Power System Controller Tuning Considering Stochastic Variations

Daniel José Turizo Arteaga

Universidad del Norte
Department of Electrical and Electronic Engineering
Barranquilla, Colombia
2017

Controller Tuning of Power System Generators Under Stochastic Loads

Daniel José Turizo Arteaga

Submitted in partial fulfillment of the requirements for the degree of:
Master of Science in Electrical Engineering

Supervisor:
Ph.D. César Orozco Henao
Co-Supervisor:
Ph.D. Javier Guerrero Sedeño

Research Line:
Power System Stability and Control
Research Group:
Electric Power Systems Research Group

Universidad del Norte
Department of Electrical and Electronic Engineering
Barranquilla, Colombia
2017

To my father, for guiding me on the path of life all this time, and being the best father in the world. This is for you, dad.

Acknowledgements

This dissertation was possible thanks to the collaboration of various people whom I think deserve to be acknowledged here.

First of all, I would like to thank my first supervisor, Dr. Javier Guerrero. I started this journey because he saw potential in me, and believed in my capabilities for successfully carrying on this research. He provided important insights and invaluable discussions about the research, even after he stopped being my official supervisor. His support has gone beyond the academic environment and I feel very grateful for being able to count on him.

I would also like to thank my current supervisor, Dr. César Orozco, for providing valuable support to the development of this research. His advises and recommendations during his time as my supervisor are much appreciated.

Very special thanks goes to my fellow students, my friends, family and loved ones. Their continuous support on my life during this research was what I needed the most.

Finally, I want to thank Universidad del Norte and its Department of Electrical and Electronic Engineering for allowing me to carry out my research and providing me with the necessary knowledge through the subjects I was allowed to take.

Abstract

Electrical power systems are vulnerable to external disturbances, such as short circuits, that can lead to damage on the equipments and even blackouts. In order to improve the system response to external disturbances, the generators of the power system are equipped with automatic controllers devised to maintain the generators working on a constant operating condition. The tuning of the controllers is performed assuming the system loads do not have time-dependent variations, but such assumption is not realistic as the power system loads are stochastically changing due to the switching on and off of every device (PCs, TVs, cellphones, etc.) connected to it.

This work proposes two new methods for the tuning of the generator controllers which takes into account the stochastic nature of the system loads. More specifically, this work proposes two new methods for the tuning of the governors and AVRs of the power system generators: one focused on the steady state response and the other focused on the fault response. First, the system response as a function of the controller parameters is calculated. As the power system is under the effect of stochastic loads, the resulting system response is stochastic. Then, a stochastic objective function which measures the quality of the system response is defined. Each tuning method uses a different objective function. Finally, the objective function is optimized using the metaheuristic Cuckoo Search, which is used for global optimization problems and can be used to optimize stochastic functions. The method was tested in different benchmark systems showing better system responses.

Keywords: Transient, stability, stochastic, controller, tuning, optimization, metaheuristic

Contents

Figure List

Table List

List of Symbols

Latin Letter Symbols

Symbol	Term
$\mathbf{B}$	Imaginary part of the admittance matrix
B_{ij}	Imaginary part of the ij element of the admittance matrix
D	Damping coefficient of the generator
E_{fd}	Generator field voltage phasor magnitude referred to stator
E'_d	Direct-axis part of the generator transient internal voltage phasor
E'_q	Quadrature-axis part of the generator transient internal voltage phasor
$\tilde{E}'_{dq}$	Transient internal voltage phasor of the generator, generator reference
$\mathbf{G}$	Real part of the admittance matrix
G_{ij}	Real part of the ij element of the admittance matrix
F	Shaft output ahead of the reheater of the governor
H	Inertia constant of the generator
I_d	Direct-axis generator current
I_q	Quadrature-axis generator current
$\tilde{I}_g$	Current phasor of the generator, synchronous reference
$\tilde{I}_{dq}$	Current phasor of the generator, generator reference
$\tilde{I}_i$	Total current phasor injected to the i^{th} node, network reference
$\vec{\tilde{I}}$	Vector of node injected current phasors
K_A	Amplifier gain of the AVR
K_E	Exciter gain of the AVR
K_F	Stabilizing feedback gain of the AVR
P_G	Active electrical power delivered by the generator
P_L	Active electrical power demanded by the load

Symbol	Term
P_{L0}	Steady state active electrical power demanded by the load
P_M	Mechanical input power of the generator
P_{MAX}	Maximum mechanical input power of the generator
P_{REF}	Governor active power setpoint
P_i	Total active electrical power injected to the i^{th} node
Q_L	Reactive power demanded by the load
Q_{L0}	Steady state reactive power demanded by the load
Q_i	Total reactive power injected to the i^{th} node
R	Governor droop (not to be confused with resistance)
R_a	Armature resistance of the generator
S_L	Complex power demanded by the load
S_{L0}	Steady state complex power demanded by the load
S_i	Total complex power injected to the i^{th} node
$\vec{S}$	Vector of node injected complex power phasors
T_A	Amplifier time constant of the AVR
T_B	Steam valve bowl time constant of the generator
T_D	Governor delay
T_E	Exciter time constant of the AVR
T_F	Stabilizing feedback time constant of the AVR
T_P	Steam reheat time constant of the governor
T_R	Regulator input time constant of the AVR
T_S	Servo time constant of the governor
T_ω	Hydro reset time constant of the governor
T'_{d0}	Transient direct-axis open circuit time constant of the generator
T'_{q0}	Transient quadrature-axis open circuit time constant of the generator
T''_{d0}	Subtransient direct-axis open circuit time constant of the generator
T''_{q0}	Subtransient quadrature-axis open circuit time constant of the generator
V_C	Regulator output (compensated) DC voltage of the AVR
V_R	Amplifier output DC voltage of the AVR
V_{REF}	AVR voltage setpoint

Symbol	Term
V_{RMAX}	Maximum amplifier output DC voltage of the AVR
V_{RMIN}	Minimum amplifier output DC voltage of the AVR
V_d	Direct-axis terminal voltage of the generator
V_f	Stabilizing feedback DC voltage of the AVR
V_q	Quadrature-axis terminal voltage of the generator
$\tilde{V}_L$	Voltage phasor of the load, network reference
$\tilde{V}_i$	Voltage phasor of the i^{th} node, network reference
$\tilde{V}_{dq}$	Terminal voltage phasor of the generator, generator reference
$\tilde{V}_t$	Terminal voltage phasor of the generator, network reference
$\tilde{V}_{t0}$	Steady state terminal voltage phasor of the generator, network reference
$\vec{\tilde{V}}$	Vector of node voltage phasors
X_d	Direct-axis steady state reactance of the generator
X_q	Quadrature-axis steady state reactance of the generator
X'_d	Direct-axis transient reactance of the generator
X'_q	Quadrature-axis transient reactance of the generator
X''_d	Direct-axis subtransient reactance of the generator
X''_q	Quadrature-axis subtransient reactance of the generator
$\mathbf{Y}$	Admittance matrix
Y_L	Load admittance
Y_{L0}	Steady state load admittance
Y_{ij}	ij element of the admittance matrix
h	Time step
i	Instant current
m	Number of generators in the power system
n	Number of nodes in the power system
p_a	Probability of detecting alien eggs (Cuckoo Search)
p_s	Population size (Cuckoo Search)
u_B	Steam valve bowl output of the governor
u_D	Delayed control signal of the governor
u_L	Limited delayed control signal of the governor

Symbol	Term
u_S	Servo output of the governor
$u\,(t)$	Unit step function evaluated at time t
v	Instant voltage
$\vec{x}$	Vector of controller parameters
$\vec{y}$	Vector of differential variables
$\vec{z}$	Vector of algebraic variables

Greek letter symbols

Symbol	Term
δ	Angle of network reference phasor voltage
γ_{ij}	Angle of the ij element of the admittance matrix
λ_i	Stochastic penetration of the load of node i
θ	Rotor angle of the generator
ξ	Standard normal random variable
ψ	Flux linkage
ρ_i	Slope of the linear variation of the load of node i
ω	Synchronous speed of the generator
ω_s	Rated synchronous speed of the generator

Subindices

Subindex	Term
L	Of the load
d	Direct axis
dq	Using generator reference (for phasors and associated variables)
i	of the i^{th} generator, node, AVR, etc. It can also refer to the i^{th} element of a vector
ij	ij element of a matrix

Subindex	Term
q	Quadrature axis
sp	Specified
0	Zero axis
∞	Steady state

Superindices

Superindex	Term
$\vec{}$	Vector
(k)	k^{th} iteration
$\tilde{}$	Phasor[1]
$\dot{}$	Time derivative
*	Complex conjugate
^{H}	Conjugate transpose

Abbreviations

Abbreviation	Term
AC	Alternating Current
ANOVA	Analysis of Variance
AVR	Automatic Voltage Regulator
CCT	Critical Clearing Time
COI	Center of Inertia
CS	Cuckoo Search
DAE	Differential Algebraic Equation
DC	Direct Current
EE	Explicit Euler
EP	Equilibrium Point

[1]Phasors written without their signature symbol $\tilde{}$ refer to their magnitude. For example: let the terminal voltage of a generator be $\tilde{V}_t = 1.02\angle 5.7°$, then its magnitude is $V_t = 1.02$.

Abbreviation	Term
EMF	Electromotive Force
FACTS	Flexible Alternating Current Transmission System
FDLF	Fast Decoupled Load Flow
GA	Genetic Algorithm
HVDC	High Voltage Direct Current
IAE	Integral Absolute Error
IE	Implicit Euler
IEEE	Institute of Electrical and Electronic Engineers
IEEE#	Power system of # nodes, used for testing in IEEE researches
NR	Newton-Raphson
ODE	Ordinary Differential Equation
OLTC	On Load Tap Changer
PDE	Partial Differential Equation
PEBS	Potential Energy Boundary Surface
PI	Proportional Integral
PID	Proportional Integral Derivative
PSO	Particle Swarm Optimization
PSS	Power System Stabilizer
RNG	Random Number Generator
SDAE	Stochastic Differential Algebraic Equation
SEP	Stable Equilibrium Point
SMIB	Single Machine Infinite Bus
SVC	Static Var Compensator
TCSC	Thyristor Controlled Series Capacitor
TEF	Transient Energy Function
WECC	Western System Coordinating Council
WGN	White Gaussian Noise
p.u.	Per Unit

1. Introduction

Electrical power systems are designed to transport the electric energy from the generation sites (hydroelectric plants, fossil fuel plants, etc.) to the consumption sites (houses, industrial facilities, etc.) in an efficient and reliable way. The power system is capable of transporting and distributing electric power, but it is not capable of storing it. Therefore it must exist, at every instant of time the system is operating, a balance between generated power injected to the system and the demanded power extracted from the system. The main problem associated with keeping this balance is that the demanded power at a future instant is not known, which forces the generators of the power system to restore the balance dynamically, at every instant.

The demanded power, although unknown, can be estimated in an approximate way using time series methods and data of past values. The aforementioned methods can be used as the demanded power normally possesses a strong periodicity associated with both the hour of the day and the day of the week. Using the estimated values of the demanded power of every system load at a given time period, the generated power of each generator is scheduled for that period, in a procedure known as *Economic Dispatch* [5]. The estimated value of the load is clearly an approximate value, and a method for balancing generated and demanded power in real time is required. For that reason, the generators of the power system are equipped with automatic controllers capable of continuously adjusting the generated power to keep the balance between generation and demand.

The generator controllers are capable of restoring the generation-demand balance by continuously modifying the generator operating condition, but doing so can cause undesired variations on the power system variables. The voltage and the frequency are the most important system variables, and they must be kept as close as possible to their rated values as large variations of these variables can lead to damage on the generators and other devices connected to the power system (electronic devices, motors, etc.). Each generator is equipped with two main controllers: the governor, which controls the generator frequency, and the AVR, which controls the generator voltage. The focus of this dissertation is the development of a tuning method for the governors and AVRs of the generators in a power system, taking into account the unknown variations of the loads. However, It must be noted that in this work not one, but two tuning methods were developed.

1.1. Objectives

1.1.1. Main Objective

- Develop a tuning method for the governors and AVRs of the generators of a power system, taking into account the stochastic variation of loads.

1.1.2. Specific Objectives

- Define the required models of the power system elements.
- Define an appropriate model for the stochastic variation of power system loads.
- Develop a metric to quantify the quality of the controllers to be tuned.
- Test the tuning method in a benchmark power system.

1.2. Scope

- The power system loads will be modelled as stochastic processes instead of the classical deterministic model.
- High-order AVR and governor models will be considered for the tuning method.
- The tuning methods to be proposed may be applied to power systems of arbitrary size.
- The performance achieved with the tuning method will be statistically tested.

1.3. Limitations

- No other controllers apart from the AVR and the governor are considered.
- The only controllable elements considered are generators

1.4. Background

Controller tuning can be performed by neglecting the interaction between each generator and the network. This allows applying analytical methods like the classical Ziegler-Nichols tuning [6]. This method was developed in 1942 by John G. Ziegler and Nathaniel B. Nichols for the tuning Proportional-Integral-Derivative (PID) controllers. The method was developed with the aim maximizing the perturbation-rejection capabilities of the controller. However, it can affect the controller normal operation.

In 1988, Sanathanan developed an analytical method for tuning the governor of a hydraulic generator based on the frequency response of said generator and its controllers [7].

The main advantage of analytical methods is that they are computationally inexpensive, but they require the assumption of no interaction between generator and network, which is unrealistic. With the computational capabilities of modern day computers and the advent of metaheuristic techniques capable of solving non-convex optimization problems, research has shifted towards tuning methods based on black box optimization techniques which allow to take into account the interaction between generators and the network.

The most common metaheuristics for optimization are Particle Swarm Optimization and Genetic Algorithms. Particle Swarm Optimization is a population metaheuristic based on the swarm behaviour of distinct species of animals [8]. A Genetic Algorithm is a population metaheuristic based on natural selection and genetics [9].

One of the most recent optimization metaheuristics is the Cuckoo Search method. This method was publicated in 2009 by Yang and Deb [10]. Is is a population metaheuristic based on the brood parasitism of the cuckoos. One important property is that it is only needed to specify one metaparameter (apart from the population size) before using it.

In 1992 Lansberry and Wozniak developed a method based on genetic algorithms to tune the governor of a hydraulic generator [9]. In 2010 Shabib, Gayed and Rashwan proposed a method for tuning a PID-type AVR using Particle Swarm Optimization [8]. In 2011 Zhang designed a procedure for tuning a PID-type AVR for a diesel generator using genetic algorithms [11]. In 2016 Shahgholian et al. devised a controller based on a combination of a fuzzy logic controller, a Proportional-Integral (PI) controller and a Thyristor Controlled Series Capacitor (TCSC) to generate an auxiliary signal for the AVR and also regulate the electrical power output of the generator in a Single Machine Infinite Bus (SMIB) system [12]. In 2017 Lomei et al. designed an approach for AVR tuning based on choosing appropriate AVR parameters to reduce the magnitude of the nonlinear characteristics of the system transient response and thus improve the system stability [13]. In 2017 Pandey and Gupta

developed a tuning method based on the Dynamic Knowledge Domain Inference concept. The method is comprised of two stages: first, an offline tuning of the controllers is performed, and second an online controller tuning is performed depending on the magnitude of the transient oscillations of the state variables during a disturbance [14].

2. Power System Elements and Models

This chapter is devoted to the development of the mathematical models describing the different elements conforming a power system. The model of each element is studied individually, and then they will be linked together to conform the complete model of the power system as a whole. This work only considers the essential elements of any power system: shunt capacitors and reactors, transformers, transmission lines, loads and generators and their controls. Some modern power system have power electronics devices (SVCs, TCSCs, etc.) that improve some of their characteristics like maximum power transfer and voltage regulation. Such systems are called *Flexible Alternating Current Transmission Systems* (FACTS). FACTS are not going to be taken into account on this work, and thus the models of the SVCs, TCSCs and other similar devices will not be developed here.

2.1. Per-Unit Representation

Before starting the development of the models for the different power system elements, the per-unit representation is going to be discussed. The per-unit representation, or *per-unit system*, is a normalization of the physical quantities of a power system that offers computational simplicity by eliminating the physical units [15]. In general, any quantity can be expressed in per unit by applying the following substitution:

$$\text{per-unit quantity value} = \frac{\text{physical quantity value}}{\text{base quantity value}}$$

The quantities in per-unit (p.u.) can be used in the same way as their physical counterparts if and only if all the related quantities are in p.u. The specific p.u. system used is completely arbitrary, and defined by choosing some of the base quantities at will. In power systems the voltage and power base quantities are freely chosen. The rest of the base quantities are not chosen, they are calculated using the basic circuit equations. Doing so ensures that the basic relationships between electrical quantities are preserved in the p.u. system. For example: let V_B and S_B be the base voltage and base power for the p.u. representation of a **single-phase** system, then the base current, impedance and admittance are calculated as:

$$I_B = \frac{S_B}{V_B}$$

$$Z_B = \frac{V_B}{I_B} = \frac{V_B^2}{S_B}$$
$$Y_B = \frac{1}{Z_B} = \frac{S_B}{V_B^2}$$

In **three-phase** systems the line voltage and three-phase power base quantities are freely chosen, and the rest of base quantities are calculated. For example: let V_{LB} and $S_{3\phi B}$ be the base line voltage and base three-phase power for the p.u. representation of a three-phase system, then the base line current and base single phase power are calculated as:

$$I_{LB} = \frac{S_{3\phi B}}{\sqrt{3}V_{LB}}$$
$$S_{1\phi B} = \frac{S_{3\phi B}}{3}$$

In a Y-connected load the base phase voltage is calculated as:

$$V_{\phi B} = \frac{V_{LB}}{\sqrt{3}}, \quad \text{(Y-connection)}$$

The base impedance and admittance are calculated assuming a Y-connection, making possible to construct single-phase equivalent systems in p.u.:

$$Z_B = \frac{V_{\phi B}^2}{S_{1\phi B}} = \frac{V_{LB}^2}{S_{3\phi B}}$$
$$Y_B = \frac{1}{Z_B} = \frac{S_{3\phi B}}{V_{LB}^2}$$

The base quantities are normally chosen so that the p.u. quantities are equal to 1 at rated operation. One important advantage of the p.u. representation is that the phase and line quantities in p.u. are equal. The p.u. representation has a wide acceptance over the industry, to the point that the data of electrical equipments are normally expressed in p.u., using the rated voltage and power of the equipment as base. When representing a power system in p.u., the base must be the same for all elements, which means the data of equipments with different p.u. systems must be converted to the p.u. system of the power system in a process known as *base changing*. Base changing is performed by calculating the physical quantity using the p.u. base of the previous p.u. system and then re-normalizing the physical quantity using the p.u. base of the new p.u. system.

The p.u. representation will be used throughout the rest of this dissertation, save some sections where the clarification will be made. The p.u. base for the models of each element developed in this chapter is calculated using the element's rated values.

2.2. Shunt Capacitor

Shunt capacitor banks are connected to a given node of the power system primarily to improve the power factor of the node, reducing losses. Another reason to use shunt capacitors is the strong dependence between reactive power and voltage magnitude: injecting reactive power to a node tends to increase the voltage magnitude of that node. The shunt capacitors act as generators of reactive power, thus increasing the node voltage in most of the cases. The admittance of the shunt capacitor can be calculated from its rated voltage and reactive power, as these are the normal parameters available from the manufacturers [16]. The complex power consumed by the shunt admittance is:

$$S_{sh} = Y_{sh}^{*} V_{sh}^{2} \tag{2-1}$$

The shunt capacitor does not consume active power, and generates reactive power, therefore:

$$\begin{aligned} S_{sh} &= Y_{sh}^{*} V_{sh}^{2} \\ -jQ_{sh} &= \left(G_{sh} + jB_{sh}\right)^{*} V_{sh}^{2} \\ -j\frac{Q_{sh}}{V_{sh}^{2}} &= G_{sh} - jB_{sh} \\ G_{sh} = 0, \qquad & B_{sh} = \frac{Q_{sh}}{V_{sh}^{2}} \end{aligned}$$

The shunt capacitor rated voltage in p.u. is 1, so the shunt admittance in p.u. is:

$$Y_{sh} = jQ_{sh} \tag{2-2}$$

Where Q_{sh} is the rated reactive power generated by the capacitor.

2.3. Shunt Reactor Model

Shunt reactors are similar to the shunt capacitors but they consume reactive power instead of generating it. They are primarily used to decrease the voltage of a given node, which can be abnormally high due to an excess of injected reactive power. The equations for the shunt capacitor apply to the shunt reactor as well, yielding that the p.u. admittance is:

$$Y_{sh} = -jQ_{sh} \tag{2-3}$$

Where Q_{sh} is the rated reactive power consumed by the reactor.

2.4. Transformer Model

Transformers are electric devices capable of changing voltage magnitude (and phase too, under special configurations) with minimal power losses. This implies transformers can change the voltage at one point of the system with almost no effect over the power flow, by changing the current flow accordingly. They are used in transmission systems to increase the voltage level, which reduces the current level and thus reduces the power losses on the transmission lines. Transformers are also used in distribution systems to reduce the voltage level to safe and practical levels for the consumers. A real transformer can be represented as a circuit with an ideal transformer plus additional elements which represent non-ideal characteristics of the real transformer, the development of the circuit can be found in [17, 18].

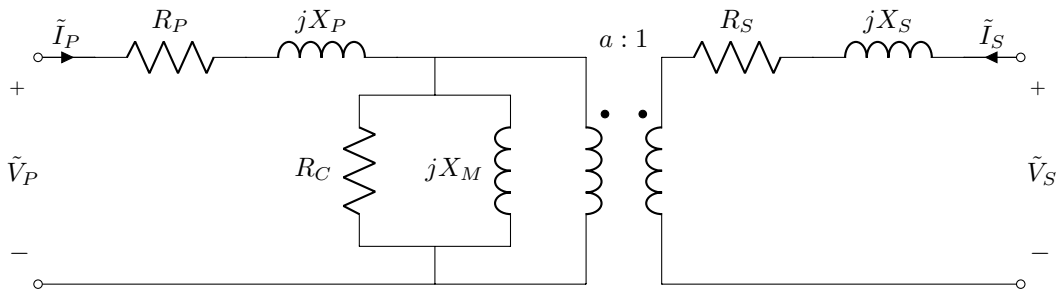

Figure 2-1.: Complete circuit model of the real transformer.

The transformer circuit is presented on Figure **2-1**, where:

- $\tilde{V}_P$ is the voltage on the primary winding, and $\tilde{V}_S$ is the voltage on the secondary winding. Similarly, $\tilde{I}_P$ is the current on the primary winding and $\tilde{I}_S$ is the current on the secondary winding.
- R_P represents the resistance of the primary winding, and R_S represents the resistance of the secondary winding.
- X_P represents the reactance due to the inductance of the primary winding, and X_S represents the reactance due to the inductance of the secondary winding.
- X_M is the magnetizing reactance. The current flowing through X_M is the *magnetizing current*, the current required to generate the oscillating magnetic flux on the transformer core.
- R_C represents the power losses on the transformer core due to the hysteresis effect and the Eddy currents. The hysteresis effect is nonlinear, but it is represented as a linear element for convenience.

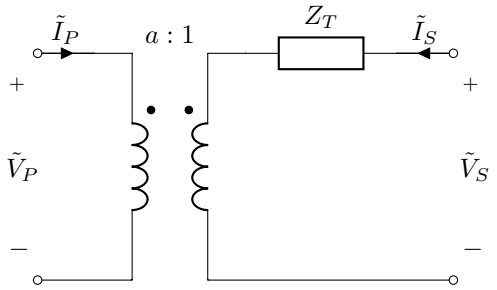

Figure 2-2.: Reduced circuit model of the transformer.

- The ideal transformer represents the magnetic link between the primary and secondary winding, due to the Faraday's law. a is the *effective voltage ratio* of the transformer and it is not equal to the turns ratio because part of the generated flux leaks out of the transformer core without linking both windings. It is possible for the voltage on the secondary side of the transformer to have a *phase shift* with respect to the voltage on the primary side, in such case a becomes a complex number with its angle representing the phase shift between the voltages.

The magnetizing current and core losses of the transformers are normally very small, which means R_C and X_M tend to have very high values. For this reason, in most studies R_C and X_M can be approximated as open circuits (they are not neglected only in special studies, where the focus is the transformer itself [15]). Furthermore, the resistance and reactance of the primary side of the transformer can be *referred* to the secondary side by dividing them by a^2 [17]. The approximated circuit of the transformer is shown in Figure **2-2**, where the resistances and reactances have been condensed into a single impedance Z_T, defined as:

$$Z_T = \left(R_P + \frac{R_S}{a^2}\right) + j\left(X_P + \frac{X_S}{a^2}\right) \tag{2-4}$$

Special considerations must be taken when using the p.u. representation in a system with transformers. The p.u. system can be designed to eliminate the ideal transformer from the circuit model of the real transformer. As the transformer changes the voltage from one side to the other, it can be considered that the base voltage from one side of the transformer is changed to the other side, dividing the power system in two *areas*, each one with a different base voltage. That way the rated p.u. voltage at both sides of the transformer is 1 (or another value, but equal for both sides), changing the value of a to 1 in such p.u. system, and thus eliminating the ideal transformer. In a power system with various transformers, the p.u. representation of that system is divided in various areas with different base voltages, and thus it is not possible to eliminate all the ideal transformers. The interested reader can find a more detailed discussion on this topic in [5].

Another way to eliminate the ideal transformer from the model is to view the real transformer as a two-port network, and describe it in terms of its admittance matrix instead of its circuit

model [19]. First of all, notice that the voltage on the primary side of the ideal transformer of Figure **2-2** is $\tilde{V}_P$; then, by definition, the voltage on the secondary side of the ideal transformer is $\frac{1}{a}\tilde{V}_P$. Applying Ohm's law to Z_T yields:

$$\begin{aligned} \tilde{I}_S Z_T &= \tilde{V}_S - \frac{1}{a}\tilde{V}_P \\ \tilde{I}_S &= -\frac{1}{aZ_T}\tilde{V}_P + \frac{1}{Z_T}\tilde{V}_S \end{aligned} \tag{2-5}$$

The power consumed by the ideal transformer must be zero, so the complex power flowing into the primary side must be equal to the power flowing out of the secondary side:

$$\begin{aligned} \tilde{V}_P \tilde{I}_P^* &= -\frac{1}{a}\tilde{V}_P \tilde{I}_S^* \\ \tilde{I}_S &= -a^* \tilde{I}_P \end{aligned} \tag{2-6}$$

Replacing Equation (2-6) in Equation (2-5):

$$\begin{aligned} -a^* \tilde{I}_P &= -\frac{1}{aZ_T}\tilde{V}_P + \frac{1}{Z_T}\tilde{V}_S \\ \tilde{I}_P &= \frac{1}{|a|^2 Z_T}\tilde{V}_P - \frac{1}{a^* Z_T}\tilde{V}_S \end{aligned} \tag{2-7}$$

Expressing equations (2-7) and (2-5) in matrix form:

$$\begin{bmatrix} \tilde{I}_P \\ \tilde{I}_S \end{bmatrix} = \begin{bmatrix} \frac{1}{|a|^2 Z_T} & -\frac{1}{a^* Z_T} \\ -\frac{1}{aZ_T} & \frac{1}{Z_T} \end{bmatrix} \begin{bmatrix} \tilde{V}_P \\ \tilde{V}_S \end{bmatrix}$$

Then the admittance matrix of the transformer is:

$$\mathbf{Y}_T = \begin{bmatrix} \frac{1}{|a|^2 Z_T} & -\frac{1}{a^* Z_T} \\ -\frac{1}{aZ_T} & \frac{1}{Z_T} \end{bmatrix} \tag{2-8}$$

The admittance matrix will be used as the default model for representing the transformer. Notice that if a has a non-zero imaginary part, then the matrix will not be symmetric, so it is not possible to construct a general standard circuit model (π or T circuit) for the transformer (for the special case that a is purely real, it is possible construct a π circuit for the transformer).

2.5. Transmission Line Model

Transmission lines are arrays of conductors used to transport electrical energy from the generating facilities to the consumers. There are two types of transmission lines: *overhead lines* and *underground cables*. Both types of lines are characterized by four main parameters [15]:

- **Series Resistance** (R_x)**:** Represents the resistance of the line conductors, with the increments due to stranding and skin effect included. This value can be obtained from the manufacturer.

- **Series Inductance** (L_x)**:** Represents the self and mutual inductances of the line conductors. This value depends on their geometric distribution, and is different for all conductors unless their distribution is symmetric. It is necessary to have equal inductances for all the conductors, in order to have a balanced transmission line (the current is the same for each phase). When the distribution is not symmetric, it is possible to make the inductances equal by transposing the conductors to ensure each one occupies each possible position.

- **Shunt Conductance** (G_x)**:** Represents the path of the leakage current that flows along insulators and due to the corona effect. This value depends on variables like the weather and the humidity of the air, which make the calculation of the shunt conductance unreliable. On top of that, the leakage current tends to be very small, which allows to completely neglect this parameter.

- **Shunt Capacitance** (C_x)**:** Represents the capacitive effect due to the potential difference between each pair of conductors and between each conductor and the ground. This value, as the inductance, depends on the geometric distribution of the conductors.

Extensive discussions on the calculation of L_x and C_x can be found in [5, 20]. The line parameters have the subscript x indicating they are parameters per unit length (Ω/km, p.u./km, etc.). These parameters are calculated assuming the conductors of the transmission line are infinitely long, which is equivalent to say the line parameters are only valid to line sections of differential length.

2.5.1. Complete Model

In order to develop the model of the complete transmission line, a line section of differential length Δx is considered, as shown in Figure **2-3**. The voltage drop and leakage current on the line section are represented as a symmetric T-circuit, because the line section is exactly equal when observed from one end or the other [21]. The T circuit is just an approximation, but it can be shown that in some cases, when the length of the line section tends to zero the circuit approximation becomes exact [4].

The voltage-current relationship for the line section when Δx tends to zero is going to be derived. Notice that the voltages and currents are expressed as arbitrary time dependent functions and not as phasors. The voltage drop of the line section, Δv, is equal to the sum

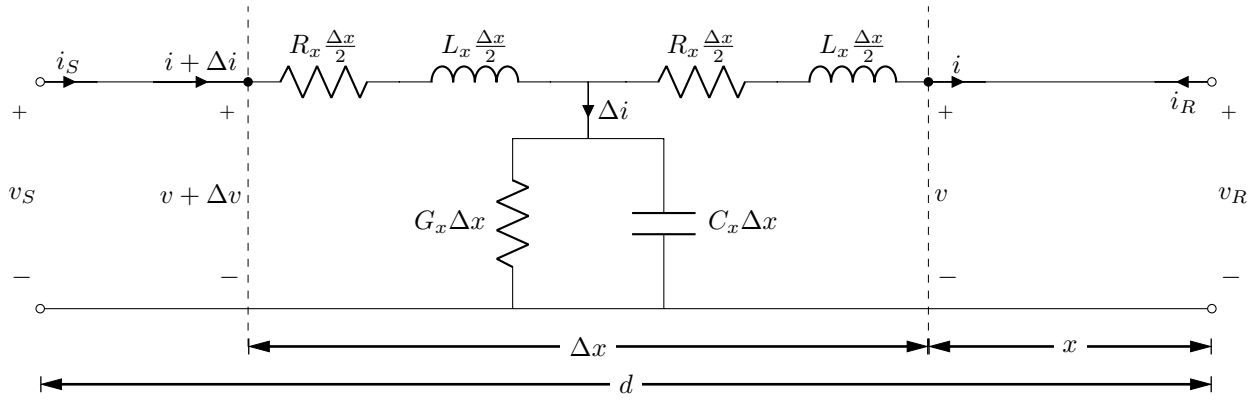

Figure 2-3.: Circuit model for the differential section of a transmission line.

of the voltage drops to the left and to the right of the shunt branch:

$$\begin{aligned}
\Delta v &= \Delta v_1 + \Delta v_2 \\
\Delta v_1 &= R_x \frac{\Delta x}{2}(i+\Delta i) + L_x \frac{\Delta x}{2}\frac{\partial (i+\Delta i)}{\partial t} \\
\Delta v_1 &= \Delta x f_v (i+\Delta i) \qquad (2\text{-}9) \\
\Delta v_2 &= R_x \frac{\Delta x}{2} i + L_x \frac{\Delta x}{2}\frac{\partial i}{\partial t} \\
\Delta v_2 &= \Delta x f_v (i) \qquad (2\text{-}10)
\end{aligned}$$

Where:

$$f_v(i) = \frac{1}{2}R_x i + \frac{1}{2}L_x \frac{\partial i}{\partial t} \qquad (2\text{-}11)$$

The voltage drop equation can be rearranged as:

$$\begin{aligned}
\Delta v &= \Delta x \left[R_x i + L_x \frac{\partial i}{\partial t} + R_x \Delta i + L_x \frac{\partial (\Delta i)}{\partial t} \right] \\
\frac{\Delta v}{\Delta x} &= R_x i + L_x \frac{\partial i}{\partial t} + \frac{1}{2}R_x \Delta i + \frac{1}{2}L_x \frac{\partial (\Delta i)}{\partial t} \qquad (2\text{-}12)
\end{aligned}$$

The leakage current equation can be calculated directly from the shunt branch:

$$\begin{aligned}
\Delta i &= G_x \Delta x (v + \Delta v_2) + C_x \Delta x \frac{\partial (v+\Delta v_2)}{\partial t} \\
\Delta i &= \Delta x \left[G_x (v + \Delta x f_v(i)) + C_x \frac{\partial (v + \Delta x f_v(i))}{\partial t} \right] \\
\Delta i &= \Delta x \left[G_x v + C_x \frac{\partial v}{\partial t} \right] + (\Delta x)^2 \left[G_x f_v(i) + C_x \frac{\partial (f_v(i))}{\partial t} \right] \\
\Delta i &= \Delta x f_i(v) + (\Delta x)^2 f_i(f_v(i)) \qquad (2\text{-}13)
\end{aligned}$$

Where:

$$f_i(v) = G_x v + C_x \frac{\partial v}{\partial t} \tag{2-14}$$

The leakage current equation can be rearranged as:

$$\frac{\Delta i}{\Delta x} = f_i(v) + \Delta x f_i(f_v(i)) \tag{2-15}$$

Applying the limit when Δx tends to zero:

$$\begin{aligned} \lim_{\Delta x \to 0} \frac{\Delta i}{\Delta x} = \frac{\partial i}{\partial x} &= f_i(v) \\ \frac{\partial i}{\partial x} &= G_x v + C_x \frac{\partial v}{\partial t} \end{aligned} \tag{2-16}$$

From Equation 2-13:

$$\frac{\partial(\Delta i)}{\partial t} = \Delta x \frac{\partial(f_i(v))}{\partial t} f_i(v) + (\Delta x)^2 \frac{\partial[f_i(f_v(i))]}{\partial t}$$

$$\lim_{\Delta x \to 0} \Delta i = 0 \tag{2-17}$$

$$\lim_{\Delta x \to 0} \frac{\partial(\Delta i)}{\partial t} = 0 \tag{2-18}$$

Applying the limit when Δx tends to zero to 2-12:

$$\begin{aligned} \lim_{\Delta x \to 0} \frac{\Delta v}{\Delta x} = \frac{\partial v}{\partial x} &= R_x i + L_x \frac{\partial i}{\partial t} + \frac{1}{2} R_x \lim_{\Delta x \to 0} \Delta i + \frac{1}{2} L_x \lim_{\Delta x \to 0} \frac{\partial(\Delta i)}{\partial t} \\ \frac{\partial v}{\partial x} &= R_x i + L_x \frac{\partial i}{\partial t} \end{aligned} \tag{2-19}$$

Equations 2-19 and 2-16 conform a set of partial differential equations (PDEs) which describes the behaviour of the voltage and current at any point of the line. These PDEs are coupled: the voltage equation depends on the current and vice versa. The PDEs can be decoupled: first, Equation 2-19 is differentiated with respect to x:

$$\frac{\partial^2 v}{\partial x^2} = R_x \frac{\partial i}{\partial x} + L_x \frac{\partial}{\partial t}\left(\frac{\partial i}{\partial x}\right)$$

Substituting Equation 2-16 into Equation 2-19:

$$\frac{\partial^2 v}{\partial x^2} = R_x G_x v + (R_x C_x + L_x G_x) \frac{\partial v}{\partial t} + L_x C_x \frac{\partial^2 v}{\partial t^2} \tag{2-20}$$

Applying the same procedure to Equation 2-16 results in the following equation:

$$\frac{\partial^2 i}{\partial x^2} = R_x G_x i + (R_x C_x + L_x G_x) \frac{\partial i}{\partial t} + L_x C_x \frac{\partial^2 i}{\partial t^2} \tag{2-21}$$

Equation 2-20 and 2-21 conform the set of decoupled PDEs that describe the voltage and current on the transmission line at any point.

2.5.2. Steady State Model

In normal steady state operation, the voltages and currents at the sending and receiving ends of the line are perfect AC (sinusoidal) waves. Equations 2-20 and 2-21 are lineal differential equations so in steady state it is possible to express the voltage and current as phasors ($\tilde{V}$ and $\tilde{I}$) instead of their time-dependent values (v and i). Equation 2-20 in phasorial form becomes:

$$\begin{aligned}\frac{d^2\tilde{V}}{dx^2} &= R_x G_x \tilde{V} + (R_x C_x + L_x G_x)\left(j\omega\tilde{V}\right) + L_x C_x\left(j^2\omega^2\tilde{V}\right)\\ \frac{\partial^2\tilde{V}}{\partial x^2} &= (R_x + j\omega L_x)(G_x + j\omega C_x)\,\tilde{V}\\ \frac{\partial^2\tilde{V}}{\partial x^2} &= z_x y_x \tilde{V} \end{aligned} \tag{2-22}$$

Where $z_x = R_x + j\omega L_x$ and $y_x = G_x + j\omega C_x$. Phasors are time independent so the derivative with respect to x is not partial anymore:

$$\frac{d^2\tilde{V}}{dx^2} = \gamma^2\tilde{V} \tag{2-23}$$

$$\gamma = +\sqrt{z_x y_x} = +\sqrt{(R_x + j\omega L_x)(G_x + j\omega C_x)} \tag{2-24}$$

Where γ is called *propagation constant* of the line. Equation 2-23 is an ordinary differential equation (ODE). More specifically, Equation 2-23 is a linear second order ODE whose general solution is:

$$\tilde{V} = A_1 e^{\gamma x} + A_2 e^{-\gamma x} \tag{2-25}$$

In order to find the general solution of the current, Equation 2-16 is expressed in phasor form:

$$\frac{\partial\tilde{I}}{\partial x} = y_x\tilde{V}$$

Substituting Equation 2-25 and integrating with respect to x:

$$\begin{aligned}\tilde{I} &= \frac{y_x}{\gamma}\left(A_1 e^{\gamma x} - A_2 e^{-\gamma x}\right)\\ \tilde{I} &= \frac{1}{\gamma/y_x}\left(A_1 e^{\gamma x} - A_2 e^{-\gamma x}\right)\\ \tilde{I} &= \frac{1}{Z_C}\left(A_1 e^{\gamma x} - A_2 e^{-\gamma x}\right) \end{aligned} \tag{2-26}$$

$$Z_C = \frac{\gamma}{y_x} = \sqrt{\frac{z_x}{y_x}} \tag{2-27}$$

Where Z_C is called *characteristic impedance* of the line. At the receiving end, where $x = 0$, the voltage and current are ($\tilde{I}_R$ has negative sign because its direction is opposite to that of $\tilde{I}_S$):

$$\tilde{V}_R = A_1 e^{\gamma 0} + A_2 e^{-\gamma 0} = A_1 + A_2$$

$$-\tilde{I}_R = \frac{1}{Z_C}\left(A_1 e^{\gamma 0} - A_2 e^{-\gamma 0}\right) = \frac{1}{Z_C}\left(A_1 - A_2\right)$$

Solving for A_1 and A_2 yields:

$$A_1 = \frac{\tilde{V}_R - \tilde{I}_R Z_C}{2}, \qquad A_2 = \frac{\tilde{V}_R + \tilde{I}_R Z_C}{2}$$

Therefore, the voltage and current of the transmission line at a distance x from the receiving end are:

$$\tilde{V}\left(x\right) = \frac{\tilde{V}_R - \tilde{I}_R Z_C}{2} e^{\gamma x} + \frac{\tilde{V}_R + \tilde{I}_R Z_C}{2} e^{-\gamma x} \tag{2-28}$$

$$\tilde{I}\left(x\right) = \frac{\tilde{V}_R - \tilde{I}_R Z_C}{2Z_C} e^{\gamma x} - \frac{\tilde{V}_R + \tilde{I}_R Z_C}{2Z_C} e^{-\gamma x} \tag{2-29}$$

At the sending end, where $x = d$, the voltage and current are:

$$\tilde{V}_S = \frac{\tilde{V}_R - \tilde{I}_R Z_C}{2} e^{\gamma d} + \frac{\tilde{V}_R + \tilde{I}_R Z_C}{2} e^{-\gamma d} \tag{2-30}$$

$$\tilde{I}_S = \frac{\tilde{V}_R - \tilde{I}_R Z_C}{2Z_C} e^{\gamma d} - \frac{\tilde{V}_R + \tilde{I}_R Z_C}{2Z_C} e^{-\gamma d} \tag{2-31}$$

The current at the receiving end can be expressed in terms of the voltages at the lines ends from Equation 2-30:

$$\begin{aligned}
\tilde{V}_S &= \tilde{V}_R \frac{e^{\gamma d} + e^{-\gamma d}}{2} - \tilde{I}_R Z_C \frac{e^{\gamma d} - e^{-\gamma d}}{2} \\
\tilde{I}_R Z_C \frac{e^{\gamma d} - e^{-\gamma d}}{2} &= -\tilde{V}_S + \tilde{V}_R \frac{e^{\gamma d} + e^{-\gamma d}}{2} \\
\tilde{I}_R &= -\tilde{V}_S \frac{1}{Z_C} \frac{2}{e^{\gamma d} - e^{-\gamma d}} + \tilde{V}_R \frac{1}{Z_C} \frac{e^{\gamma d} + e^{-\gamma d}}{e^{\gamma d} - e^{-\gamma d}}
\end{aligned} \tag{2-32}$$

Equation 2-32 can be rearranged as follows:

$$\tilde{I}_R = -\tilde{V}_S \frac{1}{Z_C} \frac{2}{e^{\gamma d} - e^{-\gamma d}} + \tilde{V}_R \frac{1}{Z_C} \left[\frac{e^{\gamma d} + e^{-\gamma d} - 2}{e^{\gamma d} - e^{-\gamma d}} + \frac{2}{e^{\gamma d} - e^{-\gamma d}}\right]$$

$$\tilde{I}_R = -\tilde{V}_S \frac{1}{Z_C} \frac{1}{\sinh\left(\gamma d\right)} + \tilde{V}_R \frac{1}{Z_C} \left[\frac{\left(e^{\gamma d/2} - e^{-\gamma d/2}\right)^2}{\left(e^{\gamma d/2} - e^{-\gamma d/2}\right)\left(e^{\gamma d/2} + e^{-\gamma d/2}\right)} + \frac{1}{\sinh\left(\gamma d\right)}\right]$$

$$\tilde{I}_R = -\tilde{V}_S \frac{1}{Z_C} \frac{1}{\sinh\left(\gamma d\right)} + \tilde{V}_R \frac{1}{Z_C} \left[\frac{\left(e^{\gamma d/2} - e^{-\gamma d/2}\right)}{\left(e^{\gamma d/2} + e^{-\gamma d/2}\right)} + \frac{1}{\sinh\left(\gamma d\right)}\right]$$

$$\tilde{I}_R = -\tilde{V}_S \frac{1}{Z_C} \frac{1}{\sinh\left(\gamma d\right)} + \tilde{V}_R \frac{1}{Z_C} \left[\tanh\left(\gamma d/2\right) + \frac{1}{\sinh\left(\gamma d\right)}\right]$$

$$\tilde{I}_R = -\tilde{V}_S \frac{1}{\sqrt{z_x/y_x}} \frac{1}{\sinh\left(\gamma d\right)} + \tilde{V}_R \left[\frac{1}{\sqrt{z_x/y_x}} \tanh\left(\gamma d/2\right) + \frac{1}{\sqrt{z_x/y_x}} \frac{1}{\sinh\left(\gamma d\right)}\right]$$

$$\tilde{I}_R = -\tilde{V}_S \frac{1}{z_x} \frac{\sqrt{z_x y_x}}{\sinh(\gamma d)} + \tilde{V}_R \left[y_x \frac{\tanh(\gamma d/2)}{\sqrt{z_x y_x}} + \frac{1}{z_x} \frac{\sqrt{z_x y_x}}{\sinh(\gamma d)} \right]$$
$$\tilde{I}_R = -\tilde{V}_S \frac{1}{z_x d} \frac{\gamma d}{\sinh(\gamma d)} + \tilde{V}_R \left[\frac{y_x d}{2} \frac{\tanh(\gamma d/2)}{\gamma d/2} + \frac{1}{z_x d} \frac{\gamma d}{\sinh(\gamma d)} \right]$$
$$\tilde{I}_R = -\tilde{V}_S \frac{1}{z} \frac{\gamma d}{\sinh(\gamma d)} + \tilde{V}_R \left[\frac{y}{2} \frac{\tanh(\gamma d/2)}{\gamma d/2} + \frac{1}{z} \frac{\gamma d}{\sinh(\gamma d)} \right] \tag{2-33}$$

Where:

$$z = z_x d \tag{2-34}$$
$$y = y_x d \tag{2-35}$$

Equation 2-31 can be rearranged as:

$$\tilde{I}_S = \tilde{V}_R \frac{1}{Z_C} \frac{e^{\gamma d} - e^{-\gamma d}}{2} - \tilde{I}_R \frac{e^{\gamma d} + e^{-\gamma d}}{2} \tag{2-36}$$

Substituting Equation 2-32:

$$\tilde{I}_S = \tilde{V}_R \frac{1}{Z_C} \frac{e^{\gamma d} - e^{-\gamma d}}{2} + \tilde{V}_S \frac{1}{Z_C} \frac{e^{\gamma d} + e^{-\gamma d}}{e^{\gamma d} - e^{-\gamma d}} - \tilde{V}_R \frac{1}{Z_C} \frac{\left(e^{\gamma d} + e^{-\gamma d}\right)^2}{2\left(e^{\gamma d} - e^{-\gamma d}\right)}$$
$$\tilde{I}_S = \tilde{V}_S \frac{1}{Z_C} \frac{e^{\gamma d} + e^{-\gamma d}}{e^{\gamma d} - e^{-\gamma d}} - \tilde{V}_R \frac{1}{Z_C} \frac{\left(e^{\gamma d} + e^{-\gamma d}\right)^2 - \left(e^{\gamma d} - e^{-\gamma d}\right)^2}{2\left(e^{\gamma d} - e^{-\gamma d}\right)}$$
$$\tilde{I}_S = \tilde{V}_S \frac{1}{Z_C} \frac{e^{\gamma d} + e^{-\gamma d}}{e^{\gamma d} - e^{-\gamma d}} - \tilde{V}_R \frac{1}{Z_C} \frac{e^{2\gamma d} + 2 + e^{-2\gamma d} - e^{2\gamma d} + 2 - e^{-2\gamma d}}{2\left(e^{\gamma d} - e^{-\gamma d}\right)}$$
$$\tilde{I}_S = \tilde{V}_S \frac{1}{Z_C} \frac{e^{\gamma d} + e^{-\gamma d}}{e^{\gamma d} - e^{-\gamma d}} - \tilde{V}_R \frac{1}{Z_C} \frac{2}{e^{\gamma d} - e^{-\gamma d}} \tag{2-37}$$

A rearrangement analogous to that of Equation 2-32 can be applied to Equation 2-37, giving the following result:

$$\tilde{I}_S = \tilde{V}_S \left[\frac{y}{2} \frac{\tanh(\gamma d/2)}{\gamma d/2} + \frac{1}{z} \frac{\gamma d}{\sinh(\gamma d)} \right] - \tilde{V}_R \frac{1}{z} \frac{\gamma d}{\sinh(\gamma d)} \tag{2-38}$$

Equations 2-38 and 2-33 can be expressed in matrix form as:

$$\begin{bmatrix} \tilde{I}_R \\ \tilde{I}_S \end{bmatrix} = \begin{bmatrix} \frac{y}{2} \frac{\tanh(\gamma d/2)}{\gamma d/2} + \frac{1}{z} \frac{\gamma d}{\sinh(\gamma d)} & -\frac{1}{z} \frac{\gamma d}{\sinh(\gamma d)} \\ -\frac{\gamma d}{z \sinh(\gamma d)} & \frac{y}{2} \frac{\tanh(\gamma d/2)}{\gamma d/2} + \frac{\gamma d}{z \sinh(\gamma d)} \end{bmatrix} \begin{bmatrix} \tilde{V}_S \\ \tilde{V}_R \end{bmatrix} \tag{2-39}$$

Let $Z = z \frac{\sinh(\gamma d)}{\gamma d}$ and $Y = y \frac{\tanh(\gamma d/2)}{\gamma d/2}$, then:

$$\begin{bmatrix} \tilde{I}_R \\ \tilde{I}_S \end{bmatrix} = \begin{bmatrix} \frac{Y}{2} + \frac{1}{Z} & -\frac{1}{Z} \\ -\frac{1}{Z} & \frac{Y}{2} + \frac{1}{Z} \end{bmatrix} \begin{bmatrix} \tilde{V}_S \\ \tilde{V}_R \end{bmatrix} \tag{2-40}$$

Therefore, the admittance matrix of the transmission line is:

$$\mathbf{Y}_L = \begin{bmatrix} \frac{Y}{2} + \frac{1}{Z} & -\frac{1}{Z} \\ -\frac{1}{Z} & \frac{Y}{2} + \frac{1}{Z} \end{bmatrix} \tag{2-41}$$

As the admittance matrix is symmetric, it is possible to represent the transmission line as a π equivalent circuit as shown in Figure **2-4**. The series impedance of the circuit is Z and the shunt admittance is Y.

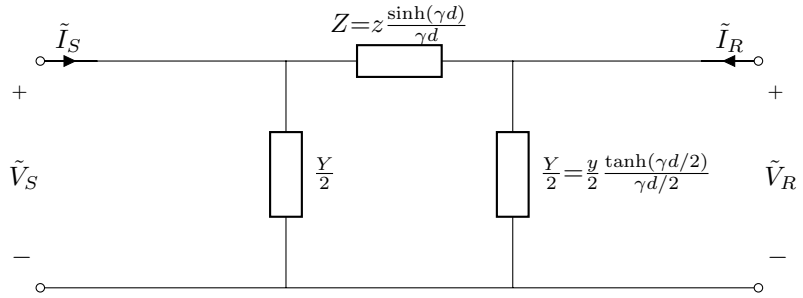

Figure 2-4.: Steady state circuit model of the transmission line.

It is typical to give the line data in terms of its series resistance R, series reactance X ($Z = R + jX$), and shunt susceptance B. The shunt conductance G, as stated previously, is negligible and taken as zero ($Y = G + jB$). It must be remembered that this circuit model is only valid for steady state. For analysis of transient events, Equations 2-20 and 2-21 should be used. However, the time constants of the line transients tend to be much smaller than the time constants of the electro-mechanic transients which are the main interest in the transient analysis of power systems. For that reason, it is common practice lo neglect the line transients and use just the circuit model in the simulations of power systems [15].

2.6. Load Model

The loads of the power system are the final users, they extract the power injected by the generators to the system. At transmission level, it is common to represent whole distribution systems as single loads, in order to simplify the analysis of the power system. A load can be modelled as a shunt element, and its specific power consumption can be modelled in different ways. Depending on the specific model a load can be classified as *static load* or *dynamic load*.

2.6.1. Static Load Models

A static load has a power consumption that is an *algebraic function* of the voltage magnitude of the node it is connected to. Static loads also do not depend of the time. Loads can depend on the frequency, but such dependence is not as strong as the voltage one (exept when the load is a motor), so throughout this work it will be assumed the loads do not depend on frequency. One of the most common load models is the *ZIP model*, where the power consumption (active and reactive) is represented as a quadratic function of the voltage magnitude [15]:

$$P_L = a_{2L}V_L^2 + a_{1L}V_L + a_{0L} \tag{2-42}$$

$$Q_L = b_{2L}V_L^2 + b_{1L}V_L + b_{0L} \tag{2-43}$$

The complex power of the load can be expressed as:

$$S_L = (a_{2L} + jb_{2L})\,V_L^2 + (a_{1L} + jb_{1L})\,V + (a_{0L} + jb_{0L}) \tag{2-44}$$

The quadratic term can be interpreted as the complex power consumed by a shunt admittance. Similarly, the linear term can be interpreted as the complex power consumed by a current source[1] and the constant term can be interpreted as the power consumed by a constant-power load. With these interpretations in mind, the coefficients of Equation 2-44 can be relabelled as:

$$S_L = Y_L V_L^2 + I_L V + S_{0L} \tag{2-45}$$

In this work the load models will be restricted to two special cases. The first case corresponds to a pure constant-admittance load:

$$S_L = Y_L V_L^2 \tag{2-46}$$

And the second case corresponds to a pure constant power load:

$$S_L = S_{0L} \tag{2-47}$$

Notice that for both cases it is implicitly assumed that the power factor of the load is constant. Also, the constant power model is nonlinear, because its voltage-current relationship is nonlinear.

[1] The complex power consumed by a constant current load is $S = \tilde{V}\tilde{I}^* = VI\angle(\theta_V - \theta_I)$ which is a function of both the voltage magnitude and angle, whereas the linear term of Equation 2-44 is a function of just the voltage magnitude, so it cannot be identically equal to the power consumed by a current source. However, the coefficient of the linear term has physical units of current, thus giving place to the current source interpretation.

2.6.2. Dynamic Load Models

A dynamic load has a power consumption that is a *differential function* of the voltage, frequency, time, or any combination of them. Dynamic load models are used for studies where the time scale is large, like long-term stability studies [15]. On top of that, typical dynamic model are deterministic, whereas the load variations considered in this work are of stochastic nature. For that reason, typical dynamic load models are not considered. For convenience, stochastic load models will be delayed to Chapter 4, where the context is more suitable.

2.7. Generator Model

Synchronous generators are the core of any power system. They are in charge of transforming mechanical power to electrical power and injecting it to the system for consumers to use. The generators are also the most complex elements of the power systems, and the complexity of their models can differ vastly depending on the application. The model that is going to be developed in this section is the *two-axis model*, which is typically used in transient stability analysis [15]. The development of the model is based on [22, 23, 15, 4].

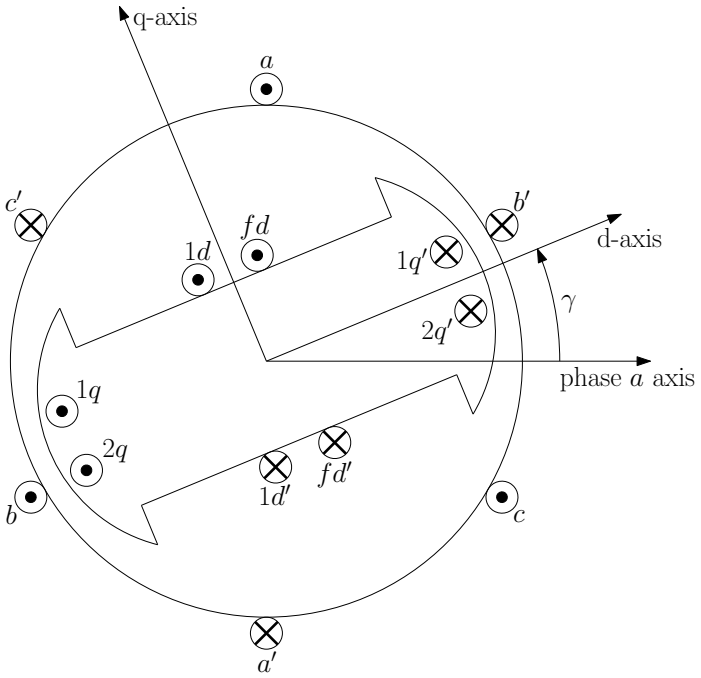

Figure 2-5.: Schematic diagram of the cross-section of a synchronous machine.

2.7.1. Time-Varying Inductances Model

Figure **2-5** shows a simplified cross section of a two-pole synchronous machine. Each stator winding is represented with a single coil accounting for all the electromotive force (EMF) induced on all the coils of the winding. Stator windings have 120° of separation between them, and the axis of each winding points in the direction of the positive flux linkage of that winding. The *direct axis*, or d-axis, points in the direction of the magnetic field produced by the field winding. The *quadrature axis*, or q-axis, leads the d-axis by 90° with respect to rotation direction of the rotor[2]. All the damper windings plus the field winding of the machine are represented as four equivalent rotor circuits (two damper windings aligned over the q-axis, one damper winding aligned over the d-axis and the field winding) which account for the total magnetic field produced by the original windings. Before developing the equations of the machine, the following assumptions are going to be made [15]:

- Stator coils are sinusoidally distributed, so the rotating magnetic flux of the rotor is perceived by the stator as a sinusoidal flux.
- The stator shape does not produce any variation of the rotor inductances with respect to the rotor position.
- Magnetic hysteresis is negligible.
- Magnetic saturation is negligible.
- The synchronous machine only has two poles.

The last assumption is made only to simplify the development of the equations, it is possible to develop the same models for machines with more than two poles, but the procedure is more extensive.

Figure **2-6** shows the circuit model of the stator windings, the stator currents are assumed to flow out of the machine because it is working as a generator. The circuit equations of the stator, using instantaneous variables, are:

$$v_a = -R_a i_a + \frac{d\psi_a}{dt} + v_n$$
$$v_b = -R_a i_b + \frac{d\psi_b}{dt} + v_n$$
$$v_c = -R_a i_c + \frac{d\psi_c}{dt} + v_n$$

[2]More generally, the q-axis leads the d-axis by $180°/p$ in a p-pole machine. Geometrically speaking, the q-axis bisects the angle formed by the d-axis, the rotor center, the pole face immediately leading the d-axis.

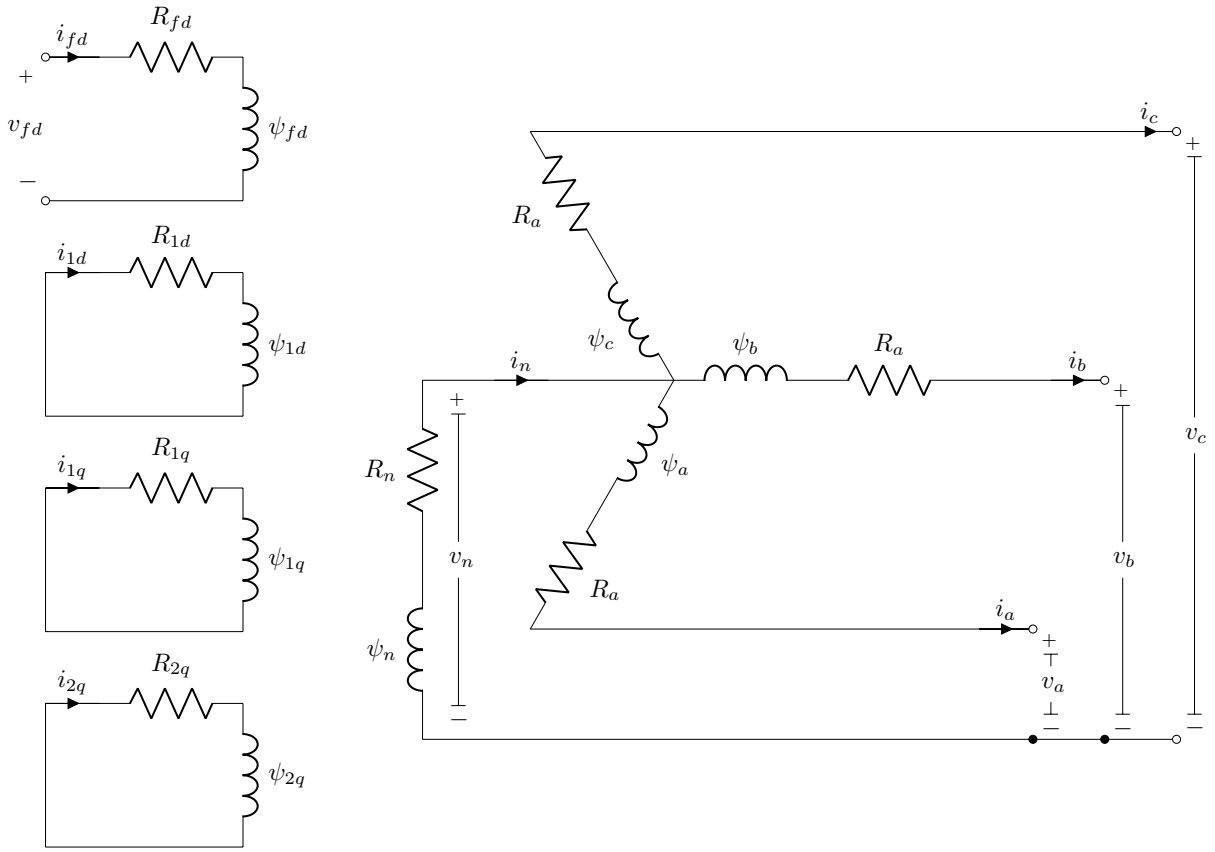

Figure 2-6.: Stator and rotor circuits of a synchronous machine.

The equations can be expressed in vector form as:

$$\vec{v}_{abc} = -R_a\vec{i}_{abc} + \frac{d\vec{\psi}_{abc}}{dt} + \vec{1}v_n \tag{2-48}$$

Where $\vec{1}$ is a vector of ones with adequate dimension. The currents of the rotor circuits are assumed to flow into their respective circuits (motor convention). The equations of the rotor circuits using instantaneous variables are:

$$\begin{aligned} v_{fd} &= R_{fd}i_{fd} + \frac{d\psi_{fd}}{dt} \\ 0 &= R_{1d}i_{1d} + \frac{d\psi_{1d}}{dt} \\ 0 &= R_{1q}i_{1q} + \frac{d\psi_{1q}}{dt} \\ 0 &= R_{2q}i_{2q} + \frac{d\psi_{2q}}{dt} \end{aligned}$$

Notice that damper windings are short circuited, so they have no sources. On the other hand, the field winding is connected to a DC source of voltage v_{fd}. The rotor equations can be expressed in vector form as:

$$\begin{bmatrix} v_{fd} \\ 0 \\ 0 \\ 0 \end{bmatrix} = \begin{bmatrix} R_{fd} & 0 & 0 & 0 \\ 0 & R_{1d} & 0 & 0 \\ 0 & 0 & R_{1q} & 0 \\ 0 & 0 & 0 & R_{2q} \end{bmatrix} \begin{bmatrix} i_{fd} \\ i_{1d} \\ i_{1q} \\ i_{2q} \end{bmatrix} + \frac{d}{dt}\left(\begin{bmatrix} \psi_{fd} \\ \psi_{1d} \\ \psi_{1q} \\ \psi_{2q} \end{bmatrix} \right)$$

Grouping variables of the d-axis circuits in a single vector, and doing the same to variables of the q-axis circuits:

$$\begin{bmatrix} \vec{v}_{f1d} \\ \vec{0} \end{bmatrix} = \begin{bmatrix} \mathbf{R}_{f1d} & \mathbf{0} \\ \mathbf{0} & \mathbf{R}_{12q} \end{bmatrix} \begin{bmatrix} \vec{i}_{f1d} \\ \vec{i}_{12q} \end{bmatrix} + \frac{d}{dt}\left(\begin{bmatrix} \vec{\psi}_{f1d} \\ \vec{\psi}_{12q} \end{bmatrix} \right)$$

Where $\vec{0}$ is a vector of zeros with adequate dimension and $\mathbf{0}$ is a matrix of zeros with adequate dimensions. Rotor and stator equations can be expressed together as:

$$\begin{bmatrix} \vec{v}_{abc} \\ \vec{v}_{f1d} \\ \vec{0} \end{bmatrix} = \begin{bmatrix} -R_a\mathbf{U} & \mathbf{0} & \mathbf{0} \\ \mathbf{0} & \mathbf{R}_{f1d} & \mathbf{0} \\ \mathbf{0} & \mathbf{0} & \mathbf{R}_{12q} \end{bmatrix} \begin{bmatrix} \vec{i}_{abc} \\ \vec{i}_{f1d} \\ \vec{i}_{12q} \end{bmatrix} + \frac{d}{dt}\left(\begin{bmatrix} \vec{\psi}_{abc} \\ \vec{\psi}_{f1d} \\ \vec{\psi}_{12q} \end{bmatrix} \right) + \begin{bmatrix} \vec{1}v_n \\ \vec{0} \\ \vec{0} \end{bmatrix} \tag{2-49}$$

Where $\mathbf{U}$ is an identity matrix with adequate dimensions. The flux linkages can be expressed in terms of the currents and the inductances coupling the different circuits:

$$\begin{bmatrix} \vec{\psi}_{abc} \\ \vec{\psi}_{f1d} \\ \vec{\psi}_{12q} \end{bmatrix} = \begin{bmatrix} -\mathbf{L}_{SS\gamma} & \mathbf{L}_{SD\gamma} & \mathbf{L}_{SQ\gamma} \\ -\mathbf{L}_{SD\gamma}^T & \mathbf{L}_{DD} & \mathbf{0} \\ -\mathbf{L}_{SQ\gamma}^T & \mathbf{0} & \mathbf{L}_{QQ} \end{bmatrix} \begin{bmatrix} \vec{i}_{abc} \\ \vec{i}_{f1d} \\ \vec{i}_{12q} \end{bmatrix} \tag{2-50}$$

Notice that d-axis circuits are decoupled from q-axis circuits. This occurs because the q-axis was specifically defined to be magnetically decoupled from the d-axis. The values of the inductance submatrices are [15]:

$$\mathbf{L}_{SS\gamma} = \begin{bmatrix} L_{aa0} + L_{aa2}\cos 2\gamma & -L_{ab0} - L_{aa2}\cos\left(2\gamma + \frac{\pi}{3}\right) & -L_{ab0} - L_{aa2}\cos\left(2\gamma - \frac{\pi}{3}\right) \\ -L_{ab0} - L_{aa2}\cos\left(2\gamma + \frac{\pi}{3}\right) & L_{aa0} + L_{aa2}\cos 2\left(\gamma - \frac{2\pi}{3}\right) & -L_{ab0} - L_{aa2}\cos\left(2\gamma - \pi\right) \\ -L_{ab0} - L_{aa2}\cos\left(2\gamma - \frac{\pi}{3}\right) & -L_{ab0} - L_{aa2}\cos\left(2\gamma - \pi\right) & L_{aa0} + L_{aa2}\cos 2\left(\gamma + \frac{2\pi}{3}\right) \end{bmatrix} \tag{2-51}$$

$$\mathbf{L}_{SD\gamma} = \begin{bmatrix} L_{afd}\cos\gamma & L_{a1d}\cos\gamma \\ L_{afd}\cos\left(\gamma - \frac{2\pi}{3}\right) & L_{a1d}\cos\left(\gamma - \frac{2\pi}{3}\right) \\ L_{afd}\cos\left(\gamma + \frac{2\pi}{3}\right) & L_{a1d}\cos\left(\gamma + \frac{2\pi}{3}\right) \end{bmatrix} \tag{2-52}$$

$$\mathbf{L}_{SQ\gamma} = \begin{bmatrix} -L_{a1q}\sin\gamma & -L_{a2q}\sin\gamma \\ -L_{a1q}\sin\left(\gamma - \frac{2\pi}{3}\right) & -L_{a2q}\sin\left(\gamma - \frac{2\pi}{3}\right) \\ -L_{a1q}\sin\left(\gamma + \frac{2\pi}{3}\right) & -L_{a2q}\sin\left(\gamma + \frac{2\pi}{3}\right) \end{bmatrix} \tag{2-53}$$

$$\mathbf{L}_{DD} = \begin{bmatrix} L_{ffd} & L_{f1d} \\ L_{f1d} & L_{11d} \end{bmatrix} \tag{2-54}$$

$$\mathbf{L}_{QQ} = \begin{bmatrix} L_{11q} & L_{12q} \\ L_{12q} & L_{22q} \end{bmatrix} \tag{2-55}$$

All the stator inductances (self and mutual) are time-varying (they depend on the *shaft angle* γ, the angle between the d-axis and the phase a axis), and this largely complicates the machine model.

2.7.2. Park's Transformation

The time-varying inductances model of the synchronous machine can be simplified by means of a variable transformation, the resultant inductance matrices for the transformed variables are constant. This transformation is the *dq0 transformation*, also called *Park's Transformation* in honour of R. H. Park [24]. To derive the transformation, let us first rearrange the equations of the flux linkages of the rotor in scalar form as:

$$\psi_{fd} = -L_{afd}\left[i_a\cos\gamma + i_b\cos\left(\gamma - \frac{2\pi}{3}\right) + i_c\cos\left(\gamma + \frac{2\pi}{3}\right)\right] + L_{ffd}i_{fd} + L_{f1d}i_{1d}$$

$$\psi_{1d} = -L_{a1d}\left[i_a\cos\gamma + i_b\cos\left(\gamma - \frac{2\pi}{3}\right) + i_c\cos\left(\gamma + \frac{2\pi}{3}\right)\right] + L_{f1d}i_{fd} + L_{11d}i_{1d}$$

$$\psi_{1q} = -L_{a1q}\left[-i_a \sin\gamma - i_b \sin\left(\gamma - \frac{2\pi}{3}\right) - i_c \sin\left(\gamma + \frac{2\pi}{3}\right)\right] + L_{11q} i_{1q} + L_{12q} i_{2q}$$

$$\psi_{2q} = -L_{a2q}\left[-i_a \sin\gamma - i_b \sin\left(\gamma - \frac{2\pi}{3}\right) - i_c \sin\left(\gamma + \frac{2\pi}{3}\right)\right] + L_{12q} i_{1q} + L_{22q} i_{2q}$$

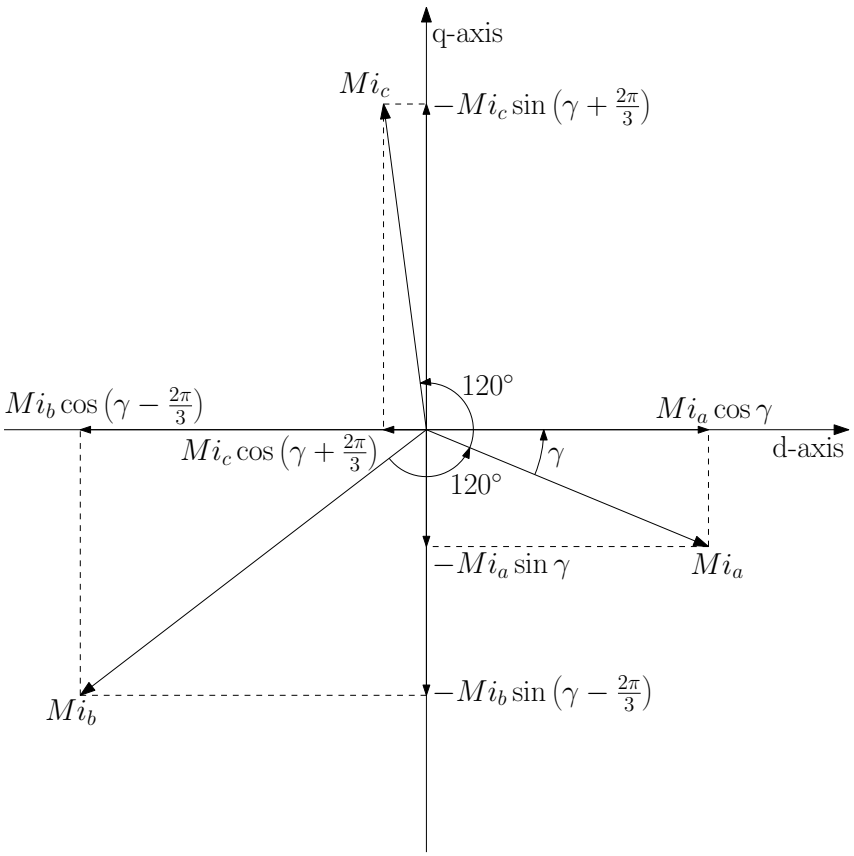

Figure 2-7.: Stator-rotor mutual fluxes projected over the d-axis and q-axis.

The stator flux perceived by the d-axis circuits is proportional to the projection of the fluxes generated by the stator windings over the d-axis, and the analogous is true for the q-axis circuits. Figure **2-7** shows these projections, where M is the mutual inductance whose value is different for each rotor circuit. The stator flux perceived by the d-axis circuits can be thought as being generated by the current of a fictitious winding which rotates at the same speed of the rotor, and is always aligned with the d-axis. Applying an analogous consideration to the stator flux perceived by the q-axis circuits, it is possible to express the currents of the two fictitious windings as:

$$i_d = k_d\left[i_a \cos\gamma + i_b \cos\left(\gamma - \frac{2\pi}{3}\right) + i_c \cos\left(\gamma + \frac{2\pi}{3}\right)\right] \tag{2-56}$$

$$i_q = -k_q\left[i_a \sin\gamma + i_b \sin\left(\gamma - \frac{2\pi}{3}\right) + i_c \sin\left(\gamma + \frac{2\pi}{3}\right)\right] \tag{2-57}$$

Where k_d and k_q are proportionality coefficients whose values can be arbitrarily chosen to simplify the machine equations. The two most common choices are:

- $k_d = k_q = 2/3$. This choice of parameters ensures better physical resemblance of the fictitious windings and currents with respect to the real stator windings [15]. However, this choice makes the inductance matrix asymmetric. It possible to recover the symmetry of the inductance matrix by expressing the equations in p.u. with an adequate selection of stator and rotor base quantities.
- $k_d = k_q = \sqrt{2/3}$. This choice is suggested by some authors [22, 23], as it preserves the symmetry of the inductance matrix, giving freedom to express the machine equations in p.u. using arbitrary base quantities.

In this work the second choice is selected as it leads, in the author's opinion, to a simpler derivation of the models. With $k_d = k_q = \sqrt{2/3}$, the transformation can be expressed in matrix form as:

$$\begin{bmatrix} i_d \\ i_q \end{bmatrix} = \sqrt{\frac{2}{3}} \begin{bmatrix} \cos\gamma & \cos\left(\gamma - \frac{2\pi}{3}\right) & \cos\left(\gamma + \frac{2\pi}{3}\right) \\ -\sin\gamma & -\sin\left(\gamma - \frac{2\pi}{3}\right) & -\sin\left(\gamma + \frac{2\pi}{3}\right) \end{bmatrix} \begin{bmatrix} i_a \\ i_b \\ i_c \end{bmatrix}$$

The transformation matrix is not square, and therefore it is not invertible (it is not possible to uniquely determine the phase currents i_a, i_b and i_c using only the transformed currents i_d and i_q). The transformation can be made invertible by adding a third transformed current. As the currents i_d i_q already account for the total flux produced by the stator windings, the third current must not produce any flux on the rotor. The neutral current satisfies this condition so it is chosen to be the last transformed current:

$$i_0 = k_0 \left(i_a + i_b + i_c\right) \tag{2-58}$$

Where i_0 is the current of a fictitious stationary winding aligned with an axis called *zero axis*, or 0-axis. This axis is called that way because the amount of flux generated by i_0 that is perceived by the rotor windings is zero. Notice also that if the machine is operating in a balanced condition, i_0 will be zero. The term k_0 is a proportionality coefficient whose value can be chosen to simplify the machine equations. In order to keep the symmetry of the inductance matrix, the value of k_0 must be $1/\sqrt{3}$. Now the dq0 transformation is complete, and it can be expressed in matrix form as:

$$\begin{aligned} \vec{i}_{abc} &= \begin{bmatrix} i_a & i_b & i_c \end{bmatrix}^T \\ \vec{i}_{dq0} &= \begin{bmatrix} i_d & i_q & i_0 \end{bmatrix}^T \\ \vec{i}_{dq0} &= \mathbf{P}\vec{i}_{abc} \end{aligned} \tag{2-59}$$

$$\mathbf{P} = \sqrt{\frac{2}{3}} \begin{bmatrix} \cos\gamma & \cos\left(\gamma - \frac{2\pi}{3}\right) & \cos\left(\gamma + \frac{2\pi}{3}\right) \\ -\sin\gamma & -\sin\left(\gamma - \frac{2\pi}{3}\right) & -\sin\left(\gamma + \frac{2\pi}{3}\right) \\ \frac{1}{\sqrt{2}} & \frac{1}{\sqrt{2}} & \frac{1}{\sqrt{2}} \end{bmatrix} \tag{2-60}$$

The inverse dq0 transformation can be defined by solving Equation 2-59 for $\vec{i}_{abc}$:

$$\vec{i}_{abc} = \mathbf{P}^{-1}\vec{i}_{dq0} \tag{2-61}$$

$$\mathbf{P}^{-1} = \sqrt{\frac{2}{3}} \begin{bmatrix} \cos\gamma & -\sin\gamma & \frac{1}{\sqrt{2}} \\ \cos\left(\gamma - \frac{2\pi}{3}\right) & -\sin\left(\gamma - \frac{2\pi}{3}\right) & \frac{1}{\sqrt{2}} \\ \cos\left(\gamma + \frac{2\pi}{3}\right) & -\sin\left(\gamma + \frac{2\pi}{3}\right) & \frac{1}{\sqrt{2}} \end{bmatrix} = \mathbf{P}^T \tag{2-62}$$

The matrix $\mathbf{P}$ is called *orthogonal*, because its inverse its equal to its transpose. Notice that the dq0 transformation and its inverse can be applied to voltages and flux linkages too:

$$\vec{v}_{dq0} = \mathbf{P}\vec{v}_{abc} \tag{2-63}$$

$$\vec{\psi}_{dq0} = \mathbf{P}\vec{\psi}_{abc} \tag{2-64}$$

$$\vec{v}_{abc} = \mathbf{P}^{-1}\vec{v}_{dq0} \tag{2-65}$$

$$\vec{\psi}_{abc} = \mathbf{P}^{-1}\vec{\psi}_{dq0} \tag{2-66}$$

Equation 2-50 can be expressed in terms of the dq0 variables as:

$$\begin{bmatrix} \mathbf{P}^{-1}\vec{\psi}_{dq0} \\ \vec{\psi}_{f1d} \\ \vec{\psi}_{12q} \end{bmatrix} = \begin{bmatrix} -\mathbf{L}_{SS\gamma} & \mathbf{L}_{SD\gamma} & \mathbf{L}_{SQ\gamma} \\ -\mathbf{L}_{SD\gamma}^T & \mathbf{L}_{DD} & \mathbf{0} \\ -\mathbf{L}_{SQ\gamma}^T & \mathbf{0} & \mathbf{L}_{QQ} \end{bmatrix} \begin{bmatrix} \mathbf{P}^{-1}\vec{i}_{dq0} \\ \vec{i}_{f1d} \\ \vec{i}_{12q} \end{bmatrix}$$

$$\begin{bmatrix} \vec{\psi}_{dq0} \\ \vec{\psi}_{f1d} \\ \vec{\psi}_{12q} \end{bmatrix} = \begin{bmatrix} -\mathbf{P}L_{SS\gamma}\mathbf{P}^{-1} & \mathbf{P}L_{SD\gamma} & \mathbf{P}L_{SQ\gamma} \\ -\mathbf{L}_{SD\gamma}^T\mathbf{P}^{-1} & \mathbf{L}_{DD} & \mathbf{0} \\ -\mathbf{L}_{SQ\gamma}^T\mathbf{P}^{-1} & \mathbf{0} & \mathbf{L}_{QQ} \end{bmatrix} \begin{bmatrix} \vec{i}_{dq0} \\ \vec{i}_{f1d} \\ \vec{i}_{12q} \end{bmatrix}$$

$$\begin{bmatrix} \vec{\psi}_{dq0} \\ \vec{\psi}_{f1d} \\ \vec{\psi}_{12q} \end{bmatrix} = \begin{bmatrix} -\mathbf{P}L_{SS\gamma}\mathbf{P}^{-1} & \mathbf{P}L_{SD\gamma} & \mathbf{P}L_{SQ\gamma} \\ -\left(\mathbf{P}L_{SD\gamma}\right)^T & \mathbf{L}_{DD} & \mathbf{0} \\ -\left(\mathbf{P}L_{SQ\gamma}\right)^T & \mathbf{0} & \mathbf{L}_{QQ} \end{bmatrix} \begin{bmatrix} \vec{i}_{dq0} \\ \vec{i}_{f1d} \\ \vec{i}_{12q} \end{bmatrix}$$

$$\begin{bmatrix} \vec{\psi}_{dq0} \\ \vec{\psi}_{f1d} \\ \vec{\psi}_{12q} \end{bmatrix} = \begin{bmatrix} -\mathbf{L}_{SS} & \mathbf{L}_{SD} & \mathbf{L}_{SQ} \\ -\mathbf{L}_{SD}^T & \mathbf{L}_{DD} & \mathbf{0} \\ -\mathbf{L}_{SQ}^T & \mathbf{0} & \mathbf{L}_{QQ} \end{bmatrix} \begin{bmatrix} \vec{i}_{dq0} \\ \vec{i}_{f1d} \\ \vec{i}_{12q} \end{bmatrix} \tag{2-67}$$

Let us define three new inductances:

$$L_d = L_{aa0} + L_{ab0} + \frac{3}{2}L_{aa2} \tag{2-68}$$

$$L_q = L_{aa0} + L_{ab0} - \frac{3}{2}L_{aa2} \tag{2-69}$$

$$L_0 = L_{aa0} - 2L_{ab0} \tag{2-70}$$

Then the new inductance submatrices of Equation 2-67 can be expressed as [22]:

$$\mathbf{L}_{SS} = \mathbf{P}L_{SS\gamma}\mathbf{P}^{-1} = \begin{bmatrix} L_d & 0 & 0 \\ 0 & L_q & 0 \\ 0 & 0 & L_0 \end{bmatrix} \tag{2-71}$$

$$\mathbf{L}_{SD} = \mathbf{P}L_{SD\gamma} = \begin{bmatrix} \sqrt{\frac{3}{2}}L_{afd} & \sqrt{\frac{3}{2}}L_{a1d} \\ 0 & 0 \\ 0 & 0 \end{bmatrix} \tag{2-72}$$

$$\mathbf{L}_{SQ} = \mathbf{P}L_{SQ\gamma} = \begin{bmatrix} 0 & 0 \\ \sqrt{\frac{3}{2}}L_{a1q} & \sqrt{\frac{3}{2}}L_{a2q} \\ 0 & 0 \end{bmatrix} \tag{2-73}$$

The inductance matrix for the dq0 variables is constant and symmetric. Furthermore, the variables of the d-axis circuits, q-axis circuits and 0-axis circuits are decoupled from each other, so it is possible to rearrange Equation 2-67 as:

$$\vec{\psi}_D = \begin{bmatrix} \psi_d & \psi_{fd} & \psi_{1d} \end{bmatrix}^T \tag{2-74}$$

$$\vec{\psi}_Q = \begin{bmatrix} \psi_q & \psi_{1q} & \psi_{2q} \end{bmatrix}^T \tag{2-75}$$

$$\begin{bmatrix} \vec{\psi}_D \\ \vec{\psi}_Q \\ \psi_0 \end{bmatrix} = \begin{bmatrix} \mathbf{L}_D & \mathbf{0} & \mathbf{0} \\ \mathbf{0} & \mathbf{L}_Q & \mathbf{0} \\ \mathbf{0} & \mathbf{0} & -L_0 \end{bmatrix} \begin{bmatrix} \vec{i}_D \\ \vec{i}_Q \\ i_0 \end{bmatrix} \tag{2-76}$$

Where:

$$\mathbf{L}_D = \begin{bmatrix} -L_d & \sqrt{\frac{3}{2}}L_{afd} & \sqrt{\frac{3}{2}}L_{a1d} \\ -\sqrt{\frac{3}{2}}L_{afd} & L_{ffd} & L_{f1d} \\ -\sqrt{\frac{3}{2}}L_{a1d} & L_{f1d} & L_{11d} \end{bmatrix} \tag{2-77}$$

$$\mathbf{L}_Q = \begin{bmatrix} -L_q & \sqrt{\frac{3}{2}}L_{a1q} & \sqrt{\frac{3}{2}}L_{a2q} \\ -\sqrt{\frac{3}{2}}L_{a1q} & L_{11q} & L_{12q} \\ -\sqrt{\frac{3}{2}}L_{a2q} & L_{12q} & L_{22q} \end{bmatrix} \tag{2-78}$$

In order to complete the machine model in dq0 variables, it is necessary to rewrite Equation 2-49. First, Let us define the extended transformation matrix:

$$\mathbf{T} = \begin{bmatrix} \mathbf{P} & \mathbf{0} & \mathbf{0} \\ \mathbf{0} & \mathbf{U}_2 & \mathbf{0} \\ \mathbf{0} & \mathbf{0} & \mathbf{U}_2 \end{bmatrix} \tag{2-79}$$

Where $\mathbf{U}_2$ is a identity matrix of size 2×2. Multiplying both sides of Equation 2-49 by $\mathbf{T}$ yields:

$$\begin{aligned}
\mathbf{T}\begin{bmatrix} \vec{v}_{abc} \\ \vec{v}_{f1d} \\ \vec{0} \end{bmatrix} &= \mathbf{T}\left(\begin{bmatrix} -R_a\mathbf{U} & \mathbf{0} & \mathbf{0} \\ \mathbf{0} & \mathbf{R}_{f1d} & \mathbf{0} \\ \mathbf{0} & \mathbf{0} & \mathbf{R}_{12q} \end{bmatrix}\begin{bmatrix} \vec{i}_{abc} \\ \vec{i}_{f1d} \\ \vec{i}_{12q} \end{bmatrix} + \frac{d}{dt}\left(\begin{bmatrix} \vec{\psi}_{abc} \\ \vec{\psi}_{f1d} \\ \vec{\psi}_{12q} \end{bmatrix}\right) + \begin{bmatrix} \vec{1}v_n \\ \vec{0} \\ \vec{0} \end{bmatrix}\right) \\
\begin{bmatrix} \vec{v}_{dq0} \\ \vec{v}_{f1d} \\ \vec{0} \end{bmatrix} &= \begin{bmatrix} -R_a\mathbf{P} & \mathbf{0} & \mathbf{0} \\ \mathbf{0} & \mathbf{R}_{f1d} & \mathbf{0} \\ \mathbf{0} & \mathbf{0} & \mathbf{R}_{12q} \end{bmatrix}\begin{bmatrix} \vec{i}_{abc} \\ \vec{i}_{f1d} \\ \vec{i}_{12q} \end{bmatrix} + \mathbf{T}\begin{bmatrix} \frac{d\vec{\psi}_{abc}}{dt} \\ \frac{d\vec{\psi}_{f1d}}{dt} \\ \frac{d\vec{\psi}_{f2q}}{dt} \end{bmatrix} + \begin{bmatrix} \mathbf{P}\vec{1}v_n \\ \vec{0} \\ \vec{0} \end{bmatrix} \\
\begin{bmatrix} \vec{v}_{dq0} \\ \vec{v}_{f1d} \\ \vec{0} \end{bmatrix} &= \begin{bmatrix} -R_a\mathbf{P} & \mathbf{0} & \mathbf{0} \\ \mathbf{0} & \mathbf{R}_{f1d} & \mathbf{0} \\ \mathbf{0} & \mathbf{0} & \mathbf{R}_{12q} \end{bmatrix}\begin{bmatrix} \mathbf{P}^{-1}\vec{i}_{dq0} \\ \vec{i}_{f1d} \\ \vec{i}_{12q} \end{bmatrix} + \begin{bmatrix} \mathbf{P}\frac{d\vec{\psi}_{abc}}{dt} \\ \frac{d\vec{\psi}_{f1d}}{dt} \\ \frac{d\vec{\psi}_{f2q}}{dt} \end{bmatrix} + \begin{bmatrix} \mathbf{P}\vec{1}v_n \\ \vec{0} \\ \vec{0} \end{bmatrix} \\
\begin{bmatrix} \vec{v}_{dq0} \\ \vec{v}_{f1d} \\ \vec{0} \end{bmatrix} &= \begin{bmatrix} -R_a\mathbf{U} & \mathbf{0} & \mathbf{0} \\ \mathbf{0} & \mathbf{R}_{f1d} & \mathbf{0} \\ \mathbf{0} & \mathbf{0} & \mathbf{R}_{12q} \end{bmatrix}\begin{bmatrix} \vec{i}_{dq0} \\ \vec{i}_{f1d} \\ \vec{i}_{12q} \end{bmatrix} + \begin{bmatrix} \mathbf{P}\frac{d}{dt}\left(\mathbf{P}^{-1}\vec{\psi}_{dq0}\right) \\ \frac{d\vec{\psi}_{f1d}}{dt} \\ \frac{d\vec{\psi}_{f2q}}{dt} \end{bmatrix} + \begin{bmatrix} \mathbf{P}\vec{1}v_n \\ \vec{0} \\ \vec{0} \end{bmatrix}
\end{aligned} \tag{2-80}$$

There are two terms that require detailed examination. The first one is the neutral voltage, which can be expressed according to Figure **2-6** as:

$$v_n = -R_n i_n + \frac{d\psi_n}{dt}$$

It can be safely assumed that the neutral circuit is not coupled to the rest of the machine circuits, therefore:

$$\psi_n = -L_n i_n$$

Where L_n is constant. Replacing in the neutral voltage equation:

$$v_n = -R_n i_n - L_n \frac{di_n}{dt}$$

The neutral current is the sum of the stator currents, then:

$$v_n = -R_n\left(i_a + i_b + i_c\right) - L_n\frac{d}{dt}\left(i_a + i_b + i_c\right)$$
$$v_n = -\sqrt{3}R_n i_0 - \sqrt{3}L_n\frac{di_0}{dt}$$

Hence:

$$\mathbf{P}\vec{1}v_n = \begin{bmatrix} 0 \\ 0 \\ \sqrt{3} \end{bmatrix} v_n$$

$$\vec{v}_{n0} = \mathbf{P}\vec{1}v_n = \begin{bmatrix} 0 \\ 0 \\ -3R_n i_0 - 3L_n\frac{di_0}{dt} \end{bmatrix} \tag{2-81}$$

The second term requiring detailed examination is the derivative of the stator flux linkages in dq0 variables:

$$\mathbf{P}\frac{d}{dt}\left(\mathbf{P}^{-1}\vec{\psi}_{dq0}\right) = \mathbf{P}\frac{d}{dt}\left(\mathbf{P}^{-1}\right)\vec{\psi}_{dq0} + \mathbf{P}\mathbf{P}^{-1}\frac{d}{dt}\left(\vec{\psi}_{dq0}\right)$$
$$\mathbf{P}\frac{d}{dt}\left(\mathbf{P}^{-1}\vec{\psi}_{dq0}\right) = \mathbf{P}\frac{d}{dt}\left(\mathbf{P}^{-1}\right)\vec{\psi}_{dq0} + \frac{d}{dt}\left(\vec{\psi}_{dq0}\right)$$

After calculating the term $\mathbf{P}\frac{d}{dt}\left(\mathbf{P}^{-1}\right)$, the result is:

$$\mathbf{P}\frac{d}{dt}\left(\mathbf{P}^{-1}\right) = \begin{bmatrix} 0 & -\frac{d\gamma}{dt} & 0 \\ \frac{d\gamma}{dt} & 0 & 0 \\ 0 & 0 & 0 \end{bmatrix} = \begin{bmatrix} 0 & -\omega & 0 \\ \omega & 0 & 0 \\ 0 & 0 & 0 \end{bmatrix}$$

Where ω is the rotor speed, and it is equal to the time derivative of γ. Now, let us define the vector of *speed voltages* as:

$$\vec{v}_\omega = \mathbf{P}\frac{d}{dt}\left(\mathbf{P}^{-1}\right)\vec{\psi}_{dq0} = \begin{bmatrix} -\omega\psi_q \\ \omega\psi_d \\ 0 \end{bmatrix} \tag{2-82}$$

Therefore:

$$\mathbf{P}\frac{d}{dt}\left(\mathbf{P}^{-1}\vec{\psi}_{dq0}\right) = \frac{d\vec{\psi}_{dq0}}{dt} + \vec{v}_\omega \tag{2-83}$$

The term accompanying the vector of speed voltages in Equation 2-82 is a vector of *transformer voltages*, which represent the induced voltages due to time variation of the flux linkages.

On the other hand, the speed voltages represent the induced voltages due to the spatial variation of the flux linkages. Replacing Equations 2-81 and 2-82 in Equation 2-80 yields the final voltage equations:

$$\begin{bmatrix} \vec{v}_{dq0} \\ \vec{v}_{f1d} \\ \vec{0} \end{bmatrix} = \begin{bmatrix} -R_a\mathbf{U} & \mathbf{0} & \mathbf{0} \\ \mathbf{0} & \mathbf{R}_{f1d} & \mathbf{0} \\ \mathbf{0} & \mathbf{0} & \mathbf{R}_{12q} \end{bmatrix} \begin{bmatrix} \vec{i}_{dq0} \\ \vec{i}_{f1d} \\ \vec{i}_{12q} \end{bmatrix} + \begin{bmatrix} \frac{d\vec{\psi}_{dq0}}{dt} \\ \frac{d\vec{\psi}_{f1d}}{dt} \\ \frac{d\vec{\psi}_{12q}}{dt} \end{bmatrix} + \begin{bmatrix} \vec{v}_{\omega} \\ \vec{0} \\ \vec{0} \end{bmatrix} + \begin{bmatrix} \vec{v}_{n0} \\ \vec{0} \\ \vec{0} \end{bmatrix} \tag{2-84}$$

The complete model of the synchronous machines in dq0 variables is given by Equations 2-76, 2-81, 2-82 and 2-84. The equations of the machine model can be solved for the derivative terms in scalar form as follows:

$$\frac{d\psi_d}{dt} = v_d + R_a i_d + \omega\psi_q \tag{2-85}$$

$$\frac{d\psi_q}{dt} = v_q + R_a i_q - \omega\psi_d \tag{2-86}$$

$$\frac{d\psi_0}{dt} = -v_0 - (R_a + 3R_n)\, i_0 - 3L_n \frac{di_0}{dt} \tag{2-87}$$

$$\frac{d\psi_{fd}}{dt} = v_{fd} - R_{fd} i_{fd} \tag{2-88}$$

$$\frac{d\psi_{1d}}{dt} = -R_{1d} i_{1d} \tag{2-89}$$

$$\frac{d\psi_{1q}}{dt} = -R_{1q} i_{1q} \tag{2-90}$$

$$\frac{d\psi_{2q}}{dt} = -R_{2q} i_{2q} \tag{2-91}$$

$$\psi_d = -L_d i_d + \sqrt{\frac{3}{2}} L_{afd} i_{fd} + \sqrt{\frac{3}{2}} L_{a1d} i_{1d} \tag{2-92}$$

$$\psi_{fd} = -\sqrt{\frac{3}{2}} L_{afd} i_d + L_{ffd} i_{fd} + L_{f1d} i_{1d} \tag{2-93}$$

$$\psi_{1d} = -\sqrt{\frac{3}{2}} L_{a1d} i_d + L_{f1d} i_{fd} + L_{11d} i_{1d} \tag{2-94}$$

$$\psi_q = -L_q i_q + \sqrt{\frac{3}{2}} L_{a1q} i_{1q} + \sqrt{\frac{3}{2}} L_{a2q} i_{2q} \tag{2-95}$$

$$\psi_{1q} = -\sqrt{\frac{3}{2}} L_{a1q} i_q + L_{11q} i_{1q} + L_{12q} i_{2q} \tag{2-96}$$

$$\psi_{2q} = -\sqrt{\frac{3}{2}} L_{a2q} i_q + L_{12q} i_{1q} + L_{22q} i_{2q} \tag{2-97}$$

$$\psi_0 = -L_0 i_0 \tag{2-98}$$

The equations conform a set of Differential Algebraic Equations (DAEs) with seven differential variables (the flux linkages) and seven algebraic variables (the circuit currents).

2.7.3. Simplifications of the Complete Model

The complete model of the synchronous machine developed in the previous subsection describes the most significant electromagnetic phenomena of the machine, leading to a model whose complexity prohibits its use in large power systems with dozens or even hundreds of machines. In order to develop a suitable model for stability studies and simplify the interfacing of the machine model with the power system model, the following simplifications are going to be made:

- The machine will be assumed to be operating in a balanced condition.
- The transformer voltages ($\frac{d\psi_d}{dt}$ and $\frac{d\psi_q}{dt}$) will be neglected.
- The rotor speed variations will be neglected (ω will be set to 1 p.u. in the equations).
- Rotor saliency will be neglected (the rotor will be assumed to be perfectly round and symmetric).

The first simplification implies the 0-axis voltages and currents are zero, so it is not necessary to consider the 0-axis equations.

Electromagnetic transients have time constants much lower than that of the electromechanical transients, so considering electromagnetic transients in stability studies would increase the *stiffness*[3] of the system and require lower time steps in the simulation of the system response, thus increasing the computational effort required [15]. The second simplification neglects the electromagnetic transients in the stator windings, avoiding the aforementioned undesired effects and making the stator equations purely algebraic. In addition, the stator quantities will be conformed only of fundamental frequency components, allowing the use of phasor representation, which will be developed further ahead in another subsection.

The third simplification counterbalances the error introduced by the second supposition in low frequency oscillations [15], and it will allow to write the model equations in terms of constant reactances. This will be done in the next subsection. Notice that neglecting speed variations is not the same as assuming constant speed. During transient events the rotor speed variations, though small, still need to be calculated.

The last simplification implies the the geometric distribution of the machine as seen from the d-axis is the same as seen from the q-axis, this in turn implies that the following inductances are equal:

$$L_d = L_q$$

[3]For more information about stiffness and stiff differential equations, see [25].

$$
\begin{aligned}
L_{ffd} &= L_{11q} \\
L_{11d} &= L_{22q} \\
L_{afd} &= L_{a1q} \\
L_{afd} &= L_{a1q} \\
L_{a1d} &= L_{a2q} \\
L_{f1d} &= L_{12q}
\end{aligned}
$$

This simplification introduces minimal errors in round rotor machines, but in salient pole machines the difference between d-axis and q-axis inductances are larger. To reduce the error, the inductances can be approximated as the average of the values of both axes:

$$L_d \approx L_q \approx \frac{L_d + L_q}{2} \tag{2-99}$$

$$L_{ffd} \approx L_{11q} \approx \frac{L_{ffd} + L_{11q}}{2} \tag{2-100}$$

$$L_{11d} \approx L_{22q} \approx \frac{L_{11d} + L_{22q}}{2} \tag{2-101}$$

$$L_{afd} \approx L_{a1q} \approx \frac{L_{afd} + L_{a1q}}{2} \tag{2-102}$$

$$L_{a1d} \approx L_{a2q} \approx \frac{L_{a1d} + L_{a2q}}{2} \tag{2-103}$$

$$L_{f1d} \approx L_{12q} \approx \frac{L_{f1d} + L_{12q}}{2} \tag{2-104}$$

The main advantage introduced by the last simplification is that it allows to represent the stator algebraic equations resulting from the second supposition as a purely linear circuit. This will be demonstrated further ahead in another subsection. Finally, the p.u. equations of the simplified model are:

$$v_d = -R_a i_d - \omega_s \psi_q \tag{2-105}$$

$$v_q = -R_a i_q + \omega_s \psi_d \tag{2-106}$$

$$\frac{d\psi_{fd}}{dt} = v_{fd} - R_{fd} i_{fd} \tag{2-107}$$

$$\frac{d\psi_{1d}}{dt} = -R_{1d} i_{1d} \tag{2-108}$$

$$\frac{d\psi_{1q}}{dt} = -R_{1q} i_{1q} \tag{2-109}$$

$$\frac{d\psi_{2q}}{dt} = -R_{2q} i_{2q} \tag{2-110}$$

$$\psi_d = -L_d i_d + \sqrt{\frac{3}{2}} L_{afd} i_{fd} + \sqrt{\frac{3}{2}} L_{a1d} i_{1d} \tag{2-111}$$

$$\psi_{fd} = -\sqrt{\frac{3}{2}} L_{afd} i_d + L_{ffd} i_{fd} + L_{f1d} i_{1d} \tag{2-112}$$

$$\psi_{1d} = -\sqrt{\frac{3}{2}} L_{a1d} i_d + L_{f1d} i_{fd} + L_{11d} i_{1d} \tag{2-113}$$

$$\psi_q = -L_q i_q + \sqrt{\frac{3}{2}} L_{a1q} i_{1q} + \sqrt{\frac{3}{2}} L_{a2q} i_{2q} \tag{2-114}$$

$$\psi_{1q} = -\sqrt{\frac{3}{2}} L_{a1q} i_q + L_{11q} i_{1q} + L_{12q} i_{2q} \tag{2-115}$$

$$\psi_{2q} = -\sqrt{\frac{3}{2}} L_{a2q} i_q + L_{12q} i_{1q} + L_{22q} i_{2q} \tag{2-116}$$

The equations of the simplified model conform a set of DAEs with four differential variables (the flux linkages of the rotor circuits) and eight algebraic variables (ψ_d, ψ_q and the circuit currents).

2.7.4. Simplified Model in Terms of Measurable Parameters

The flux linkage equations of the simplified model can be eliminated by substituting them in the rest of equations, reducing the size of the model from twelve equations to six (four differential equations and two algebraic equations of the stator). The stator algebraic equations are used to interface the machine model with the power system model, and for that reason they are not eliminated.

Before eliminating the flux linkage equations it is convenient to express the model equations in terms of parameters that can be physically measured from machine tests. First, it will be assumed that the field circuit and circuit *1q* encompass the d-axis and q-axis components of the original damper windings with slow dynamics, respectively[4]. Similarly, it will be assumed that the damper windings *1d* and *2q* encompass the d-axis and q-axis components of the original damper windings with fast dynamics, respectively. Then, let us define the following machine parameters [23]:

- **Steady State Direct-Axis Reactance:**

$$X_d \triangleq \omega L_d \tag{2-117}$$

- **Steady State Quadrature-Axis Reactance:**

$$X_q \triangleq \omega L_q \tag{2-118}$$

[4]The field winding normally has a slow dynamic (its electrical transients decay slowly) and in the machine model it is lumped together with the d-axis components of the damper windings with slow dynamics, forming a single equivalent circuit

- **Transient Direct-Axis Reactance:**

$$X'_d \triangleq \omega \left(L_d - \frac{\frac{3}{2}L_{afd}^2}{L_{fd}} \right) \tag{2-119}$$

- **Transient Quadrature-Axis Reactance:**

$$X'_q \triangleq \omega \left(L_q - \frac{\frac{3}{2}L_{a1q}^2}{L_{1q}} \right) \tag{2-120}$$

- **Subtransient Direct-Axis Reactance:**

$$X''_d \triangleq \omega \left(L_d - \frac{\frac{3}{2}L_{afd}^2 L_{1d} + \frac{3}{2}L_{a1d}^2 L_{fd} - 2\sqrt{\frac{3}{2}}L_{afd}\sqrt{\frac{3}{2}}L_{a1d}L_{f1d}}{L_{1d}L_{fd} - L_{f1d}^2} \right) \tag{2-121}$$

- **Subtransient Quadrature-Axis Reactance:**

$$X''_q \triangleq \omega \left(L_q - \frac{\frac{3}{2}L_{a1q}^2 L_{2q} + \frac{3}{2}L_{a2q}^2 L_{1q} - 2\sqrt{\frac{3}{2}}L_{a1q}\sqrt{\frac{3}{2}}L_{a2q}L_{12q}}{L_{2q}L_{1q} - L_{12q}^2} \right) \tag{2-122}$$

- **Transient Direct-Axis Open Circuit Time Constant:**

$$T'_{d0} \triangleq \frac{L_{fd}}{R_{fd}} \tag{2-123}$$

- **Transient Quadrature-Axis Open Circuit Time Constant:**

$$T'_{q0} \triangleq \frac{L_{1q}}{R_{1q}} \tag{2-124}$$

- **Subtransient Direct-Axis Open Circuit Time Constant:**

$$T''_{d0} \triangleq \frac{L_{fd}L_{1d} - L_{f1d}^2}{R_{1d}L_{fd}} \tag{2-125}$$

- **Subtransient Quadrature-Axis Open Circuit Time Constant:**

$$T''_{q0} \triangleq \frac{L_{1q}L_{2q} - L_{12q}^2}{R_{2q}L_{1q}} \tag{2-126}$$

Notice that the previously defined reactances are constant because speed variations are being neglected, they can be easily calculated by replacing ω with ω_s in therir definitions. These parameters can be measured from various standard machine tests [15]. It is convenient to rewrite the model equations in terms of variables that simplify such equations instead of keeping the flux linkages. Therefore, new convenient variables are defined [23]:

- **Transient Direct-Axis Electromotive Force:**

$$e'_d \triangleq -\omega_s \frac{\sqrt{\frac{3}{2}} L_{a1q}}{L_{1q}} \psi_{1q} \tag{2-127}$$

- **Transient Quadrature-Axis Electromotive Force:**

$$e'_q \triangleq \omega_s \frac{\sqrt{\frac{3}{2}} L_{afd}}{L_{fd}} \psi_{fd} \tag{2-128}$$

- **Subtransient Direct-Axis Electromotive Force:**

$$e''_d \triangleq -\omega_s \left(\frac{\sqrt{\frac{3}{2}} L_{a1q} L_{2q} - \sqrt{\frac{3}{2}} L_{a2q} L_{12q}}{L_{1q} L_{2q} - L_{12q}^2} \psi_{1q} + \frac{\sqrt{\frac{3}{2}} L_{a2q} L_{1q} - \sqrt{\frac{3}{2}} L_{a1q} L_{12q}}{L_{1q} L_{2q} - L_{12q}^2} \psi_{2q} \right) \tag{2-129}$$

- **Subtransient Quadrature-Axis Electromotive Force:**

$$e''_q \triangleq \omega_s \left(\frac{\sqrt{\frac{3}{2}} L_{afd} L_{1d} - \sqrt{\frac{3}{2}} L_{a1d} L_{f1d}}{L_{fd} L_{1d} - L_{f1d}^2} \psi_{fd} + \frac{\sqrt{\frac{3}{2}} L_{a1d} L_{fd} - \sqrt{\frac{3}{2}} L_{afd} L_{f1d}}{L_{fd} L_{1d} - L_{f1d}^2} \psi_{1d} \right) \tag{2-130}$$

- **Field Voltage Referred to Stator:**

$$e_{fd} \triangleq \omega_s \frac{\sqrt{\frac{3}{2}} L_{afd}}{R_{fd}} v_{fd} \tag{2-131}$$

Substituting Equations 2-117 to 2-131 into Equations 2-105 to 2-116 gives the model equations in terms of measurable parameters:

$$v_d = -R_a i_d + X''_q i_q + e''_d \tag{2-132}$$

$$v_q = -R_a i_q - X''_d i_d + e''_q \tag{2-133}$$

$$T'_{q0} \frac{de'_d}{dt} = -e'_d + \left(X_q - X'_q \right) i_q \tag{2-134}$$

$$T'_{d0} \frac{de'_q}{dt} = e_{fd} - e'_q - \left(X_d - X'_d \right) i_d \tag{2-135}$$

$$T''_{q0} \frac{de''_d}{dt} = e'_d - e''_d + \left(X'_q - X''_q \right) i_q \tag{2-136}$$

$$T''_{d0} \frac{de''_q}{dt} = e'_q - e''_q - \left(X'_d - X''_d \right) i_d \tag{2-137}$$

This model is called *Subtransient Dynamic Model* [4], and its equations conform a set of DAEs with four differential variables (the transient and subtransient EMFs) and two algebraic variables (the d-axis and q-axis terminal voltages).

2.7.5. Model Equations in Phasor Form

As discussed previously, by neglecting the stator transients the voltages will be composed only of fundamental frequency components. Therefore, the phase voltages may be written as:

$$\vec{v}_{abc} = \begin{bmatrix} v_a \\ v_b \\ v_c \end{bmatrix} = \begin{bmatrix} \sqrt{2}V_t \cos(\omega_s t + \delta_0) \\ \sqrt{2}V_t \cos\left(\omega_s t + \delta_0 - \frac{2\pi}{3}\right) \\ \sqrt{2}V_t \cos\left(\omega_s t + \delta_0 + \frac{2\pi}{3}\right) \end{bmatrix} \tag{2-138}$$

The magnitude and angle of the phase voltages may change with respect to time due to transient events, but their mathematical form remains unchanged. The electrical angular speed is equal to the synchronous speed ω_s because the machine is assumed to have two poles. For machines with more than two poles the angular speeds are different but the same results that are going to be derived here can be achieved. From Equation 2-138 it is clear that the terminal voltage phasor is:

$$\tilde{V}_t = V_t e^{j\delta_0} = V_t \angle \delta_0 \tag{2-139}$$

The phasor uses the angle of phase a because that phase is the one used in single-phase equivalent circuits. The phase voltages transformed to dq0 variables are:

$$\vec{v}_{dq0} = \begin{bmatrix} v_d \\ v_q \\ v_0 \end{bmatrix} = \begin{bmatrix} \sqrt{3}V_t \cos(\omega_s t + \delta_0 - \gamma) \\ \sqrt{3}V_t \sin(\omega_s t + \delta_0 - \gamma) \\ 0 \end{bmatrix} \tag{2-140}$$

Notice that at steady state both terms, $\omega_s t$ and γ change at the same rate and their difference is a constant. Therefore it is convenient to express γ in terms of an angle that at steady state must be constant. Then the *rotor angle* is defined as:

$$\theta \triangleq \gamma - \omega_s t + \frac{\pi}{2} \tag{2-141}$$

The term $\pi/2$ in the definition of the rotor angle represents a 90° phase shift. The term is added for convenience as it will be seen in a latter subsection. Expressing the dq0 voltages in terms of θ gives:

$$\vec{v}_{dq0} = \begin{bmatrix} v_d \\ v_q \\ v_0 \end{bmatrix} = \begin{bmatrix} \sqrt{3}V_t \cos\left(\delta_0 + \frac{\pi}{2} - \theta\right) \\ \sqrt{3}V_t \sin\left(\delta_0 + \frac{\pi}{2} - \theta\right) \\ 0 \end{bmatrix} \tag{2-142}$$

The voltages v_d and v_q can be expressed in complex form as:

$$v_d + jv_q = \sqrt{3}V_t \angle \left(\delta_0 + \frac{\pi}{2} - \theta\right) \tag{2-143}$$

$$v_d + jv_q = \sqrt{3}\tilde{V}_{dq} \tag{2-144}$$

Where $\tilde{V}_{dq}$ is the *terminal voltage phasor in dq0 variables*, and is defined as:

$$\tilde{V}_{dq} = V_d + jV_q = \tilde{V}_t \left[1\angle\left(\frac{\pi}{2} - \theta\right)\right] \tag{2-145}$$

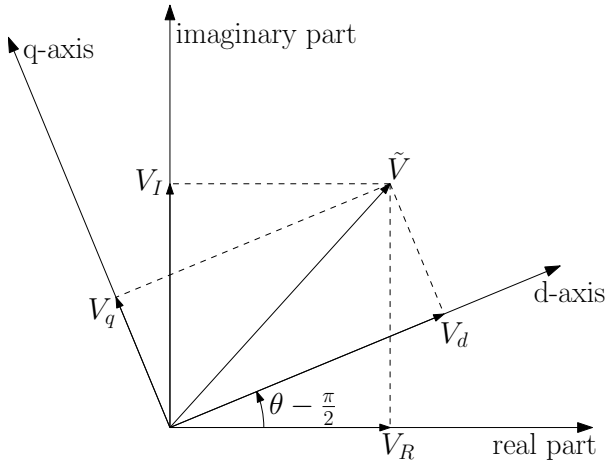

Figure 2-8.: Voltage phasor components in network and generator reference frame.

Equation 2-145 defines the *Park's transformation for phasors*, and it can be extended to other phasor quantities like currents. The real part of the dq0 phasor is proportional to the d-axis component of that variable and the imaginary part is proportional to the q-axis component. It must be noted that the transformation just applies a rotation of angle $\pi/2 - \theta$ to the original phasor, as it can be seen in Figure **2-8**. For that reason, the angle reference of the original (phase) phasors is the *network reference*, whereas the angle reference of the dq0 phasors is the *generator reference*. It also must be noted that, as the rotor angles of different machines are not necessarily equal, the angle reference of the dq0 phasors is different for each machine.

The network phasor can be easily recovered from the dq0 phasor using the *inverse Park's transformation for phasors*:

$$\tilde{V}_t = \tilde{V}_{dq} \left[1\angle\left(\theta - \frac{\pi}{2}\right)\right] \tag{2-146}$$

Equation 2-146 also applies to other phasor quantities like currents.

Finally, d-axis and q-axis components of the dq0 phasor can be expressed in terms of the d-axis and q-axis voltages as:

$$V_d = \frac{1}{\sqrt{3}} v_d \tag{2-147}$$

$$V_q = \frac{1}{\sqrt{3}} v_q \tag{2-148}$$

The other model variables can be expressed in phasor form in an analogous way:

$$\tilde{I}_{dq} = I_d + jI_q = \frac{1}{\sqrt{3}}\left(i_d + ji_q\right) \tag{2-149}$$

$$\tilde{E}'_{dq} = E'_d + jE'_q = \frac{1}{\sqrt{3}}\left(e'_d + je'_q\right) \tag{2-150}$$

$$\tilde{E}''_{dq} = E''_d + jE''_q = \frac{1}{\sqrt{3}}\left(e''_d + je''_q\right) \tag{2-151}$$

$$\tilde{E}_{fd} = 0 + jE_{fd} = \frac{1}{\sqrt{3}}\left(0 + je_{fd}\right) \tag{2-152}$$

The d-axis and q-axis components of the previously defined phasors are:

$$I_d = \frac{1}{\sqrt{3}} i_d \tag{2-153}$$

$$I_q = \frac{1}{\sqrt{3}} i_q \tag{2-154}$$

$$E'_d = \frac{1}{\sqrt{3}} e'_d \tag{2-155}$$

$$E'_q = \frac{1}{\sqrt{3}} e'_q \tag{2-156}$$

$$E''_d = \frac{1}{\sqrt{3}} e''_d \tag{2-157}$$

$$E''_q = \frac{1}{\sqrt{3}} e''_q \tag{2-158}$$

$$E_{fd} = \frac{1}{\sqrt{3}} e_{fd} \tag{2-159}$$

The model equations expressed in terms of the phasor quantities are:

$$V_d = -R_a I_d + X''_q I_q + E''_d \tag{2-160}$$

$$V_q = -R_a I_q - X''_d I_d + E''_q \tag{2-161}$$

$$T'_{q0}\frac{dE'_d}{dt} = -E'_d + \left(X_q - X'_q\right) I_q \tag{2-162}$$

$$T'_{d0}\frac{dE'_q}{dt} = E_{fd} - E'_q - \left(X_d - X'_d\right) I_d \tag{2-163}$$

$$T''_{q0}\frac{dE''_d}{dt} = E'_d - E''_d + \left(X'_q - X''_q\right) I_q \tag{2-164}$$

$$T''_{d0}\frac{dE''_q}{dt} = E'_q - E''_q - \left(X'_d - X''_d\right) I_d \tag{2-165}$$

With the model equations in phasor form, it is possible to interface them with the power system equations in phasor form.

2.7.6. Model Equations in p.u.

As discussed in previous sections, it is common practice to express electrical equations and quantities in p.u. with reference to certain base quantities. It is possible to choose different p.u. base quantities for each generator circuit, in the same way the windings of a transformer have different p.u. base quantities. In Subsection 2.7.4, the process of substituting the rotor flux linkages by the defined EMFs is equivalent to *referring* the rotor variables to the stator, in the same way the impedance of the primary winding of a transformer is referred to the secondary winding (Section 2.4). Therefore, only base quantities of the stator windings need to be considered [23]. In the special case that a rotor variable is desired, the referred quantity along with Equations 2-127 to 2-131 can be used to obtain the original rotor quantity . If the rotor circuit associated to that quantity has a different p.u. base than that of the stator circuit, the base of the referred quantity must be changed to that of the rotor circuit.

This work assumes that any arbitrary p.u. base may be used for the machine circuits, with the sole restriction that the base time must be 1s. Hence, the terms of the model equations can be expressed in p.u. without changing the equations in any way. Care must be taken that the variable t and the time constants will still keep units of time.

2.7.7. Two-Axis Model

The subtransient time constants are normally small compared to the time constant of the electromechanical transients, so the dynamics of the subtransient damper windings tend to be much faster than the electromechanical dynamics. Therefore, it is possible to neglect the subtransient dynamics in the same way the stator electromagnetic transients are neglected. The machine model with subtransients dynamics can be obtained by setting T''_{d0} and T''_{q0} to zero[5]:

$$
\begin{aligned}
V_d &= -R_a I_d + X''_q I_q + E''_d \\
V_q &= -R_a I_q - X''_d I_d + E''_q \\
T'_{q0}\frac{dE'_d}{dt} &= -E'_d + \left(X_q - X'_q\right) I_q \\
T'_{d0}\frac{dE'_q}{dt} &= E_{fd} - E'_q - \left(X_d - X'_d\right) I_d \\
0 &= E'_d - E''_d + \left(X'_q - X''_q\right) I_q \\
0 &= E'_q - E''_q - \left(X'_d - X''_d\right) I_d
\end{aligned}
$$

[5]Setting the subtransient time constants to zero is equivalent to assume the subtransient EMFs react instantaneously fast to perturbations, becoming algebraic variables

The subtransient EMFs can be eliminated from the model using substitution, obtaining the following reduced model:

$$V_d = -R_a I_d + X'_q I_q + E'_d \tag{2-166}$$

$$V_q = -R_a I_q - X'_d I_d + E'_q \tag{2-167}$$

$$T'_{q0}\frac{dE'_d}{dt} = -E'_d + \left(X_q - X'_q\right) I_q \tag{2-168}$$

$$T'_{d0}\frac{dE'_q}{dt} = E_{fd} - E'_q - \left(X_d - X'_d\right) I_d \tag{2-169}$$

This reduced model is called *Two-Axis Model* [4], and is a standard choice for transient stability analysis. It must be noted that the algebraic equations for V_d and V_q can be expressed phasor form as:

$$\tilde{V}_{dq} = -\left(R_a + jX'_d\right)\tilde{I}_{dq} + \tilde{E}'_{dq} + \left(X'_q - X'_d\right)\mathfrak{Im}\left\{\tilde{I}_{dq}\right\} \tag{2-170}$$

which is a nonlinear circuit equation because of the last term. However, as the machine saliency is being neglected, X'_q and X'_d are equal, and the equation becomes:

$$\tilde{V}_{dq} = -\left(R_a + jX_d\right)\tilde{I}_{dq} + \tilde{E}'_{dq} \tag{2-171}$$

which is a linear circuit equation. The phasors can be expressed using the network reference, giving:

$$\tilde{V}_t = -\left(R_a + jX_d\right)\tilde{I}_{dq}\left[1\angle\left(\theta - \frac{\pi}{2}\right)\right] + \tilde{E}'_{dq}\left[1\angle\left(\theta - \frac{\pi}{2}\right)\right] \tag{2-172}$$

The equivalent circuit of the generator in network reference is shown in Figure **2-9**.

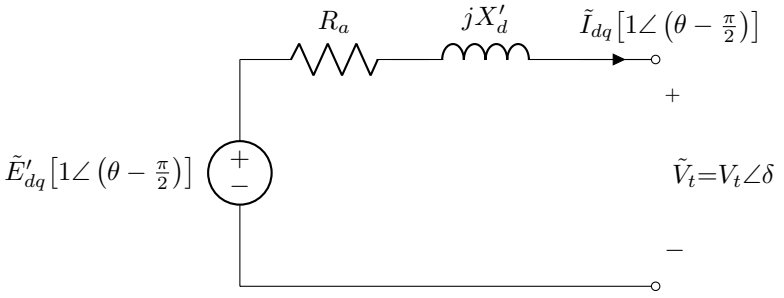

Figure 2-9.: Equivalent circuit of the generator using the Two-Axis Model.

2.7.8. Swing Equation

The Two-Axis Model describes the electrical dynamics of the synchronous machine with sufficient detail for transient stability analysis, but in order to have a complete electromechanical model of the machine, it is necessary to derive another set of equations to describe

the mechanical dynamics of the generator. The first equation of this new set is called the *swing equation*, and is obtained by applying Newton's Second Law to the machine rotor [15]:

$$J\frac{d\omega}{dt} = \tau_M - \tau_e$$

Where τ_M is the mechanical torque moving the rotor (it can be produced a turbine in a thermal plant, or the water flow in a hydraulic plant), τ_e is the induced electromagnetic torque that opposes the rotor movement, and J is the combined inertia moment of the rotor and any other elements coupled to it (a turbine for example). The friction torque is normally very small and is neglected. Notice that all quantities are in physical units. Multiplying by ω_s yields:

$$J\omega_s\frac{d\omega}{dt} = \omega_s\left(\tau_M - \tau_e\right)$$
$$J\omega_s\frac{d\omega}{dt} = \frac{\omega_s}{\omega}\left(\omega\tau_M - \omega\tau_e\right)$$

As speed variations are being neglected, the fraction ω_s/ω can be approximated to 1. Power is equal to the product of angular speed and torque, so the equation can be expressed in terms of powers after neglecting speed variations as:

$$J\omega_s\frac{d\omega}{dt} = P_M - P_e$$

It is customary to express the swing equation in terms of the *inertia constant* H, which is defined as the ratio of the kinetic energy stored in the rotor (including the coupled elements) at synchronous speed to the rated three-phase power of the machine:

$$H = \frac{\frac{1}{2}J\omega_s^2}{S_{rated}} \tag{2-173}$$

Notice that H has units of seconds. The swing equation in terms of H becomes:

$$2H\frac{S_{rated}}{\omega_s}\frac{d\omega}{dt} = P_M - P_e$$

The electrical power of the electromagnetic torque equals the power generated by the stator EMFs:

$$P_e = \frac{d\psi_a}{dt}i_a + \frac{d\psi_b}{dt}i_b + \frac{d\psi_c}{dt}i_c$$

By the Energy Conservation Principle, the power generated by the stator EMFs must be equal to the output power plus the power losses on the stator windings and the neutral circuit:

$$P_e = v_a i_a + v_b i_b + v_c i_c + R_a\left(i_a^2 + i_b^2 + i_c^2\right) + R_n\left(i_a + i_b + i_c\right)^2$$
$$P_e = \vec{v}_{abc}^{T}\vec{i}_{abc} + R_a\vec{i}_{abc}^{T}\vec{i}_{abc} + R_n\left(i_a + i_b + i_c\right)^2$$

The electrical power can be expressed in terms of dq0 variables as:

$$P_e = \vec{v}_{dq0}^T \mathbf{P}^T \mathbf{P} \vec{i}_{dq0} + R_a \vec{i}_{dq0}^T \mathbf{P}^T \mathbf{P} \vec{i}_{dq0} + R_n i_0^2$$
$$P_e = \vec{v}_{dq0}^T \vec{i}_{dq0} + R_a \vec{i}_{dq0}^T \vec{i}_{dq0} + R_n i_0^2$$
$$P_e = v_d i_d + v_q i_q + v_0 i_0 + R_a \left(i_d^2 + i_q^2 + i_0^2\right) + R_n i_0^2$$

As the machine is assumed to be operating in a balanced condition, the zero sequence components vanish:

$$P_e = v_d i_d + v_q i_q + R_a \left(i_d^2 + i_q^2\right)$$

The electrical power in terms of phasor components is:

$$P_e = 3\left[V_d I_d + V_q I_q + R_a \left(I_d^2 + I_q^2\right)\right]$$

If the Two-Axis Model is being used, the electrical power can be expressed in terms of the transient EMFs as:

$$P_e = 3\left[E'_d I_d + E'_q I_q + \left(X'_q - X'_d\right) I_d I_q\right]$$

As the transient saliency is being neglected, X'_d and X'_q are equal:

$$P_e = 3\left(E'_d I_d + E'_q I_q\right)$$

Replacing in the swing equation:

$$2H \frac{S_{rated}}{\omega_s} \frac{d\omega}{dt} = P_M - 3\left(E'_d I_d + E'_q I_q\right)$$
$$2H \frac{d}{dt}\left(\frac{\omega}{\omega_s}\right) = \frac{P_M}{S_{rated}} - \frac{3\left(E'_d I_d + E'_q I_q\right)}{S_{rated}}$$

The rated three-phase power can be expressed in terms of the rated phase voltage and current:

$$S_{rated} = 3 V_{\phi rated} I_{\phi rated}$$

Replacing:

$$2H \frac{d}{dt}\left(\frac{\omega}{\omega_s}\right) = \frac{P_M}{S_{rated}} - \frac{3\left(E'_d I_d + E'_q I_q\right)}{3 V_{\phi rated} I_{\phi rated}}$$
$$2H \frac{d}{dt}\left(\frac{\omega}{\omega_s}\right) = \frac{P_M}{S_{rated}} - \frac{E'_d}{V_{\phi rated}} \frac{I_d}{I_{\phi rated}} - \frac{E'_q}{V_{\phi rated}} \frac{I_q}{I_{\phi rated}}$$

Expressing all quantities in p.u. (except the ones with units of time) using the machine rated quantities as base:

$$2H \frac{d\omega}{dt} = P_M - E'_d I_d - E'_q I_q$$

If the Two-Axis Model is being used, the *asynchronous torque* produced by the subtransient damper windings will be neglected[6] [23]. The effect of the asynchronous torque can be included approximately as a torque proportional to the speed deviation [23, 4]:

$$2H\frac{d\omega}{dt} = P_M - E'_d I_d - E'_q I_q - D\left(\omega - 1\right) \tag{2-174}$$

Where D is in p.u. of power. The speed equation was derived assuming a 2-pole machine, but the equation is exactly equal in p.u. for a p-pole machine, the only difference is the synchronous speed.

In order to interface the electromechanical model of the machine with the model of the power system, the dq0 phasors must be transformed to network phasors, and to do this it is necessary to calculate the variations of the rotor angle with respect to time. This variations are quantified by the derivative of the rotor angle, which can be calculated from the definition of the rotor angle:

$$\frac{d\theta}{dt} = \frac{d\gamma}{dt} - \omega_s$$
$$\frac{d\theta}{dt} = \omega - \omega_s$$

Where ω and ω_s have units of rad/s. The equation can be expressed as:

$$\frac{d\theta}{dt} = \omega_s\left(\omega - 1\right) \tag{2-175}$$

Where ω is now in p.u. and ω_s still has units of rad/s. Notice that θ has units of radians. As the angle variables like θ are dimensionless, there is no need to express them in p.u., they will be always be expressed in radians (or degrees, depending on the context).

The final electromechanical model of the synchronous machine is comprised of the following equations:

$$\frac{d\theta}{dt} = \omega_s\left(\omega - 1\right) \tag{2-176}$$
$$2H\frac{d\omega}{dt} = P_M - E'_d I_d - E'_q I_q - D\left(\omega - 1\right) \tag{2-177}$$
$$T'_{q0}\frac{dE'_d}{dt} = -E'_d + \left(X_q - X'_q\right) I_q \tag{2-178}$$
$$T'_{d0}\frac{dE'_q}{dt} = E_{fd} - E'_q - \left(X_d - X'_d\right) I_d \tag{2-179}$$

[6]Damper windings produce a torque that tries to keep the rotor at synchronous speed, like the electrical torque of an induction machine. One of the main reasons for having damper windings in a synchronous machine is that the torque they produce can start the rotor movement from standstill.

$$V_d = -R_a I_d + X'_q I_q + E'_d \tag{2-180}$$
$$V_q = -R_a I_q - X'_d I_d + E'_q \tag{2-181}$$

These equations conform a set of DAEs with four differential variables and two algebraic variables.

2.7.9. Steady State Characteristics

In steady state, if the machine operating condition is stable[7], the variations with respect to time of the model variables will be zero, which implies the derivatives of the model variables will be zero. It must be noted that it cannot be stated a priori that the derivative of the rotor angle is zero, because the rotor angle is a variable created for convenience, and it has no direct physical meaning (although physical interpretations can be constructed). The machine model in steady state can be simplified as follows:

$$\begin{aligned}
\frac{d\theta_\infty}{dt} &= \omega_s \left(\omega_\infty - 1\right) \\
0 &= P_{M\infty} - E'_{d\infty} I_{d\infty} - E'_{q\infty} I_{q\infty} - D\left(\omega_\infty - 1\right) \\
0 &= -E'_{d\infty} + \left(X_q - X'_q\right) I_{q\infty} \\
0 &= E_{fd\infty} - E'_{q\infty} - \left(X_d - X'_d\right) I_{d\infty} \\
V_{d\infty} &= -R_a I_{d\infty} + X'_q I_{q\infty} + E'_{d\infty} \\
V_{q\infty} &= -R_a I_{q\infty} - X'_d I_{d\infty} + E'_{q\infty}
\end{aligned}$$

The subscript ∞ indicates a steady state quantity. The machine is normally equipped with automatic controllers responsible of keeping the rotor speed equal to the synchronous speed (1 p.u.), so in steady state $\omega_\infty = 1$. Replacing:

$$\frac{d\theta_\infty}{dt} = 0 \tag{2-182}$$
$$0 = P_{M\infty} - E'_{d\infty} I_{d\infty} - E'_{q\infty} I_{q\infty} \tag{2-183}$$
$$0 = -E'_{d\infty} + \left(X_q - X'_q\right) I_{q\infty} \tag{2-184}$$
$$0 = E_{fd\infty} - E'_{q\infty} - \left(X_d - X'_d\right) I_{d\infty} \tag{2-185}$$
$$V_{d\infty} = -R_a I_{d\infty} + X'_q I_{q\infty} + E'_{d\infty} \tag{2-186}$$
$$V_{q\infty} = -R_a I_{q\infty} - X'_d I_{d\infty} + E'_{q\infty} \tag{2-187}$$

As the derivative of the rotor angle in steady state is zero, the value of θ_∞ must be a constant which will be calculated shortly. First, the values of $E'_{d\infty}$ and $E'_{q\infty}$ will be calculated by

[7] Generators are designed to work in stable operating conditions. It can happen in real situations that a generator ends up working in an unstable operating condition after a disturbance, this problem is known as the *voltage stability problem* and it conforms a field of study in itself [15, 23].

expressing the equations of $V_{d\infty}$ and $V_{q\infty}$ in phasor form:

$$\tilde{V}_{dq\infty} = -\left(R_a + jX'_d\right)\tilde{I}_{dq\infty} + \tilde{E}'_{dq\infty} + \left(X'_q - X'_d\right)\mathfrak{Im}\left\{\tilde{I}_{dq\infty}\right\}$$

As transient saliency is being neglected, X'_q and X'_d are equal:

$$\tilde{V}_{dq\infty} = -\left(R_a + jX'_d\right)\tilde{I}_{dq\infty} + \tilde{E}'_{dq\infty}$$

The equation can be expressed in network reference by multiplying both sides by $[1\angle(\theta_\infty - \pi/2)]$:

$$\tilde{V}_{t\infty} = -\left(R_a + jX'_d\right)\tilde{I}_{g\infty} + \tilde{E}'_{dq\infty}\left[1\angle\left(\theta_\infty - \frac{\pi}{2}\right)\right]$$

Where the steady state generator voltage and current are $\tilde{V}_{t\infty}$ and $\tilde{I}_{g\infty}$ respectively. The transient EMFs can be expressed in terms of $\tilde{V}_{t\infty}$ and $\tilde{I}_{g\infty}$ as follows:

$$\begin{aligned}
\tilde{E}'_{dq\infty} &= \left[\tilde{V}_{t\infty} + \left(R_a + jX'_d\right)\tilde{I}_{g\infty}\right]\left[1\angle\left(\frac{\pi}{2} - \theta_\infty\right)\right] \\
E'_{d\infty} &= \mathfrak{Re}\left\{\left[\tilde{V}_{t\infty} + \left(R_a + jX'_d\right)\tilde{I}_{g\infty}\right]\left[1\angle\left(\frac{\pi}{2} - \theta_\infty\right)\right]\right\} \\
E'_{q\infty} &= \mathfrak{Im}\left\{\left[\tilde{V}_{t\infty} + \left(R_a + jX'_d\right)\tilde{I}_{g\infty}\right]\left[1\angle\left(\frac{\pi}{2} - \theta_\infty\right)\right]\right\}
\end{aligned}$$

In order to calculate θ_∞ and $E_{fd\infty}$, let us retake the original equations of $V_{d\infty}$ and $V_{q\infty}$. The transient EMFs can be eliminated from the Equations 2-186 and 2-187 by substitution of Equations 2-184 and 2-185, yielding:

$$\begin{aligned}
V_{d\infty} &= -R_a I_{d\infty} + X_q I_{q\infty} \\
V_{q\infty} &= -R_a I_{q\infty} - X_d I_{d\infty} + E_{fd\infty}
\end{aligned}$$

In phasor form:

$$\tilde{V}_{dq\infty} = -\left(R_a + jX_q\right)\tilde{I}_{dq\infty} + j\left[E_{fd\infty} + \left(X_q - X_d\right)\mathfrak{Re}\left\{\tilde{I}_{dq\infty}\right\}\right]$$

As transient saliency is being neglected, X_q and X_d are equal:

$$\tilde{V}_{dq\infty} = -\left(R_a + jX_q\right)\tilde{I}_{dq\infty} + jE_{fd\infty}$$

In network reference:

$$\begin{aligned}
\tilde{V}_{t\infty} &= -\left(R_a + jX_q\right)\tilde{I}_{g\infty} + jE_{fd\infty}\left[1\angle\left(\theta_\infty - \frac{\pi}{2}\right)\right] \\
\tilde{V}_{t\infty} &= -\left(R_a + jX_q\right)\tilde{I}_{g\infty} + E_{fd\infty}\left(1\angle\theta_\infty\right) \\
\tilde{V}_{t\infty} &= -\left(R_a + jX_q\right)\tilde{I}_{g\infty} + E_{fd\infty}\angle\theta_\infty
\end{aligned}$$

The equivalent circuit in network reference of the generator in steady state is shown in Figure **2-10**. It is possible express both $E_{fd\infty}$ and θ_∞ in terms of the generator voltage and current as:

$$E_{fd\infty}\angle\theta_\infty = \tilde{V}_{t\infty} + \left(R_a + jX_q\right)\tilde{I}_{g\infty}$$

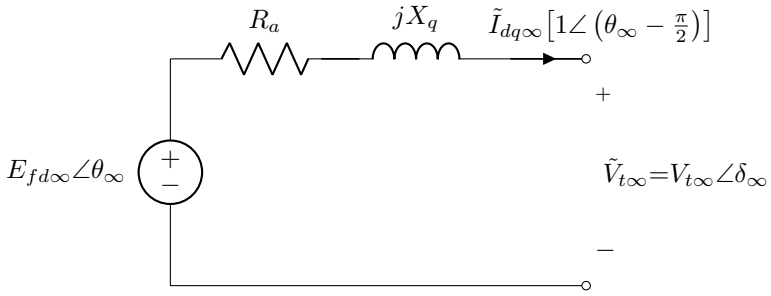

Figure 2-10.: Equivalent circuit of the generator in steady state.

$$E_{fd\infty} = \left|\tilde{V}_{t\infty} + (R_a + jX_q)\,\tilde{I}_{g\infty}\right| \tag{2-188}$$

$$\theta_\infty = \mathrm{Arg}\left\{\tilde{V}_{t\infty} + (R_a + jX_q)\,\tilde{I}_{g\infty}\right\} \tag{2-189}$$

The steady state mechanical input power $P_{m\infty}$ can be calculated from Equation 2-183 as:

$$\begin{aligned}
P_{M\infty} &= E'_{d\infty} I_{d\infty} + E'_{q\infty} I_{q\infty} \\
P_{M\infty} &= \mathfrak{Re}\left\{\tilde{E}'_{dq\infty}\tilde{I}^*_{dq\infty}\right\} \\
P_{M\infty} &= \mathfrak{Re}\left\{\left[\tilde{V}_{dq\infty} + (R_a + jX'_d)\,\tilde{I}_{dq\infty}\right]\tilde{I}^*_{dq\infty}\right\} \\
P_{M\infty} &= \mathfrak{Re}\left\{\left[\tilde{V}_{g\infty} + (R_a + jX'_d)\,\tilde{I}_{g\infty}\right]\left[1\angle\left(\frac{\pi}{2} - \theta_\infty\right)\right]\left(\tilde{I}_{g\infty}\left[1\angle\left(\frac{\pi}{2} - \theta_\infty\right)\right]\right)^*\right\} \\
P_{M\infty} &= \mathfrak{Re}\left\{\left[\tilde{V}_{g\infty} + (R_a + jX'_d)\,\tilde{I}_{g\infty}\right]\tilde{I}^*_{g\infty}\right\} \\
P_{M\infty} &= \mathfrak{Re}\left\{\tilde{V}_{g\infty}\tilde{I}^*_{g\infty} + (R_a + jX'_d)\,I^2_{g\infty}\right\} \\
P_{M\infty} &= \mathfrak{Re}\left\{\tilde{V}_{g\infty}\tilde{I}^*_{g\infty}\right\} + R_a I^2_{g\infty}
\end{aligned} \tag{2-190}$$

The generator voltage and current in steady state are normally calculated from the power system equations, as it will be seen in a latter chapter.

2.8. Automatic Voltage Regulator (AVR)

The automatic voltage regulator (AVR) is an automatic controller responsible for keeping constant the magnitude of the terminal voltage of a generator. The AVR controls the generator voltage by manipulating the field voltage. Each generator has its own AVR so the model can vary greatly from generator to generator, however most AVRs can be represented as one of the standard models defined by IEEE [26]. In this work all AVRs are represented with a simplified version of the Type DC1A AVR model [26], whose block diagram can be seen in Figure **2-11**. The equations of the AVR model in p.u. (generator base) are:

$$\frac{dV_C}{dt} = \frac{1}{T_R}\,(V_t - V_C) \tag{2-191}$$

$$\frac{dV_R}{dt} = \frac{1}{T_A}\left[K_A\left(V_{REF} - V_C - V_f\right) - V_R\right] u\left(V_R - V_{RMIN}\right) u\left(V_{RMAX} - V_R\right) \tag{2-192}$$

$$\frac{dE_{fd}}{dt} = \frac{1}{T_E}\left(V_R - K_E E_{fd}\right) \tag{2-193}$$

$$\frac{dV_f}{dt} = \frac{1}{T_F}\left(K_F \frac{dE_{fd}}{dt} - V_f\right) \tag{2-194}$$

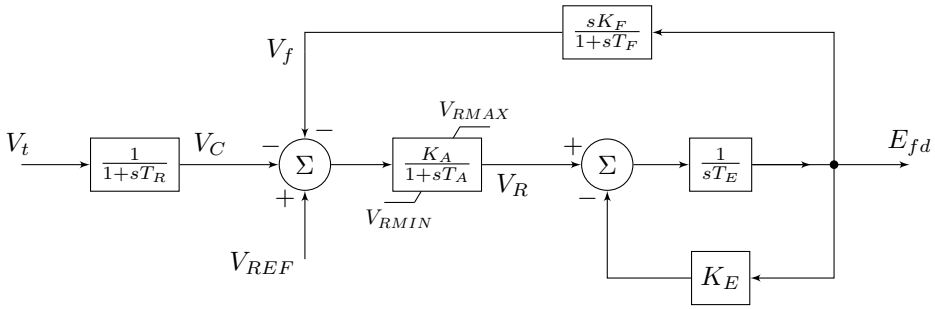

Figure 2-11.: AVR block diagram.

Where $u\left(x\right)$ denotes the unit step function, V_t is the magnitude of the generator terminal voltage, V_C is the compensated voltage[8], V_R is the regulator output voltage, the term E_{fd} is the same used on the machine model, V_f is the stabilizing feedback output, V_{REF} is the AVR setpoint and K_A is the regulator gain. The rest are AVR constants.

The tunable parameter of the AVR is the regulator gain K_A. The value of the AVR setpoint, V_{REF}, is a constant defined by the steady state operation of the generator. The values of the rest of parameters are defined by the AVR physical characteristics. The interested reader is referred to [27], where this and other AVR models are explained in detail. Some stabilizing feedbacks have variable parameters (K_F and T_F), but in this work they are considered constant. As it will be seen later, the proposed tuning method can be extended to consider any set of variable parameters without loss of generality.

2.9. Speed Governor

The speed governor is an automatic controller responsible for keeping constant the rotor speed of the generator. The governor controls the speed by manipulating the mechanical

[8]In most AVRs the compensated voltage is just a rectified measurement of the terminal voltage using a potential transformer. In some AVRs the controlled voltage is not at the generator terminals but at some other point of the system (the high voltage side of the generator transformer, for example), but the measurement is still taken at the generator terminals. In those cases, the measurement is *compensated* by adding a current-dependent term that simulates an impedance drop, effectively regulating the voltage at some point different than the generator terminals [26].

power. There are two main types of governors [27]:

- **Isochronous governor:** It uses an integral control to keep the speed constant. It has a very small stability margin and is commonly used for generators in small, isolated systems.
- **Droop governor:** It uses a proportional control to keep the speed constant. It has a larger stability margin than the isochronous governor and is commonly used for generators connected to large power systems.

Each generator has its own governor, and it is assumed in this work that all generator have droop governors. The model can vary greatly from generator to generator, however most models can be transformed to the equivalent general purpose model proposed in [27]. In this work all governors are represented with the general purpose model, whose block diagram is shown in Figure **2-12**. The equations of the governor model in p.u. (generator base) are:

$$\frac{du_D}{dt} = \frac{1}{T_D}\left[\frac{(\omega - 1)}{R} + \frac{T_\omega}{R}\frac{d\omega}{dt} - u_D\right] \tag{2-195}$$

$$u_L = \max\left\{\min\left\{P_{REF} - u_D, P_{MAX}\right\}, 0\right\} \tag{2-196}$$

$$\frac{du_S}{dt} = \frac{1}{T_S}\left(u_L - u_S\right) \tag{2-197}$$

$$\frac{du_B}{dt} = \frac{1}{T_B}\left(u_S - u_B\right) \tag{2-198}$$

$$\frac{dP_M}{dt} = \frac{1}{T_P}\left(u_B + FT_P\frac{du_B}{dt} - P_M\right) \tag{2-199}$$

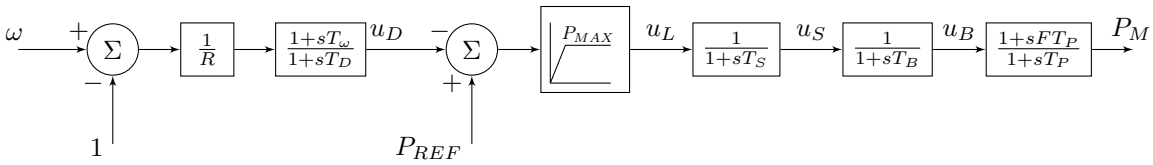

Figure 2-12.: Governor block diagram.

Where P_M is the mechanical input power of the generator, u_D, u_L, u_S and u_B are the other differential variables of the model (their physical meaning depends on the original governor model), P_{REF} is the governor setpoint and R is the governor *droop* (not to be confused with resistance). The rest are governor constants.

The tunable parameter of the governor is the droop R. The value of the governor sepoint, P_{REF}, is a constant defined by the steady state operation of the generator. The values of the rest of parameters are defined by the governor physical characteristics. The interested reader is referred to [27], where this and other governor models are explained in detail.

3. Power System Analysis

This chapter is focused on the methods and techniques required for the study of power systems in two different states: steady state and transient state. For the rest of this work the following suppositions are going to be made:

- The power system works in a balanced operating condition. Therefore, it is possible to represent the system with a single-phase equivalent representation.
- There are no harmonic components present in the system, so it is possible to represent voltages and currents as phasors.

The scope of this chapter is limited to the methods used to implement the proposed solution.

3.1. Steady State Analysis: Power Flow

The steady state analysis of a power system involves the calculation of electric variables like voltages, currents and powers given specific conditions at each node. Such calculations become trivial if the voltages of all nodes are known, so the main problem of the analysis reduces to determining the node voltages. This is known as the *power flow problem*, or *load flow problem* [5].

3.1.1. Node types

The steady state performance of the system is determined by the operative conditions of each node, which provide the necessary information to determine the node voltages. The node conditions are normally expressed in terms of two of the following four electric quantities: injected active power P, injected reactive power Q, voltage magnitude V and voltage angle δ. Each node can be classified, depending on the specified quantities, as one of the following types [15]:

- **Load (PQ) node:** Injected active and reactive power are known. This type of nodes normally have loads connected to them, when no loads are connected the node is called *transit node* and its injected powers are zero. Nodes with linear (constant admittance)

loads also have zero injected powers, because it is considered that only sources and nonlinear devices inject power into the node.

- **Voltage-controlled (PV) node:** Injected active power and voltage magnitude are known. This type of nodes normally have generators, SVCs or or other voltage-controlling devices attached to them. The reactive power capability of the voltage-controlling device is limited and when the limit is reached, the voltage control is lost and the node type becomes PQ [5]. The reactive capability limits are typically known so those cases can be managed programatically. In this work it is assumed that the only voltage-controlling devices are synchronous generators, and their reactive capability limits are expressed in terms of their AVR limits, so the case when a PV node becomes a PQ node will be neglected.

- **Slack or swing ($V\delta$) node:** Voltage magnitude and angle are specified. A system must have at least one slack node in order to have an angle reference, otherwise the power flow would have infinite solutions (one for each angle reference). The slack node has a voltage-controlling device which normally has limited reactive power capability, much like the PV node.

- **Limited slack ($Q\delta$) node:** Injected reactive power and voltage angle are known. When the reactive capability limit of the voltage-controlling device of the slack node is reached, the voltage control is lost and the injected power is fixed at the limiting value. In such case, V becomes an unknown variable and Q becomes a known variable. As with the PV nodes, the case in which a $V\delta$ node becomes a $Q\delta$ will be neglected.

- **Device node:** A node of this type has attached a device that imposes special conditions to the node's electric variables that do not fit in any of the previous node types (a HVDC converter, for example [15]). Nodes of this type are not considered in this work.

3.1.2. Network Equations

The relationship between node voltages and injected node currents depends on the elements linking them. In this work it is considered that two nodes can be connected only through a transformer or a transmission line (a series capacitor, reactor or resistance is possible too), or a parallel combination of them, so any pair of nodes is connected through linear elements (constant admittances). Therefore the voltage-current relationship between any pair of nodes (excluding ground) is linear, and it can be expressed by means of the node equations as [5]:

$$\begin{bmatrix} \tilde{I}_1 \\ \tilde{I}_2 \\ \vdots \\ \tilde{I}_n \end{bmatrix} = \begin{bmatrix} Y_{11} & Y_{12} & \cdots & Y_{1n} \\ Y_{21} & Y_{22} & \cdots & Y_{2n} \\ \vdots & \vdots & \ddots & \vdots \\ Y_{n1} & Y_{n2} & \cdots & Y_{nn} \end{bmatrix} \begin{bmatrix} \tilde{V}_1 \\ \tilde{V}_2 \\ \vdots \\ \tilde{V}_n \end{bmatrix} \tag{3-1}$$

Where [15]:

n	is the total number of nodes
Y_{ii}	is the self admittance of node i
	= sum of all admittances connected to node i
Y_{ij}	is the mutual admittance between nodes i and j
	= negative of the sum of all admittances between nodes i and j
$\tilde{V}_i$	is the phasor voltage of node i with respect to ground
	$= V_i \angle \delta_i$
$\tilde{I}_i$	is the phasor injected current by sources and nonlinear elements to node i

The self admittances include the shunt admittances and the constant admittance loads, so it is considered that only sources and nonlinear loads contribute to the node injected current. The node equations can be expressed in compact form as:

$$\vec{\tilde{I}} = \mathbf{Y}\vec{\tilde{V}} \tag{3-2}$$

Where:

$\mathbf{Y}$	is the admittance matrix
$\vec{\tilde{V}}$	is the vector of node voltages
$\vec{\tilde{I}}$	is the vector of injected currents

If the injected currents were known, the node equations would be purely linear, and finding the node voltages would be trivial. However, in most cases only the injected powers are known. The injected current of node i can be expressed in terms of its injected active a reactive power as:

$$\tilde{I}_i = \frac{P_i - jQ_i}{\tilde{V}_i^*} = \frac{S_i^*}{\tilde{V}_i^*} \tag{3-3}$$

The whole system of equations can be expressed as:

$$\vec{S}^* \oslash \vec{\tilde{V}}^* = \mathbf{Y}\vec{\tilde{V}} \tag{3-4}$$

$$\vec{S}^* = \vec{\tilde{V}}^* \circ \left(\mathbf{Y}\vec{\tilde{V}}\right) \tag{3-5}$$

$$\vec{S} = \vec{\tilde{V}} \circ \left(\mathbf{Y}\vec{\tilde{V}}\right)^* \tag{3-6}$$

$$\vec{0} = \vec{\tilde{V}} \circ \left(\mathbf{Y}\vec{\tilde{V}}\right)^* - \vec{S} \tag{3-7}$$

Where $\circ$ is the Hadamard (elementwise) product, and $\oslash$ is the Hadamard (elementwise) division. The scalar equation for an arbitrary node i is:

$$\tilde{V}_i \left(\sum_{k=1}^{n} Y_{ik} \tilde{V}_k \right)^* - S_i = 0 \tag{3-8}$$

Equation 3-8 is called *power mismatch equation*. The relationship between $\tilde{V}_i$ and S_i in Equation 3-8 depends on the type of node. In PQ nodes S_i is a known constant but $\tilde{V}_i$ is not known. In PV nodes V_i and P_i are known but Q_i and δ_i are unknown. In slack nodes $\tilde{V}_i$ is known but S_i is not. In $Q\delta$ nodes Q_i and δ_i are known but V_i and P_i are unknown. Device nodes specify the relationship between P_i, Q_i, V_i and δ_i as a set of two equations (typically nonlinear).

In general, each node has four real variables to be found: P_i, Q_i, V_i and δ_i. In order to find them all, four equations per node are required: the complex node equations contribute with 2 real equations per node, and the node type specifications add two more equations per node. When no device nodes are present, it is possible to replace the nodes' specifications into the node equations, yielding a set of n complex equations that can be solved to find the n node voltage phasors. The complex node equations can also be expressed in real and imaginary components, giving a set of $2n$ real equations that can be solved to find $2n$ variables: the node voltage magnitudes and angles.

3.1.3. Newton-Raphson Method

The Newton-Raphson method is one of the most popular iterative techniques used to solve systems of real nonlinear equations [28]. Let $\vec{f}(\vec{x}) = [f_1(\vec{x}) \;\; f_2(\vec{x}) \;\; \cdots \;\; f_{nf}(\vec{x})]^T$ be a vector of nf functions dependent of the variable vector $\vec{x} = [x_1 \; x_2 \; \cdots \; x_{nf}]^T$, where the solution of the following vector equation is required:

$$\vec{f}(\vec{x}) = \vec{0} \tag{3-9}$$

The method starts with an initial estimate of the solution $\vec{x}^{(0)}$, provided by the user. The method performs a series of iterations, each one yielding a new estimate that is (hopefully) closer to the real solution than the previous ones. Assuming iteration k has been executed and its estimate $\vec{x}^{(k)}$ is known, iteration $k+1$ is executed by performing the following steps:

- Evaluate the function using the current estimate:

$$\vec{f}^{(k)} = \vec{f}\left(\vec{x}^{(k)}\right) \tag{3-10}$$

- Calculate the Jacobian of $\vec{f}(\vec{x})$ using the current estimate:

$$\mathbf{J}^{(k)} = \left.\frac{\partial \vec{f}(\vec{x})}{\partial \vec{x}^T}\right|_{\vec{x}^{(k)}} = \left.\begin{bmatrix} \frac{\partial f_1(\vec{x})}{\partial x_1} & \frac{\partial f_1(\vec{x})}{\partial x_2} & \dots & \frac{\partial f_1(\vec{x})}{\partial x_{nf}} \\ \frac{\partial f_2(\vec{x})}{\partial x_1} & \frac{\partial f_2(\vec{x})}{\partial x_2} & \dots & \frac{\partial f_2(\vec{x})}{\partial x_{nf}} \\ \vdots & \vdots & \ddots & \vdots \\ \frac{\partial f_{nf}(\vec{x})}{\partial x_1} & \frac{\partial f_{nf}(\vec{x})}{\partial x_2} & \dots & \frac{\partial f_{nf}(\vec{x})}{\partial x_{nf}} \end{bmatrix}\right|_{\vec{x}^{(k)}} \tag{3-11}$$

- Approximate the difference between the real solution and the actual estimate as the solution of the following system of linear equations:

$$\vec{f}^{(k)} = -\mathbf{J}^{(k)}\Delta\vec{x}^{(k)} \tag{3-12}$$

- Calculate the new estimate as:

$$\vec{x}^{(k+1)} = \vec{x}^{(k)} + \Delta\vec{x}^{(k)} \tag{3-13}$$

Subsequent iterations are executed by repeating the previous steps, until a specific termination criterion is met. Normally the method is implemented with the following two criteria:

- If the absolute value of all the elements of $\vec{f}(\vec{x})$ are lesser than a specified tolerance ϵ, that is, if:

$$\max_i \left| f_i\left(\vec{x}^{(k)}\right)\right| = \left\|\vec{f}^{(k)}\right\|_\infty < \epsilon \tag{3-14}$$

  Then the method is considered to have converged to a solution $\vec{x}^{(k)}$ and the execution stops.

- If the method reaches a specified number of iterations before satisfying the first criterion, it is considered that the method failed to find any valid solution and the execution stops. This does not imply that the system of equations has no solutions, and remedial measures can be taken (changing the initial estimate or trying another method, for example).

The Newton-Raphson method has *quadratic convergence*: the error of a given iteration's estimate is proportional to the square of the error of the previous iteration's estimate [29]. Because of the previous property, this method can converge to a solution in very few iterations. However, the computational cost of the method is very high due to the following reasons:

- To calculate the Jacobian matrix it is required to calculate the partial derivatives of each element of the function vector, and these calculations must be repeated for each iteration. The exact calculations of the partial derivatives are, except for special cases, computationally costly.

- The Jacobian matrix must be factored in order to solve Equation 3-12. This matrix changes with each iteration, so the factoring must be performed once per iteration.

There exist some modifications of the method that avoid those problems:

- **Quasi-Newton:** The Jacobian matrix is approximated by estimating the partial derivatives with numerical methods instead of calculating their exact values [30].
- **Dishonest Newton-Raphson:** The Jacobian matrix is not recalculated at every iteration but instead it is left unchanged during a predetermined number of iterations. It can also be recalculated prematurely when slow convergence is detected [29].
- **Very Dishonest Newton-Raphson:** Equation 3-12 is solved using the SAME matrix at all iterations. That matrix does not necessarily have to be the Jacobian [29].

One of the most popular methods for solving the power flow problem is the Fast Decoupled Load Flow (FDLF) which is a Very Dishonest Newton-Raphson adapted to the power flow problem. It was proposed by Stott and Alsac in 1974 [31]. In this work the full Newton-Raphson method was used to solve the power flow problem, as proposed originally by Tinney and Hart in 1967 [32].

3.1.4. Power Flow Solution Using Newton-Raphson Method

Before applying the Newton-Raphson method, Equation 3-7 must decomposed in two real equations, corresponding to its real and imaginary part (the the subscript *sp* to denotes the specified complex power of the nodes):

$$\begin{bmatrix} \mathfrak{Re}\left\{\vec{\bar{V}} \circ \left(\mathbf{Y}\vec{\bar{V}}\right)^* - \vec{S}_{sp}\right\} \\ \mathfrak{Im}\left\{\vec{\bar{V}} \circ \left(\mathbf{Y}\vec{\bar{V}}\right)^* - \vec{S}_{sp}\right\} \end{bmatrix} = \begin{bmatrix} \vec{0} \\ \vec{0} \end{bmatrix} \tag{3-15}$$

$$\begin{bmatrix} \Delta\vec{P} \\ \Delta\vec{Q} \end{bmatrix} = \begin{bmatrix} \vec{0} \\ \vec{0} \end{bmatrix} \tag{3-16}$$

Where $\vec{S}_{sp} = \vec{S}_G - \vec{S}_L$. The subscript G means generated (injected) power, whereas the subscript L means consumed (extracted) power. Equation 3-16 can be expressed as:

$$\Delta\vec{P} = \vec{P} - \vec{P}_{sp} = \vec{P} - \left(\vec{P}_G - \vec{P}_L\right) \tag{3-17}$$

$$\Delta\vec{Q} = \vec{Q} - \vec{Q}_{sp} \tag{3-18}$$

$$\vec{P} = \mathfrak{Re}\left\{\vec{\bar{V}} \circ \left(\mathbf{Y}\vec{\bar{V}}\right)^*\right\} \tag{3-19}$$

$$\vec{Q} = \mathfrak{Im}\left\{\vec{\bar{V}} \circ \left(\mathbf{Y}\vec{\bar{V}}\right)^*\right\} \tag{3-20}$$

Notice that the elements of $\vec{Q}_{sp}$ corresponding to the PV or slack nodes are not defined. Similarly, the elements $\vec{P}_{sp}$ corresponding to the slack and $Q\delta$ nodes are not defined. For now it will be assumed that all nodes are of type PQ, and the case with PV, slack and $Q\delta$ nodes will be treated later. Vectors $\vec{P}$ and $\vec{P}$ depend on the node voltage phasors. but the variable vector must be composed only of real numbers. In order to achieve that, the nodes voltages will be expressed in terms of their magnitude and angle as:

$$\vec{\tilde{V}} = \vec{V} \circ e^{j\vec{\delta}} \tag{3-21}$$

Where the exponential function is applied individually to each angle δ_i. The objective function and variable vector of the Newton-Raphson method are defined as:

$$\vec{f}\,(\vec{x}) = \left[\Delta\vec{P}\ \Delta\vec{Q}\right]^T \tag{3-22}$$

$$\vec{x} = \left[\vec{\delta}\ \vec{V}\right]^T \tag{3-23}$$

The Jacobian matrix can be calculated as:

$$\mathbf{J} = \begin{bmatrix} \frac{\partial\Delta\vec{P}}{\partial\vec{\delta}^T} & \frac{\partial\Delta\vec{P}}{\partial\vec{V}^T} \\ \frac{\partial\Delta\vec{Q}}{\partial\vec{\delta}^T} & \frac{\partial\Delta\vec{Q}}{\partial\vec{V}^T} \end{bmatrix} \tag{3-24}$$

$$\mathbf{J} = \begin{bmatrix} \mathbf{H} & \mathbf{N} \\ \mathbf{M} & \mathbf{L} \end{bmatrix} \tag{3-25}$$

The submatrix $\mathbf{H}$ can be expressed as:

$$\mathbf{H} = \frac{\partial\Delta\vec{P}}{\partial\vec{\delta}^T} \tag{3-26}$$

$$\mathbf{H} = \frac{\partial}{\partial\vec{\delta}^T}\left(\vec{P} - \vec{P}_{sp}\right) \tag{3-27}$$

$$\mathbf{H} = \frac{\partial}{\partial\vec{\delta}^T}\left(\mathfrak{Re}\left\{\vec{\tilde{V}} \circ \left(\mathbf{Y}\vec{\tilde{V}}\right)^*\right\}\right) \tag{3-28}$$

The real part function $\mathfrak{Re}\{\cdot\}$ can be commuted with the (vectorial) derivative with respect to a real (vector) variable:

$$\mathbf{H} = \mathfrak{Re}\left\{\frac{\partial}{\partial\vec{\delta}^T}\left(\vec{\tilde{V}} \circ \left(\mathbf{Y}\vec{\tilde{V}}\right)^*\right)\right\} \tag{3-29}$$

In order to calculate the vectorial derivative of a complex Hadamard product, the matrix calculus theory proposed in [33] and expanded in [34] is required. First, consider $\vec{\delta}$ to be the real part of an arbitrary complex vector variable $\vec{\zeta}$ defined as:

$$\vec{\zeta} = \vec{\delta} + j\vec{\varepsilon} \tag{3-30}$$

In scalar form:

$$\zeta_i = \delta_i + j\varepsilon_i \tag{3-31}$$

For the scalar case, the derivative of an arbitrary complex function g with respect to δ_i can be expressed in terms of Wirtinger derivatives as [35]:

$$\frac{\partial g}{\partial \delta_i} = \frac{\partial g}{\partial \zeta_i} + \frac{\partial g}{\partial \zeta_i^*} \tag{3-32}$$

The previous equation can be easily extended to the vectorial case as:

$$\frac{\partial \vec{g}}{\partial \vec{\delta}^T} = \frac{\partial \vec{g}}{\partial \vec{\zeta}^T} + \frac{\partial \vec{g}}{\partial \vec{\zeta}^H} \tag{3-33}$$

Where the superscript H denotes conjugate transpose. Let $\vec{g} = \vec{g}_1 \circ \vec{g}_2$ be the Hadamard product of two arbitrary vector functions, then the Wirtinger derivatives of $\vec{g}_1 \circ \vec{g}_2$ are [33, 34]:

$$\frac{\partial}{\partial \vec{\zeta}^T}\left(\vec{g}_1 \circ \vec{g}_2\right) = \operatorname{diag}\left(\vec{g}_2\right)\frac{\partial \vec{g}_1}{\partial \vec{\zeta}^T} + \operatorname{diag}\left(\vec{g}_1\right)\frac{\partial \vec{g}_2}{\partial \vec{\zeta}^T} \tag{3-34}$$

$$\frac{\partial}{\partial \vec{\zeta}^H}\left(\vec{g}_1 \circ \vec{g}_2\right) = \operatorname{diag}\left(\vec{g}_2\right)\frac{\partial \vec{g}_1}{\partial \vec{\zeta}^H} + \operatorname{diag}\left(\vec{g}_1\right)\frac{\partial \vec{g}_2}{\partial \vec{\zeta}^H} \tag{3-35}$$

Where the operator $\operatorname{diag}(\cdot)$ transforms the input vector into a square diagonal matrix whose diagonal elements are equal to those of the input vector. In mathematical terms:

$$\begin{aligned} &\vec{g}_1 \in \mathbb{R}^n, \qquad \operatorname{diag}\left(\vec{g}_1\right) \in \mathbb{R}^{n\times n} \\ &\left\{\operatorname{diag}\left(\vec{g}_1\right)\right\}_{ii} = \left\{\vec{g}_1\right\}_i \\ &\left\{\operatorname{diag}\left(\vec{g}_1\right)\right\}_{ij} = 0, \qquad i \neq j \end{aligned}$$

Three important properties of the operator $\operatorname{diag}(\cdot)$ that are going to be needed next are:

$$\begin{aligned} \operatorname{diag}\left(\vec{v}_1\right)^* &= \operatorname{diag}\left(\vec{v}_1^*\right) \\ \operatorname{diag}\left(\vec{v}_1\right)\vec{v}_2 &= \operatorname{diag}\left(\vec{v}_1 \circ \vec{v}_2\right) \\ \operatorname{diag}\left(\vec{v}_1\right)\operatorname{diag}\left(\vec{v}_2\right) &= \operatorname{diag}\left(\vec{v}_1 \circ \vec{v}_2\right), \qquad \vec{v}_1, \vec{v}_2 \in \mathbb{R}^n \end{aligned}$$

Adding the Equations 3-34 and 3-35 together:

$$\left[\frac{\partial}{\partial \vec{\zeta}^T}\left(\vec{g}_1 \circ \vec{g}_2\right) + \frac{\partial}{\partial \vec{\zeta}^H}\left(\vec{g}_1 \circ \vec{g}_2\right)\right] = \operatorname{diag}\left(\vec{g}_2\right)\left[\frac{\partial \vec{g}_1}{\partial \vec{\zeta}^T} + \frac{\partial \vec{g}_1}{\partial \vec{\zeta}^H}\right] + \operatorname{diag}\left(\vec{g}_1\right)\left[\frac{\partial \vec{g}_2}{\partial \vec{\zeta}^T} + \frac{\partial \vec{g}_2}{\partial \vec{\zeta}^H}\right] \tag{3-36}$$

$$\frac{\partial}{\partial \vec{\delta}^T}\left(\vec{g}_1 \circ \vec{g}_2\right) = \operatorname{diag}\left(\vec{g}_2\right)\frac{\partial \vec{g}_1}{\partial \vec{\delta}^T} + \operatorname{diag}\left(\vec{g}_1\right)\frac{\partial \vec{g}_2}{\partial \vec{\delta}^T} \tag{3-37}$$

Therefore, Equation 3-29 can be rewritten as:

$$\mathbf{H} = \mathfrak{Re}\left\{\operatorname{diag}\left(\left(\mathbf{Y}\vec{V}\right)^*\right)\frac{\partial \vec{V}}{\partial \vec{\delta}^T} + \operatorname{diag}\left(\vec{V}\right)\frac{\partial}{\partial \vec{\delta}^T}\left(\left(\mathbf{Y}\vec{V}\right)^*\right)\right\} \tag{3-38}$$

The conjugate operator $*$ can be commuted with the (vectorial) derivative with respect to a real (vector) variable:

$$\mathbf{H} = \mathfrak{Re}\left\{ \text{diag}\left(\left(\mathbf{Y}\vec{\vec{V}}\right)^*\right) \frac{\partial \vec{\vec{V}}}{\partial \vec{\delta}^T} + \text{diag}\left(\vec{\vec{V}}\right) \left(\frac{\partial \mathbf{Y}\vec{\vec{V}}}{\partial \vec{\delta}^T}\right)^* \right\} \tag{3-39}$$

$$\mathbf{H} = \mathfrak{Re}\left\{ \text{diag}\left(\left(\mathbf{Y}\vec{\vec{V}}\right)^*\right) \frac{\partial \vec{\vec{V}}}{\partial \vec{\delta}^T} + \text{diag}\left(\vec{\vec{V}}\right) \mathbf{Y}^* \left(\frac{\partial \vec{\vec{V}}}{\partial \vec{\delta}^T}\right)^* \right\} \tag{3-40}$$

The derivative of the voltage vector is calculated as:

$$\frac{\partial \vec{\vec{V}}}{\partial \vec{\delta}^T} = \frac{\partial}{\partial \vec{\delta}^T}\left(\vec{V} \circ e^{j\vec{\delta}}\right) \tag{3-41}$$

$$\frac{\partial \vec{\vec{V}}}{\partial \vec{\delta}^T} = \text{diag}\left(e^{j\vec{\delta}}\right) \frac{\partial \vec{V}}{\partial \vec{\delta}^T} + \text{diag}\left(\vec{V}\right) \frac{\partial e^{j\vec{\delta}}}{\partial \vec{\delta}^T} \tag{3-42}$$

$$\frac{\partial \vec{\vec{V}}}{\partial \vec{\delta}^T} = \text{diag}\left(e^{j\vec{\delta}}\right) \mathbf{0} + \text{diag}\left(\vec{V}\right) j\text{diag}\left(e^{j\vec{\delta}}\right) \tag{3-43}$$

$$\frac{\partial \vec{\vec{V}}}{\partial \vec{\delta}^T} = j\text{diag}\left(\vec{\vec{V}}\right) \tag{3-44}$$

Replacing Equation 3-44 in Equation 3-40:

$$\mathbf{H} = \mathfrak{Re}\left\{ \text{diag}\left(\left(\mathbf{Y}\vec{\vec{V}}\right)^*\right) j\text{diag}\left(\vec{\vec{V}}\right) + \text{diag}\left(\vec{\vec{V}}\right) \mathbf{Y}^* \left(j\text{diag}\left(\vec{\vec{V}}\right)\right)^* \right\} \tag{3-45}$$

$$\mathbf{H} = \mathfrak{Re}\left\{ j\text{diag}\left(\vec{\vec{V}} \circ \left(\mathbf{Y}\vec{\vec{V}}\right)^*\right) - j\text{diag}\left(\vec{\vec{V}}\right) \mathbf{Y}^* \text{diag}\left(\vec{\vec{V}}\right)^* \right\} \tag{3-46}$$

Let $\vec{S} = \vec{\vec{V}} \circ \left(\mathbf{Y}\vec{\vec{V}}\right)^*$ denote the vector of injected complex powers given the node voltage vector $\vec{\vec{V}}$, then:

$$\mathbf{H} = \mathfrak{Re}\left\{ j\text{diag}\left(\vec{S}\right) - j\text{diag}\left(\vec{\vec{V}}\right) \mathbf{Y}^* \text{diag}\left(\vec{\vec{V}}\right)^* \right\} \tag{3-47}$$

$$\mathbf{H} = \mathfrak{Re}\left\{ -j\left(\text{diag}\left(\vec{\vec{V}}\right) \mathbf{Y}^* \text{diag}\left(\vec{\vec{V}}\right)^* - \text{diag}\left(\vec{S}\right)\right) \right\} \tag{3-48}$$

$$\mathbf{H} = \mathfrak{Im}\left\{ \text{diag}\left(\vec{\vec{V}}\right) \mathbf{Y}^* \text{diag}\left(\vec{\vec{V}}\right)^* - \text{diag}\left(\vec{S}\right) \right\} \tag{3-49}$$

The other submatrices can be calculated by applying a similar process, yielding the following results:

$$\mathbf{M} = -\mathfrak{Re}\left\{ \text{diag}\left(\vec{\vec{V}}\right) \mathbf{Y}^* \text{diag}\left(\vec{\vec{V}}\right)^* - \text{diag}\left(\vec{S}\right) \right\} \tag{3-50}$$

$$\mathbf{N} = \mathfrak{Re}\left\{ \text{diag}\left(\vec{\vec{V}}\right) \mathbf{Y}^* \text{diag}\left(e^{j\vec{\delta}}\right)^* + \text{diag}\left(\vec{S} \oslash \vec{V}\right) \right\} \tag{3-51}$$

$$\mathbf{L} = \mathfrak{Im}\left\{\text{diag}\left(\vec{\vec{V}}\right)\mathbf{Y}^{*}\text{diag}\left(e^{j\vec{\delta}}\right)^{*} + \text{diag}\left(\vec{S} \oslash \vec{V}\right)\right\} \tag{3-52}$$

It must be noted that $\vec{\vec{V}}$ is the vector of node voltage **phasors**, whereas $\vec{V}$ is the vector of node voltage **magnitudes**.

Let $\vec{x}^{(k)} = \left[\vec{\delta}^{(k)}\ \vec{V}^{(k)}\right]^{T}$ be the estimate at iteration k. The change in the estimate, $\Delta\vec{x}^{(k)} = \left[\Delta\vec{\delta}^{(k)}\ \Delta\vec{V}^{(k)}\right]^{T}$, is calculated by solving the following system of linear equations:

$$\begin{bmatrix} \Delta\vec{P}^{(k)} \\ \Delta\vec{Q}^{(k)} \end{bmatrix} = \begin{bmatrix} \mathbf{H}^{(k)} & \mathbf{N}^{(k)} \\ \mathbf{M}^{(k)} & \mathbf{L}^{(k)} \end{bmatrix} \begin{bmatrix} \Delta\vec{\delta}^{(k)} \\ \Delta\vec{V}^{(k)} \end{bmatrix} \tag{3-53}$$

The superscript (k) in the power mismatches and the Jacobian submatrices indicate that they are evaluated using $\vec{x}^{(k)}$.

Equation 3-53 was obtained assuming that all nodes were of type PQ, but it can be extended to other cases as well. Suppose node i is of type PV, then there is no specified reactive power Q_{spi}, and the reactive power mismatch $\Delta Q_i^{(k)}$ is undefined. Also, as the true value of V_i is already known, $\Delta V_i^{(k)}$ must be zero. The row associated with $\Delta Q_i^{(k)}$ must be removed from Equation 3-53 in order to remove the undefined mismatch. Similarly, the column associated with $\Delta V_i^{(k)}$ be removed from Equation 3-53 as there is no need to estimate V_i. In conclusion, a PV node only contributes with one equation (ΔP_i) and one unknown variable ($\Delta\delta_i$).

A similar procedure can be performed for slack and $Q\delta$ nodes, so in general Equation 3-53 can be constructed by assuming all nodes are PQ and then removing the rows of the undefined mismatch equations and the columns of the already known variables. The total number of rows (and columns) of the final Jacobian matrix is:

$$\begin{aligned}(\textit{total rows}) = {} & 2\,(\#\ \textit{of nodes}) - (\#\ \textit{of PV nodes}) - (\#\ \textit{of } Q\delta\ \textit{nodes}) \\ & - 2\,(\#\ \textit{of slack nodes})\end{aligned} \tag{3-54}$$

After solving Equation 3-53, the new estimate can be calculated by applying Equation 3-13.

3.2. Transient Stability Analysis: Time-Domain Simulation

The previous section discussed how to calculate the steady-state performance of a power system. When the system is disturbed by an event (a short-circuit, for example), the electrical and mechanical variables start to change with respect to time in what is known as the

transient response. The transient response of a real power system can be simulated. In order to do that, it is necessary to solve the differential equations describing the system variables. At the same time, the variables must satisfy the power flow equations described in the previous section at any time. This leads to a set of Differential Algebraic Equations (DAEs) that must be solved over the time range of interest to obtain the transient response [15, 4, 23]. Before deriving the set of DAEs, the following assumptions are going to be made:

- Electromagnetic transients are neglected, because their time constants are small compared to those of electro-mechanical transients (stiffer system). Also, they have little impact on transient stability [15]. For these reasons, the electric network is modelled with just algebraic equations (power flow equations).
- Variations of the speed of the generators are small, so the total frequency of the system can be assumed to be constant, and thus the network reactances do not vary.
- Saturation and salient poles effects are neglected by taking each machines' direct and quadrature axis reactances as constants equal to the average of the two real values. This is done for the reactances of each period (subtransient, transient and steady state).

The previous assumptions allow using the two-axis machine model developed in the previous chapter. The first assumption is specially important as its greatly reduces the amount of differential equations that must be solved, thus reducing the complexity of the model. The first assumption also implies that the only elements contributing with differential equations to the set of DAEs are the generators and their controllers. In the next subsection the set of DAEs will be derived.

3.2.1. Power System DAEs

In order to construct the set of DAEs, let us first define all the algebraic equations. All algebraic equations will expressed in the form $f(x) = 0$. The first ones are the power flow equations. Let n be the number of system nodes and m the number of generators. Assume nodes number 1 to m are the generator nodes (node numbering can be changed when required to fit the numbering proposed here). These nodes must be type PV or slack, as the generators' AVRs keep the voltage magnitude constant. The remaining nodes must be of type PQ. During the transient response, the voltage magnitude of the PV and slack nodes vary, and in order to calculate it the generator model must be used. The circuit model of each generator adds one node to the system, for a new total of $n+m$ nodes (nodes $n+1$ to $n+m$ are the generators' internal nodes). The new system including the generator circuits is called *extended system*. During the transient response nodes 1 to m are considered PQ with zero power injection, and nodes $n+1$ to $n+m$ are considered slack. The power flow

equations of the extended system at a time t are:

$$\begin{bmatrix} \mathfrak{Re}\left\{\tilde{V}_1\left(\sum_{k=1}^{n+m} Y_{1k}(t)\,\tilde{V}_k\right)^* - S_{sp1}(t)\right\} \\ \vdots \\ \mathfrak{Re}\left\{\tilde{V}_n\left(\sum_{k=1}^{n+m} Y_{nk}(t)\,\tilde{V}_k\right)^* - S_{spn}(t)\right\} \\ \mathfrak{Im}\left\{\tilde{V}_1\left(\sum_{k=1}^{n+m} Y_{1k}(t)\,\tilde{V}_k\right)^* - S_{sp1}(t)\right\} \\ \vdots \\ \mathfrak{Im}\left\{\tilde{V}_n\left(\sum_{k=1}^{n+m} Y_{nk}(t)\,\tilde{V}_k\right)^* - S_{spn}(t)\right\} \end{bmatrix} = \vec{g}_{PQ} = \vec{0} \tag{3-55}$$

Where:

$$\tilde{V}_{n+i} = \tilde{E}'_{dqi} \cdot 1\angle\left(\theta_i - \frac{\pi}{2}\right), \qquad 1 \le i \le m \tag{3-56}$$

Replacing:

$$\begin{bmatrix} \mathfrak{Re}\left\{\tilde{V}_1\left(\sum_{k=1}^{n} Y_{1k}(t)\,\tilde{V}_k + \sum_{k=1}^{m} Y_{1(n+k)}(t)\,\tilde{E}'_{dqk}\cdot 1\angle\left(\theta_k - \frac{\pi}{2}\right)\right)^* - S_{sp1}(t)\right\} \\ \vdots \\ \mathfrak{Re}\left\{\tilde{V}_n\left(\sum_{k=1}^{n} Y_{nk}(t)\,\tilde{V}_k + \sum_{k=1}^{m} Y_{n(n+k)}(t)\,\tilde{E}'_{dqk}\cdot 1\angle\left(\theta_k - \frac{\pi}{2}\right)\right)^* - S_{spn}(t)\right\} \\ \mathfrak{Im}\left\{\tilde{V}_1\left(\sum_{k=1}^{n} Y_{1k}(t)\,\tilde{V}_k + \sum_{k=1}^{m} Y_{1(n+k)}(t)\,\tilde{E}'_{dqk}\cdot 1\angle\left(\theta_k - \frac{\pi}{2}\right)\right)^* - S_{sp1}(t)\right\} \\ \vdots \\ \mathfrak{Im}\left\{\tilde{V}_n\left(\sum_{k=1}^{n} Y_{nk}(t)\,\tilde{V}_k + \sum_{k=1}^{m} Y_{n(n+k)}(t)\,\tilde{E}'_{dqk}\cdot 1\angle\left(\theta_k - \frac{\pi}{2}\right)\right)^* - S_{spn}(t)\right\} \end{bmatrix} = \vec{g}_{PQ} = \vec{0} \tag{3-57}$$

Notice that the power flow equations are only considered for nodes 1 to n, because the voltages of the generators' internal nodes (generators' EMFs) are calculated by applying Equation 3-56 after solving the differential equations of E'_{di} and E'_{qi}. Basically, nodes $n+1$ to $n+m$ are treated as slack nodes. It must also be noted that certain disturbances produce continuous changes on the injected powers, and for that reason the time dependence is explicitly stated. Some disturbances can also change the system topology, modifying the admittances matrix, and for that reason the time dependence is also explicitly stated.

The next algebraic equations to be considered are ones of the generators' currents, which can be calculated by solving the generators' circuits:

$$\tilde{I}_{dqi} = \frac{\tilde{E}'_{dqi} - \tilde{V}_i \cdot 1\angle\left(\frac{\pi}{2} - \theta_i\right)}{R_{ai} + jX'_{di}} \tag{3-58}$$

$$I_{di} = \mathfrak{Re}\left\{\frac{\tilde{E}'_{dqi} - \tilde{V}_i \cdot 1\angle\left(\frac{\pi}{2} - \theta_i\right)}{R_{ai} + jX'_{di}}\right\} \tag{3-59}$$

$$I_{qi} = \mathfrak{Im}\left\{\frac{\tilde{E}'_{dqi} - \tilde{V}_i \cdot 1\angle\left(\frac{\pi}{2} - \theta_i\right)}{R_{ai} + jX'_{di}}\right\}, \qquad 1 \le i \le m \tag{3-60}$$

In vector form:

$$\begin{bmatrix} \mathfrak{Re}\left\{\frac{\tilde{E}'_{dq1} - \tilde{V}_1 \cdot 1\angle\left(\frac{\pi}{2} - \theta_1\right)}{R_{a1} + jX'_{d1}}\right\} - I_{d1} \\ \vdots \\ \mathfrak{Re}\left\{\frac{\tilde{E}'_{dqm} - \tilde{V}_m \cdot 1\angle\left(\frac{\pi}{2} - \theta_m\right)}{R_{am} + jX'_{dm}}\right\} - I_{dm} \\ \mathfrak{Im}\left\{\frac{\tilde{E}'_{dq1} - \tilde{V}_1 \cdot 1\angle\left(\frac{\pi}{2} - \theta_1\right)}{R_{a1} + jX'_{d1}}\right\} - I_{q1} \\ \vdots \\ \mathfrak{Im}\left\{\frac{\tilde{E}'_{dqm} - \tilde{V}_m \cdot 1\angle\left(\frac{\pi}{2} - \theta_m\right)}{R_{am} + jX'_{dm}}\right\} - I_{qm} \end{bmatrix} = \vec{g}_{IDQ} = \vec{0} \tag{3-61}$$

The set of algebraic equations is completed by adding the limiter equations of the generators' governors (Equation 2-197):

$$u_{Li} = \max\left\{\min\{P_{REFi} - u_{Di}, P_{MAXi}\}, 0\right\}, \qquad 1 \le i \le m \tag{3-62}$$

The complete set of DAEs comprising all system equations can be expressed as:

$$\dot{\vec{y}} = \vec{f}\left(\vec{x}, \vec{y}, \vec{z}\right) \tag{3-63a}$$

$$\vec{0} = \vec{g}\left(\vec{y}, \vec{z}, t\right) \tag{3-63b}$$

Where the dot superscript means time derivative and:

$$\begin{aligned} \vec{x} &= \left[K_{A1} \ \cdots \ K_{Am} \ R_1 \ \cdots \ R_m\right]^T \\ \vec{y} &= \big[\theta_1 \ \omega_1 \ E'_{d1} \ E'_{q1} \ V_{C1} \ V_{R1} \ E_{fd1} \ V_{f1} \ u_{D1} \ u_{S1} \ u_{B1} \ P_{M1} \ \cdots \\ &\quad \cdots \ \theta_m \ \omega_m \ E'_{dm} \ E'_{qm} \ V_{Cm} \ V_{Rm} \ E_{fdm} \ V_{fm} \ u_{Dm} \ u_{Sm} \ u_{Bm} \ P_{Mm}\big]^T \\ \vec{z} &= \left[\delta_1 \ \cdots \ \delta_n \ V_1 \ \cdots \ V_n \ I_{d1} \ \cdots \ I_{dm} \ I_{q1} \ \cdots \ I_{qm} \ u_{L1} \ \cdots \ u_{Lm}\right]^T \end{aligned}$$

$$\vec{g}\left(\vec{y}, \vec{z}, t\right) = \begin{bmatrix} \vec{g}_{PQ}\left(\vec{y}, \vec{z}, t\right) \\ \vec{g}_{IDQ}\left(\vec{y}, \vec{z}\right) \\ \max\left\{\min\{P_{REF1} - u_{D1}, P_{MAX1}\}, 0\right\} - u_{L1} \\ \vdots \\ \max\left\{\min\{P_{REFm} - u_{Dm}, P_{MAXm}\}, 0\right\} - u_{Lm} \end{bmatrix} \tag{3-64}$$

$$\vec{f}(\vec{x},\vec{y},\vec{z}) = \begin{bmatrix} \omega_s\left(\omega_1 - 1\right) \\ \frac{1}{2H_1}\left(P_{M1} - E'_{d1}I_{d1} - E'_{q1}I_{q1} - D_1\left(\omega_1 - 1\right)\right) \\ \frac{1}{T'_{q01}}\left(-E'_{d1} + \left(X_{q1} - X'_{q1}\right)I_{q1}\right) \\ \frac{1}{T'_{d01}}\left(E_{fd1} - E'_{q1} - \left(X_{d1} - X'_{d1}\right)I_{d1}\right) \\ \frac{1}{T_{R1}}\left(V_1 - V_{C1}\right) \\ \frac{1}{T_{A1}}\left[K_{A1}\left(V_{REF1} - V_{C1} - V_{f1}\right) - V_{R1}\right] u\left(V_{R1} - V_{RMIN1}\right) u\left(V_{RMAX1} - V_{R1}\right) \\ \frac{1}{T_{E1}}\left(V_{R1} - K_{E1}E_{fd1}\right) \\ \frac{1}{T_{F1}}\left(K_{F1}\frac{dE_{fd1}}{dt} - V_{f1}\right) \\ \frac{1}{T_{D1}}\left[\frac{1}{R_1}\left(\omega_1 - 1 + T_{\omega 1}\frac{d\omega_1}{dt}\right) - u_{D1}\right] \\ \frac{1}{T_{S1}}\left(u_{L1} - u_{S1}\right) \\ \frac{1}{T_{B1}}\left(u_{S1} - u_{B1}\right) \\ \frac{1}{T_{P1}}\left(u_{B1} + F_1 T_{P1}\frac{du_{B1}}{dt} - P_{M1}\right) \\ \vdots \\ \omega_s\left(\omega_m - 1\right) \\ \frac{1}{2H_m}\left(P_{Mm} - E'_{dm}I_{dm} - E'_{qm}I_{qm} - D_m\left(\omega_m - 1\right)\right) \\ \frac{1}{T'_{q0m}}\left(-E'_{dm} + \left(X_{qm} - X'_{qm}\right)I_{qm}\right) \\ \frac{1}{T'_{d0m}}\left(E_{fdm} - E'_{qm} - \left(X_{dm} - X'_{dm}\right)I_{dm}\right) \\ \frac{1}{T_{Rm}}\left(V_m - V_{Cm}\right) \\ \frac{1}{T_{Am}}\left[K_{Am}\left(V_{REFm} - V_{Cm} - V_{fm}\right) - V_{Rm}\right] u\left(V_{Rm} - V_{RMINm}\right) u\left(V_{RMAXm} - V_{Rm}\right) \\ \frac{1}{T_{Em}}\left(V_{Rm} - K_{Em}E_{fdm}\right) \\ \frac{1}{T_{Fm}}\left(K_{Fm}\frac{dE_{fdm}}{dt} - V_{fm}\right) \\ \frac{1}{T_{Dm}}\left[\frac{1}{R_m}\left(\omega_m - 1 + T_{\omega m}\frac{d\omega_m}{dt}\right) - u_{Dm}\right] \\ \frac{1}{T_{Sm}}\left(u_{Lm} - u_{Sm}\right) \\ \frac{1}{T_{Bm}}\left(u_{Sm} - u_{Bm}\right) \\ \frac{1}{T_{Pm}}\left(u_{Bm} + F_m T_{Pm}\frac{du_{Bm}}{dt} - P_{Mm}\right) \end{bmatrix} \tag{3-65}$$

Vector $\vec{z}$ correspond to the system algebraic variables. Vector $\vec{y}$ correspond to the system differential variables. Vector $\vec{x}$ correspond to the tunable parameters of the generators' controllers. It must be noted the the set of DAEs was constructed assuming all generators have AVRs and governors. This is not necessarily true (synchronous condensers do not have governor, and some machines may have simpler models than the ones exposed in this work), but it possible to remove or adjust the equations accordingly to fit the machines' characteristics.

The system transient response to a disturbance for the controller parameter values of $\vec{x}$ is given by $\vec{y}(\vec{x}, t)$ and $\vec{z}(\vec{x}, t)$, which are found by solving Equation 3-63. The simulation results are analysed to determine whether the system is stable (withstands the fault) or not (collapses). Instability can be detected when some of the differential variables, normally the rotor angles, diverge (increase or decrease without bounds). An example of a stable and an unstable system response of a power system with two generators is given in Figure **3-1**.

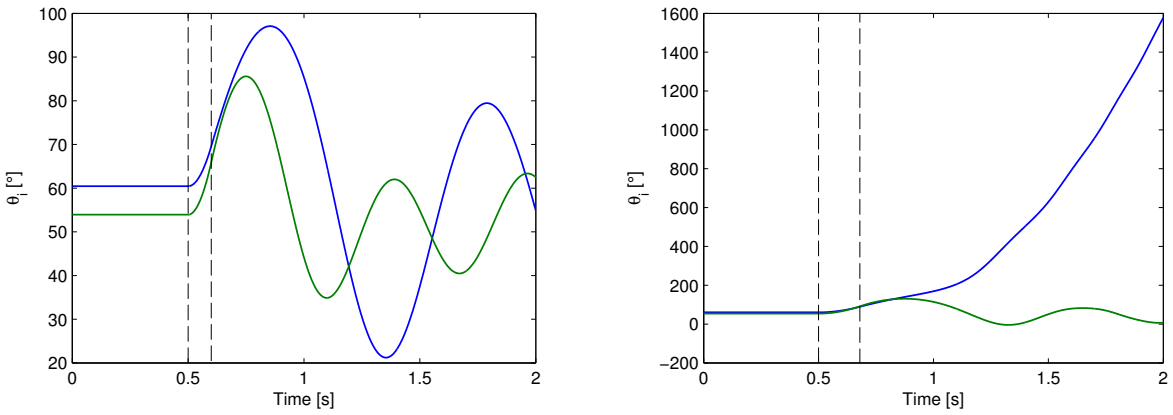

(a) Fault cleared at time 0.6 s (stable).

(b) Fault cleared at time 0.68 s (unstable).

Figure 3-1.: Rotor angles of the generators of a power system disturbed by a short-circuit at time 0.5 s. The fault is cleared at different times.

The set of DAEs has no explicit solution, so it must be solved numerically to find an approximate discretization of the transient response. The next subsections discuss the numerical methods implemented in the software developed in this work.

3.2.2. Explicit Euler Method

Consider the following first-order vectorial differential equation with initial value condition:

$$\dot{\vec{y}}(t) = \vec{f}(\vec{y}(t), t), \qquad \vec{y}(t_0) = \vec{y}_0 \tag{3-66}$$

The previous equation can be solved as:

$$\vec{y}(t) = \vec{y}_0 + \int_{t_0}^{t} \vec{f}(\vec{y}(\tau), \tau)\, d\tau \tag{3-67}$$

If the vector function $\vec{f}(\vec{y}(t), t)$ cannot be integrated analytically, then it is not possible to find the exact solution $\vec{y}(t)$. However, it is possible to approximate the solution as a discrete sequence of time-vector pairs $(t_0, \vec{y}[0])$, $(t_1, \vec{y}[1])$, $\cdots$. The sequence should be a

good approximation of the true time-vector solution pairs $(t_0, \vec{y}(t_0))$, $(t_1, \vec{y}(t_1))$, $\cdots$. The smaller the time between pairs, the better will be the sequence as an approximation of the exact solution. As the true value of $\vec{y}(t_0)$ is known (initial value condition), $\vec{y}[0]$ is set equal to $\vec{y}(t_0)$. The next term of the sequence (term 1) can be calculated as:

$$\vec{y}(t_1) = \vec{y}(t_0) + \int_{t_0}^{t_1} \vec{f}(\vec{y}(\tau), \tau)\, d\tau \tag{3-68}$$

$$\vec{y}(t_1) = \vec{y}[0] + \int_{t_0}^{t_1} \vec{f}(\vec{y}(\tau), \tau)\, d\tau \tag{3-69}$$

If the time difference $t_1 - t_0$ is small enough, it is possible to approximate the function $\vec{f}(\vec{y}(\tau), \tau)$ inside the integral as a function whose integral can be calculated analytically. The main difference between the numerical methods considered in this work lies in the approximation used for the integrand. For this reason, the numerical methods used to solve differential equations are also called *numerical integration methods*.

The Explicit Euler method assumes the integrand is constant and equal to the value of the original function at the time of the previous term, that is:

$$\vec{y}(t_1) \approx \vec{y}[0] + \int_{t_0}^{t_1} \vec{f}(\vec{y}(t_0), t_0)\, d\tau = \vec{y}[0] + \int_{t_0}^{t_1} \vec{f}(\vec{y}[0], t_0)\, d\tau \tag{3-70}$$

$$\vec{y}(t_1) \approx \vec{y}[0] + (t_1 - t_0)\, \vec{f}(\vec{y}[0], t_0) \tag{3-71}$$

$$\vec{y}(t_1) \approx \vec{y}[0] + h\vec{f}(\vec{y}[0], t_0) \tag{3-72}$$

Where $h = t_1 - t_0$ is called *step size*. The sequence term $\vec{y}[1]$ is set equal to this numerical approximation:

$$\vec{y}[1] = \vec{y}[0] + h\vec{f}(\vec{y}[0], t_0) \tag{3-73}$$

Assume the sequence is equally spaced in time, that is $t_k = t_0 + kh$. Then the rest of terms can be calculated inductively as:

$$\vec{y}[k+1] = \vec{y}[k] + h\vec{f}(\vec{y}[k], t_k) \tag{3-74}$$

The Explicit Euler method is of order 1, because the global approximation error is proportional to h^1. This method is called explicit because the term $k+1$ of the sequence can be calculated directly using the term k. One of the main disadvantages of the Explicit Euler method is that it is not A-stable [25]. This means the numerical solution may diverge (unstable) even when the true solution does not. Another problem is that the stability region of the method is relatively small. This implies that in order to generate a convergent solution it is normally required to use very small step sizes, and this greatly increases the computation time required to execute the method.

Notice that the Explicit Euler method (and the other methods that are going to be presented here) approximate the differential equations as algebraic equations. A set of DAEs can be solved by applying this or another numerical method and then solving the whole set of algebraic equations at each time step. By applying the Explicit Euler method to Equation 3-63, the following set of algebraic equations is obtained:

$$\vec{y}\left[\vec{x}, k+1\right] = \vec{y}\left[\vec{x}, k\right] + h\vec{f}\left[\vec{x}, \vec{y}\left[\vec{x}, k\right], \vec{z}\left[\vec{x}, k\right]\right] \tag{3-75a}$$

$$\vec{0} = \vec{g}\left[\vec{y}\left[\vec{x}, k+1\right], \vec{z}\left[\vec{x}, k+1\right], t_0 + (k+1)\,h\right] \tag{3-75b}$$

Where:

$$\begin{aligned} &\vec{y}\left[\vec{x}, k\right] \approx \vec{y}\left(\vec{x}, t_0 + kh\right) \\ &\vec{z}\left[\vec{x}, k\right] \approx \vec{z}\left(\vec{x}, t_0 + kh\right), \qquad \forall k > 0 \\ &\vec{y}\left[\vec{x}, 0\right] = \vec{y}\left(\vec{x}, t_0\right) \\ &\vec{z}\left[\vec{x}, 0\right] = \vec{z}\left(\vec{x}, t_0\right) \end{aligned}$$

Equation 3-75a can be evaluated directly. After that, Equation 3-75b is solved numerically to find $\vec{z}\left[\vec{x}, k+1\right]$. The calculation of the initial values $y\left(\vec{x}, t_0\right)$ and $\vec{z}\left(\vec{x}, t_0\right)$ is going to be discussed later.

3.2.3. Implicit Euler Method

The Implicit Euler method assumes the integrand in Equation 3-69 is constant and equal to the value of the original function at the time of the next term, that is:

$$\vec{y}\left(t_1\right) \approx \vec{y}\left[0\right] + \int_{t_0}^{t_1} \vec{f}\left(\vec{y}\left(t_1\right), t_1\right) d\tau \tag{3-76}$$

As $\vec{y}\left(t_1\right)$ cannot be exactly known, it is replaced by its approximation $\vec{y}\left[1\right]$:

$$\vec{y}\left(t_1\right) \approx \vec{y}\left[0\right] + \int_{t_0}^{t_1} \vec{f}\left(\vec{y}\left[1\right], t_1\right) d\tau \tag{3-77}$$

$$\vec{y}\left(t_1\right) \approx \vec{y}\left[0\right] + \left(t_1 - t_0\right)\vec{f}\left(\vec{y}\left[1\right], t_1\right) \tag{3-78}$$

$$\vec{y}\left(t_1\right) \approx \vec{y}\left[0\right] + h\vec{f}\left(\vec{y}\left[1\right], t_1\right) \tag{3-79}$$

The sequence term $\vec{y}\left[1\right]$ is set equal to this numerical approximation:

$$\vec{y}\left[1\right] = \vec{y}\left[0\right] + h\vec{f}\left(\vec{y}\left[1\right], t_1\right) \tag{3-80}$$

Assume the sequence is equally spaced in time, that is $t_k = t_0 + kh$. Then the rest of terms can be calculated inductively as:

$$\vec{y}\left[k+1\right] = \vec{y}\left[k\right] + h\vec{f}\left(\vec{y}\left[k+1\right], t_{k+1}\right) \tag{3-81}$$

The Implicit Euler method is of order 1, because the global approximation error is proportional to h[1]. This method is called implicit because the term $k+1$ is defined as a function of itself. For that reason, the term must be calculated by numerically solving Equation 3-81 (with Newton-Raphson method, for example). Therefore, one step of the Implicit Euler method requires a computation time much longer than one step of the Explicit Euler method. This is the main disadvantage of this method. On the other hand, this method is A-stable [25]. This implies that if the true solution is stable, then the numerical solution will be stable too[1] (the converse is not necessarilly true). Moreover, this method is L-stable [25], which means it can rapidly dampen oscillations produced by the stiff components of the equations[2]. One of the main advantages of this method is that it allows using large time steps without losing stability[3].

By applying the Implicit Euler method to Equation 3-63, the following set of algebraic equations is obtained:

$$\vec{y}\left[\vec{x}, k+1\right] = \vec{y}\left[\vec{x}, k\right] + h\vec{f}\left[\vec{x}, \vec{y}\left[\vec{x}, k+1\right], \vec{z}\left[\vec{x}, k+1\right]\right] \tag{3-82a}$$

$$\vec{0} = \vec{g}\left[\vec{y}\left[\vec{x}, k+1\right], \vec{z}\left[\vec{x}, k+1\right], t_0 + (k+1)\,h\right] \tag{3-82b}$$

Where:

$$\begin{aligned} &\vec{y}\left[\vec{x}, k\right] \approx \vec{y}\left(\vec{x}, t_0 + kh\right) \\ &\vec{z}\left[\vec{x}, k\right] \approx \vec{z}\left(\vec{x}, t_0 + kh\right), \qquad \forall k > 0 \\ &\vec{y}\left[\vec{x}, 0\right] = \vec{y}\left(\vec{x}, t_0\right) \\ &\vec{z}\left[\vec{x}, 0\right] = \vec{z}\left(\vec{x}, t_0\right) \end{aligned}$$

Equation 3-82a cannot be evaluated directly, so in order to find $\vec{y}\left[\vec{x}, k+1\right]$ and $\vec{z}\left[\vec{x}, k+1\right]$ both Equation 3-82a and Equation 3-82b must be solved simultaneously using a numerical method.

3.2.4. Implicit Trapezoidal Method

The Implicit Trapeziodal method assumes the integrand in Equation 3-69 varies linearly during the integration interval (the integral becomes simply the area of a trapezium), that

[1] The property of A-stability is defined for linear differential equations, so it might not hold true for nonlinear differential equations. However, in most cases the nonlinear equations can be approximated as linear ones. The A-stability also holds true for those cases.

[2] Again, the property of L-stability is defined for linear differential equations, but it also holds true for a large set of nonlinear differential equations.

[3] When solving DAEs, the Implicit Euler method with a large time step can even be faster than the Explicit Euler method. In this work that was the case.

is:

$$\vec{y}(t_1) \approx \vec{y}[0] + \int_{t_0}^{t_1} \left[\vec{f}(\vec{y}(t_0), t_0) + \frac{\tau - t_0}{t_1 - t_0} \left(\vec{f}(\vec{y}(t_1), t_1) - \vec{f}(\vec{y}(t_0), t_0) \right) \right] d\tau \tag{3-83}$$

$$\vec{y}(t_1) \approx \vec{y}[0] + \int_{t_0}^{t_1} \left[\vec{f}(\vec{y}[0], t_0) + \frac{\tau - t_0}{t_1 - t_0} \left(\vec{f}(\vec{y}(t_1), t_1) - \vec{f}(\vec{y}[0], t_0) \right) \right] d\tau \tag{3-84}$$

As $\vec{y}(t_1)$ cannot be exactly known, it is replaced by its approximation $\vec{y}[1]$:

$$\vec{y}(t_1) \approx \vec{y}[0] + \int_{t_0}^{t_1} \left[\vec{f}(\vec{y}[0], t_0) + \frac{\tau - t_0}{t_1 - t_0} \left(\vec{f}(\vec{y}[1], t_1) - \vec{f}(\vec{y}[0], t_0) \right) \right] d\tau \tag{3-85}$$

$$\vec{y}(t_1) \approx \vec{y}[0] + \frac{t_1 - t_0}{2} \left(\vec{f}(\vec{y}[0], t_0) + \vec{f}(\vec{y}[1], t_1) \right) \tag{3-86}$$

$$\vec{y}(t_1) \approx \vec{y}[0] + \frac{h}{2} \left(\vec{f}(\vec{y}[0], t_0) + \vec{f}(\vec{y}[1], t_1) \right) \tag{3-87}$$

The sequence term $\vec{y}[1]$ is set equal to this numerical approximation:

$$\vec{y}[1] = \vec{y}[0] + \frac{h}{2} \left(\vec{f}(\vec{y}[0], t_0) + \vec{f}(\vec{y}[1], t_1) \right) \tag{3-88}$$

Assume the sequence is equally spaced in time, that is $t_k = t_0 + kh$. Then the rest of terms can be calculated inductively as:

$$\vec{y}[k+1] = \vec{y}[k] + \frac{h}{2} \left(\vec{f}(\vec{y}[k], t_k) + \vec{f}(\vec{y}[k+1], t_{k+1}) \right) \tag{3-89}$$

The Implicit Trapezoidal method is of order 2, because the global approximation error is proportional to h^2. This method is called implicit because the term $k+1$ is defined as a function of itself. For that reason, the term must be calculated by numerically solving Equation 3-89 (with Newton-Raphson method, for example). Therefore, one step of the Implicit Trapezoidal method requires a computation time similar to one step of the Implicit Euler method, which is much longer than one step of the Explicit Euler method. This is the main disadvantage of this method. On the other hand, this method is marginally A-stable [25]. This implies that the numerical solution will be stable if and only if the true solution is stable too (in some cases when solving nonlinear differential equations, this might not hold true). However, this method is not L-stable [25], which means the stiff components of the equations can affect the solution by generating abnormally large oscillations that are not correctly damped. One of the main advantages of this method is that it allows using large time steps without losing stability.

Let us compare the Implicit Trapezoidal method with the Implicit Euler method. Implicit Trapezoidal has an order of accuracy of 2, but it is not L-stable. Implicit Euler is L-stable, but its order of accuracy is 1. Basically, Implicit Trapezoidal method is more accurate than the Euler methods (explicit and implicit). However, in some cases it can suffer heavy numerical oscillations in the solution, a problem that does not affect the Implicit Euler method.

Depending on the application and stiffness of the system, one method may be preferable over the other.

By applying the Implicit Trapezoidal method to Equation 3-63, the following set of algebraic equations is obtained:

$$\vec{y}\left[\vec{x}, k+1\right] = \vec{y}\left[\vec{x}, k\right] + \frac{h}{2}\left(\vec{f}\left[\vec{x}, \vec{y}\left[\vec{x}, k\right], \vec{z}\left[\vec{x}, k\right]\right] + \vec{f}\left[\vec{x}, \vec{y}\left[\vec{x}, k+1\right], \vec{z}\left[\vec{x}, k+1\right]\right]\right) \tag{3-90a}$$

$$\vec{0} = \vec{g}\left[\vec{y}\left[\vec{x}, k+1\right], \vec{z}\left[\vec{x}, k+1\right], t_0 + (k+1)\,h\right] \tag{3-90b}$$

Where:

$$\begin{aligned} &\vec{y}\left[\vec{x}, k\right] \approx \vec{y}\left(\vec{x}, t_0 + kh\right) \\ &\vec{z}\left[\vec{x}, k\right] \approx \vec{z}\left(\vec{x}, t_0 + kh\right), \qquad \forall k > 0 \\ &\vec{y}\left[\vec{x}, 0\right] = \vec{y}\left(\vec{x}, t_0\right) \\ &\vec{z}\left[\vec{x}, 0\right] = \vec{z}\left(\vec{x}, t_0\right) \end{aligned}$$

Equation 3-90a cannot be evaluated directly, so in order to find $\vec{y}\left[\vec{x}, k+1\right]$ and $\vec{z}\left[\vec{x}, k+1\right]$ both Equation 3-90a and Equation 3-90b must be solved simultaneously using a numerical method.

3.2.5. Heun (Explicit Trapezoidal) Method

The Heun method belongs to the family of predictor-corrector methods [15]. It assumes the integrand in Equation 3-69 varies linearly during the integration interval, just like the Implicit Trapezoidal method. However, instead of replacing the term $\vec{y}\left(t_1\right)$ in Equation 3-84 by its approximation $\vec{y}\left[1\right]$, the Heun method replaces it by the *predictor step* $\vec{y}\left[1\right]^{(p)}$:

$$\vec{y}\left(t_1\right) \approx \vec{y}\left[0\right] + \int_{t_0}^{t_1}\left[\vec{f}\left(\vec{y}\left[0\right], t_0\right) + \frac{\tau - t_0}{t_1 - t_0}\left(\vec{f}\left(\vec{y}\left[1\right]^{(p)}, t_1\right) - \vec{f}\left(\vec{y}\left[0\right], t_0\right)\right)\right] d\tau \tag{3-91}$$

$$\vec{y}\left(t_1\right) \approx \vec{y}\left[0\right] + \frac{t_1 - t_0}{2}\left(\vec{f}\left(\vec{y}\left[0\right], t_0\right) + \vec{f}\left(\vec{y}\left[1\right]^{(p)}, t_1\right)\right) \tag{3-92}$$

$$\vec{y}\left(t_1\right) \approx \vec{y}\left[0\right] + \frac{h}{2}\left(\vec{f}\left(\vec{y}\left[0\right], t_0\right) + \vec{f}\left(\vec{y}\left[1\right]^{(p)}, t_1\right)\right) \tag{3-93}$$

The sequence term $\vec{y}\left[1\right]$ is set equal to the *corrector step*, which corresponds to the previous numerical approximation:

$$\vec{y}\left[1\right] = \vec{y}\left[0\right] + \frac{h}{2}\left(\vec{f}\left(\vec{y}\left[0\right], t_0\right) + \vec{f}\left(\vec{y}\left[1\right]^{(p)}, t_1\right)\right) \tag{3-94}$$

Assume the sequence is equally spaced in time, that is $t_k = t_0 + kh$. Then the rest of terms can be calculated inductively as:

$$\vec{y}\left[k+1\right] = \vec{y}\left[k\right] + \frac{h}{2}\left(\vec{f}\left(\vec{y}\left[k\right], t_k\right) + \vec{f}\left(\vec{y}\left[k+1\right]^{(p)}, t_{k+1}\right)\right) \tag{3-95}$$

The predictor step $\vec{y}\,[k+1]^{(p)}$ is calculated by performing one step of the Explicit Euler method:

$$\vec{y}\,[k+1]^{(p)} = \vec{y}\,[k] + h\vec{f}\,(\vec{y}\,[k]\,, t_k) \tag{3-96}$$

The Heun method is of order 2, because the global approximation error is proportional to h^2. This method is of explicit type because the term $k+1$ can be calculated by direct evaluation of Equations 3-96 and 3-95. Therefore, one step of the Heun method requires a computation time much shorter than one step of either the Implicit Euler method or the Implicit Trapezoidal method. However, this method requires two evaluations of $\vec{f}$ per step, whereas the Explicit Euler method requires only one, and thus it is roughly two times faster. One of the main disadvantages of this method is that is not A-stable [25]. This means that the numerical solution may be unstable even when the true solution is stable. Another problem is that the stability region of this method is relatively small (although not as small as the stability region of the Explicit Euler method). This implies that in order to generate a convergent solution it is normally required to use very small step sizes, and this greatly increases the computation time required to execute the method.

By applying the Heun method to Equation 3-63, the following set of algebraic equations is obtained:

$$\vec{y}\,[\vec{x}, k+1]^{(p)} = \vec{y}\,[\vec{x}, k] + h\vec{f}\,[\vec{x}, \vec{y}\,[\vec{x}, k]\,, \vec{z}\,[\vec{x}, k]] \tag{3-97a}$$

$$\vec{0} = \vec{g}\left[\vec{y}\,[\vec{x}, k+1]^{(p)}\,, \vec{z}\,[\vec{x}, k+1]^{(p)}\,, t_0 + (k+1)\,h\right] \tag{3-97b}$$

$$\vec{y}\,[\vec{x}, k+1] = \vec{y}\,[\vec{x}, k] + \frac{h}{2}\left(\vec{f}\,[\vec{x}, \vec{y}\,[\vec{x}, k]\,, \vec{z}\,[\vec{x}, k]] + \vec{f}\left[\vec{x}, \vec{y}\,[\vec{x}, k+1]^{(p)}\,, \vec{z}\,[\vec{x}, k+1]^{(p)}\right]\right) \tag{3-97c}$$

$$\vec{0} = \vec{g}\,[\vec{y}\,[\vec{x}, k+1]\,, \vec{z}\,[\vec{x}, k+1]\,, t_0 + (k+1)\,h] \tag{3-97d}$$

Where:

$$\begin{aligned} &\vec{y}\,[\vec{x}, k] \approx \vec{y}\,(\vec{x}, t_0 + kh) \\ &\vec{z}\,[\vec{x}, k] \approx \vec{z}\,(\vec{x}, t_0 + kh)\,, \qquad \forall k > 0 \\ &\vec{y}\,[\vec{x}, 0] = \vec{y}\,(\vec{x}, t_0) \\ &\vec{z}\,[\vec{x}, 0] = \vec{z}\,(\vec{x}, t_0) \end{aligned}$$

Equation 3-97a can be evaluated directly. After that, Equation 3-97b is solved numerically to find $\vec{z}\,[\vec{x}, k+1]^{(p)}$. This procedure is then repeated for Equations 3-97c and 3-97d.

3.2.6. Initial Conditions and Setpoints of the Power System DAEs

As discussed at the start of the section, the objective of the time domain simulation is to study the behaviour of a power system after being perturbed by an external event. Before the

occurrence of the event the power system is, by design, operating at steady state. Therefore the initial value conditions required to implement any of the previously discussed methods are the steady state values of the power system differential and algebraic variables.

The steady state values can be found by performing the following procedure:

- First, let the controller parameter values be given by the vector $\vec{x}$:

$$[K_{A1} \ \cdots \ K_{Am} \ R_1 \ \cdots \ R_m]^T = \vec{x}$$

- The power flow of the original system (NOT the extended one) is solved to get the steady state voltages of the original system[4] $\vec{\tilde{V}}_{s0}$. Then the voltage angles and magnitudes are calculated as:

$$\vec{\delta}_0 = \arg\left\{\vec{\tilde{V}}_{s0}\right\} \tag{3-98}$$

$$\vec{V}_0 = \left|\vec{\tilde{V}}_{s0}\right| \tag{3-99}$$

- The admittance value of each constant admittance load is calculated as:

$$Y_{L0i} = \frac{S_{L0i}}{\left|\tilde{V}_{s0i}\right|^2} \tag{3-100}$$

  Where S_{L0i} is the steady state consumption of the load of node i. This step is only performed for nodes with constant admittance loads.

- The generator injected currents are calculated using the node equations (Equation 3-2):

$$\vec{\tilde{I}}_{G0} = \begin{bmatrix} \sum_{k=1}^{n} Y_{s1k}\tilde{V}_{s0k} \\ \vdots \\ \sum_{k=1}^{n} Y_{smk}\tilde{V}_{s0k} \end{bmatrix} + \left(\vec{S}_{L0} \oslash \vec{\tilde{V}}_{s0}\right)^* \tag{3-101}$$

  Where Y_{sij} is the ij of the admittance matrix of the original system and $\vec{S}_{L0}$ is the vector of steady state load consumptions.

- The steady state and transient EMFs in network reference are calculated as:

$$\vec{\tilde{E}}_0 = \begin{bmatrix} V_{s01} \\ \vdots \\ V_{s0m} \end{bmatrix} + \left(\begin{bmatrix} R_{a1} \\ \vdots \\ R_{am} \end{bmatrix} + j \begin{bmatrix} X_{q1} \\ \vdots \\ X_{qm} \end{bmatrix} \right) \circ \vec{\tilde{I}}_{G0} \tag{3-102}$$

[4] In steady state all loads are normally specified in terms of their consumed power. Hence, all loads must be treated as constant power loads during this initial power flow. The model parameters of the loads can be determined with using the voltages of the initial power flow [5].

$$\vec{\tilde{E}}'_0 = \begin{bmatrix} V_{s01} \\ \vdots \\ V_{s0m} \end{bmatrix} + \left(\begin{bmatrix} R_{a1} \\ \vdots \\ R_{am} \end{bmatrix} + j \begin{bmatrix} X'_{d1} \\ \vdots \\ X'_{dm} \end{bmatrix} \right) \circ \vec{\tilde{I}}_{G0} \tag{3-103}$$

- The steady state rotor angle is calculated as:

$$\vec{\theta}_0 = \arg\left\{ \vec{\tilde{E}}_0 \right\} \tag{3-104}$$

- The steady state values of the transient EMFs and currents in generator reference are calculated as:

$$\vec{\tilde{E}}'_{0dq} = \vec{\tilde{E}}'_0 \circ \left[1\angle \left(\frac{\pi}{2} - \vec{\theta}_0 \right) \right] \tag{3-105}$$

$$\vec{\tilde{I}}_{0dq} = \vec{\tilde{I}}_{G0} \circ \left[1\angle \left(\frac{\pi}{2} - \vec{\theta}_0 \right) \right] \tag{3-106}$$

  The subscript $0dq$ indicates the steady state value of the respective phasor. That subscript was selected over the subscript $dq0$ to avoid confusion, as the quantities here have nothing to do with the zero-axis.

- The steady state value of the converted electrical powers (provided by the transient EMFs) is:

$$\begin{aligned} \vec{P}_{e0} &= \mathfrak{Re}\left\{ \vec{\tilde{E}}'_{0dq} \right\} \circ \mathfrak{Re}\left\{ \vec{\tilde{I}}_{0dq} \right\} + \mathfrak{Im}\left\{ \vec{\tilde{E}}'_{0dq} \right\} \circ \mathfrak{Im}\left\{ \vec{\tilde{I}}_{0dq} \right\} \\ \vec{P}_{e0} &= \mathfrak{Re}\left\{ \vec{\tilde{E}}'_{0dq} \circ \vec{\tilde{I}}^{*}_{0dq} \right\} \end{aligned} \tag{3-107}$$

- The steady state speed of the generators is 1 p.u.:

$$\vec{\omega}_0 = \left[\vec{1} \right]_{m \times 1} \tag{3-108}$$

- In steady state, all derivatives are zero. Therefore the steady state mechanical powers of the generators are calculated using the differential equations of the speeds:

$$\begin{aligned} \vec{0} &= \vec{1} \oslash \begin{bmatrix} 2H_1 \\ \vdots \\ 2H_m \end{bmatrix} \circ \left(\vec{P}_{M0} - \vec{P}_{e0} - \begin{bmatrix} D_1 \\ \vdots \\ D_m \end{bmatrix} \circ \left(\vec{\omega}_0 - \vec{1} \right) \right) \\ \vec{P}_{M0} &= \vec{P}_{e0} \end{aligned} \tag{3-109}$$

- The steady state value of the differential variables of the generators' governors is found by setting the derivatives in the governors' equations and solving:

$$\vec{u}_{D0} = \left[\vec{0} \right]_{m \times 1} \tag{3-110}$$

$$\vec{u}_{L0} = \vec{P}_{M0} \tag{3-111}$$

$$\vec{u}_{S0} = \vec{P}_{M0} \tag{3-112}$$

$$\vec{u}_{B0} = \vec{P}_{M0} \tag{3-113}$$

- The steady state value of the generators' field voltages referred to stator is calculated from the differential equations of E'_{qi}:

$$\vec{0} = \vec{1} \oslash \begin{bmatrix} T'_{d01} \\ \vdots \\ T'_{d0m} \end{bmatrix} \circ \left(\vec{E}_{fd0} - \mathfrak{Im}\left\{\vec{\tilde{E}}'_{0dq}\right\} - \begin{bmatrix} X_{d1} - X'_{d1} \\ \vdots \\ X_{dm} - X'_{dm} \end{bmatrix} \circ \mathfrak{Re}\left\{\vec{\tilde{I}}_{0dq}\right\} \right)$$

$$\vec{E}_{fd0} = \mathfrak{Im}\left\{\vec{\tilde{E}}'_{0dq}\right\} + \begin{bmatrix} X_{d1} - X'_{d1} \\ \vdots \\ X_{dm} - X'_{dm} \end{bmatrix} \circ \mathfrak{Re}\left\{\vec{\tilde{I}}_{0dq}\right\} \tag{3-114}$$

- The steady state value of the differential variables of the generators' AVRs is found by setting the derivatives in the AVRs' equations and solving:

$$\vec{V}_{C0} = \begin{bmatrix} \left|\tilde{V}_{s01}\right| \\ \vdots \\ \left|\tilde{V}_{s0m}\right| \end{bmatrix} \tag{3-115}$$

$$\vec{V}_{R0} = \begin{bmatrix} K_{E1} \\ \vdots \\ K_{Em} \end{bmatrix} \circ \vec{E}_{fd0} \tag{3-116}$$

$$\vec{V}_{f0} = \left[\vec{0}\right]_{m\times 1} \tag{3-117}$$

- The initial values of the vectors $\vec{y}$ and $\vec{z}$ are:

$$\vec{y}\,(\vec{x}, t_0) = \mathrm{vec}\left(\left[\vec{\theta}_0 \ \vec{\omega}_0 \ \mathfrak{Re}\left\{\vec{\tilde{E}}'_{0dq}\right\} \ \mathfrak{Im}\left\{\vec{\tilde{E}}'_{0dq}\right\} \ \vec{V}_{C0} \ \vec{V}_{R0} \ \vec{E}_{fd0} \ \vec{V}_{f0} \ \vec{u}_{D0} \ \vec{u}_{S0} \ \vec{u}_{B0} \ \vec{P}_{M0} \right]^T \right) \tag{3-118}$$

$$\vec{z}\,(\vec{x}, t_0) = \mathrm{vec}\left(\left[\vec{\delta}_0 \ \vec{V}_0 \ \mathfrak{Re}\left\{\vec{\tilde{I}}_{0dq}\right\} \ \mathfrak{Im}\left\{\vec{\tilde{I}}_{0dq}\right\} \ \vec{u}_{L0} \right]^T \right) \tag{3-119}$$

Where the operator vec $(\cdot)$ transforms the input matrix into a column vector by concatenating the columns of the input matrix[5].

It must be noted that the AVR variable V_{Ri} and the governor variable u_{Li} are limited, so their steady state values must satisfy the following inequalities:

$$V_{RMINi} \leq V_{R0i} \leq V_{RMAXi} \tag{3-120a}$$

$$0 \leq u_{L0i} \leq P_{MAXi}, \qquad \forall\ 1 \leq i \leq m \tag{3-120b}$$

If the inequality does not hold for all the steady state values of the variables, that means the steady state for a power system those specific parameters does not exist.

To solve the set of DAEs, the setpoint value of the generators' controllers is also required. These can be found from the system steady state performance. The setpoints of the AVRs are calculated from the differential equations of V_{Ri}. As Inequality 3-120 must hold true, the limits of the equations can be ignored:

$$\vec{0} = \vec{1} \oslash \begin{bmatrix} T_{A1} \\ \vdots \\ T_{Am} \end{bmatrix} \circ \left(\begin{bmatrix} K_{A1} \\ \vdots \\ K_{Am} \end{bmatrix} \circ \left(\begin{bmatrix} V_{REF1} \\ \vdots \\ V_{REFm} \end{bmatrix} - \vec{V}_{C0} - \vec{V}_{f0} \right) - \vec{V}_{R0} \right)$$

$$\begin{bmatrix} V_{REF1} \\ \vdots \\ V_{REFm} \end{bmatrix} = \begin{bmatrix} K_{E1} \\ \vdots \\ K_{Em} \end{bmatrix} \oslash \begin{bmatrix} K_{A1} \\ \vdots \\ K_{Am} \end{bmatrix} \circ \vec{E}_{fd0} + \begin{bmatrix} \left|\tilde{V}_{s01}\right| \\ \vdots \\ \left|\tilde{V}_{s0m}\right| \end{bmatrix} \tag{3-121}$$

Similarly, the setpoints of the governors are calculated from the equations of u_{Li}:

$$\begin{bmatrix} P_{REF1} \\ \vdots \\ P_{REFm} \end{bmatrix} = \vec{P}_{M0} \tag{3-122}$$

[5]Let us define the matrix $\mathbf{A} \in \mathbb{R}^{n \times m}$ as:

$$\mathbf{A} = [\vec{a}_1\ \cdots\ \vec{a}_m], \qquad \vec{a}_i \in \mathbb{R}^n, \qquad 1 \leq i \leq m$$

Then the operator vec $(\cdot)$ is defined as:

$$\text{vec}\,(\mathbf{A}) = \left[\vec{a}_1^T\ \cdots\ \vec{a}_m^T\right]^T \in \mathbb{R}^{nm}$$

Where vec $(\mathbf{A})$ is a column vector of size nm.

3.2.7. Step Calculation of Numerical Integration Methods

As discussed before, the implicit methods for solving differential equations have their step defined as the solution of a system of nonlinear equations. This means each step must be calculated by numerically solving those equations. When explicit methods are used to solve a set of DAEs, it is also required to solve a system of nonlinear equations at each step. In this work the step calculation is performed by applying a modified variant of the Dishonest NR (Newton-Raphson) method. The objective of this subsection is to discuss the implementation of that method.

In order to generalize the implementation, the integration methods discussed in this work (except Heun method) will be treated as special cases of the more general *theta method* [36]. The step equations of the theta method is the following:

$$\vec{y}\left[k+1\right] = \vec{y}\left[k\right] + h\left(\left(1-\theta_{th}\right)\vec{f}\left(\vec{y}\left[k\right], t_k\right) + \theta_{th}\vec{f}\left(\vec{y}\left[k+1\right], t_{k+1}\right)\right) \tag{3-123}$$

Where the parameter θ_{th} (not to be confused with rotor angle) is constant during all steps. Notice that for $\theta_{th} = 0$, the theta method reduces to the Explicit Euler method. Similarly, Implicit Trapezoidal is a theta method with $\theta_{th} = \frac{1}{2}$ and Implicit Euler is a theta method with $\theta_{th} = 1$. Heun method does not correspond to any theta method, but nevertheless the implementation that is going to be discussed next can be easily applied to it. The step equation of theta method applied to the poser system DAEs is the following (for convenience it is assumed the simulation starts at $t_0 = 0$):

$$\vec{y}\left[\vec{x}, k+1\right] = \vec{y}\left[\vec{x}, k\right] + h\left(\left(1-\theta_{th}\right)\vec{f}\left[\vec{x}, \vec{y}\left[\vec{x}, k\right], \vec{z}\left[\vec{x}, k\right]\right] + \theta_{th}\vec{f}\left[\vec{x}, \vec{y}\left[\vec{x}, k+1\right], \vec{z}\left[\vec{x}, k+1\right]\right]\right) \tag{3-124a}$$

$$\vec{0} = \vec{g}\left[\vec{y}\left[\vec{x}, k+1\right], \vec{z}\left[\vec{x}, k+1\right], \left(k+1\right)h\right] \tag{3-124b}$$

Where:

$$\vec{y}\left[\vec{x}, 0\right] = \vec{y}\left(\vec{x}, 0\right)$$
$$\vec{z}\left[\vec{x}, 0\right] = \vec{z}\left(\vec{x}, 0\right)$$

The objective function that must be solved for the step calculation is:

$$\vec{f}_{th}\left(\vec{y}_{st}, \vec{z}_{st}, k\right) = \begin{bmatrix} \vec{y}\left[\vec{x}, k\right] + h\left(\left(1-\theta_{th}\right)\vec{f}\left[\vec{x}, \vec{y}\left[\vec{x}, k\right], \vec{z}\left[\vec{x}, k\right]\right] + \theta_{th}\vec{f}\left[\vec{x}, \vec{y}_{st}, \vec{z}_{st}\right]\right) - \vec{y}_{st} \\ \vec{g}\left[\vec{y}_{st}, \vec{z}_{st}, \left(k+1\right)h\right] \end{bmatrix} \tag{3-125}$$

In explicit methods $\vec{f}_{th}$ does not include the first term. The Jacobian of the objective function

is:

$$\mathbf{J}_{th} = \begin{bmatrix} \theta_{th}\frac{\partial \vec{f}[\vec{x},\vec{y}_{st},\vec{z}_{st}]}{\partial y_{st}^T} - \mathbf{I} & \theta_{th}\frac{\partial \vec{f}[\vec{x},\vec{y}_{st},\vec{z}_{st}]}{\partial z_{st}^T} \\ \frac{\partial \vec{g}[\vec{y}_{st},\vec{z}_{st},(k+1)h]}{\partial y_{st}^T} & \frac{\partial \vec{g}[\vec{y}_{st},\vec{z}_{st},(k+1)h]}{\partial z_{st}^T} \end{bmatrix} \tag{3-126}$$

Where $\mathbf{I}$ is an identity matrix of appropriate dimensions. In explicit methods the Jacobian only includes the last submatrix (the lower right one).

The algorithm to solve the power systems DAEs using an implicit integration method with Dishonest NR method for step calculation can be expressed as the following sequence of steps:

1. Define the time step h and the final simulation time t_{max}.
2. Define the following algorithm parameters: tol, $thresh$, $iter_{max}$. The default values used in this work for these parameters are:

$$\begin{aligned} tol &\leftarrow 10^{-3} \\ thresh &\leftarrow 5 \\ iter_{max} &\leftarrow 20 \end{aligned}$$

3. Calculate the steady state vectors $\vec{y}\,(\vec{x},0)$, $\vec{y}\,(\vec{x},0)$ and the controllers' setpoints. The initial values of the solution are:

$$\begin{aligned} \vec{y}\,[\vec{x},0] &\leftarrow \vec{y}\,(\vec{x},0) \\ \vec{z}\,[\vec{x},0] &\leftarrow \vec{z}\,(\vec{x},0) \end{aligned}$$

4. Calculate the Jacobian $\mathbf{J}_{th}$. The Jacobian will be kept the same during all the steps. Exceptions to this are the steps when a disturbance occurs or when slow convergence is detected. In both cases the Jacobian is recalculated.
5. $k \leftarrow 1$
6. If $kh > t_{max}$ go to step 17.
7. If a disturbance occurs at this step (or between this step and the previous one), update the admittance matrix and recalculate $\mathbf{J}_{th}$.
8. $\begin{bmatrix} \vec{y}\,[\vec{x},k] \\ \vec{z}\,[\vec{x},k] \end{bmatrix} \leftarrow \begin{bmatrix} \vec{y}\,[\vec{x},k-1] \\ \vec{z}\,[\vec{x},k-1] \end{bmatrix}$
9. $l \leftarrow 0, \quad l_2 \leftarrow 0$

10. $\vec{f}_{thl} \leftarrow \vec{f}_{th}\left(\vec{y}\left[\vec{x},k\right],\vec{z}\left[\vec{x},k\right],k\right)$

11. $$\begin{bmatrix} \vec{y}\left[\vec{x},k\right] \\ \vec{z}\left[\vec{x},k\right] \end{bmatrix} \leftarrow \begin{bmatrix} \vec{y}\left[\vec{x},k\right] \\ \vec{z}\left[\vec{x},k\right] \end{bmatrix} - \mathbf{J}_{th}^{-1}\vec{f}_{thl}$$

12. $l \leftarrow l+1, \quad l_2 \leftarrow l_2+1$

13. If $\left\|\vec{y}\left[\vec{x},k\right]\right\|_\infty < tol$ and $\left\|\vec{z}\left[\vec{x},k\right]\right\|_\infty < tol$ the next step has been found. Assign $k \leftarrow k+1$ and go back to step 6.

14. If $l \geq iter_{max}$ the next step could not be calculated. Print error message and go to step 18.

15. If $l_2 \geq thresh$ there is slow convergence. Recalculate $\mathbf{J}_{th}^{-1}$ and assign $l_2 \leftarrow 0$.

16. Go back to step 10.

17. Return solutions $\vec{y}$ and $\vec{z}$.

18. End algorithm.

The algorithm can be easily adapted to explicit methods by calculating $\vec{y}\left[\vec{x},k\right]$ directly and removing it from steps 8 and 11. Special care must be taken when implementing the Heun method, as it requires two NR iterations per step (see Equation 3-97).

3.3. Transient Stability Analysis: Energy Functions

One of the most important questions of transient stability analysis is how much time can a power system withstand a disturbance (fault) without becoming unstable. The maximum value of such time is called *Critical Clearing Time* (CCT) of that specific fault. The value of the CCT depends on the type of fault, its location, and the power system characteristics. The CCT of the fault presented in Figure **3-1** lies between 0.10 s and 0.18 s. The exact value of the CCT is of great interest for the design and coordination of the power system protections.

The CCT for a specific fault can be calculated using time-domain simulation by performing various simulations with different fault durations in a bisection-like procedure [28]. Each new simulation narrows down the range where the CCT lies until the desired accuracy is achieved. This procedure is basically a brute force approach and as such the computation time required is too high.

The evident need of fast methods of calculating the CCT is a problem that has been extensively studied in the past decades [1, 37, 38, 39, 40]. For the simple case of the Single Machine Infinite Bus (SMIB) system, the CCT can be calculated directly using a method known as the *Equal Area Criterion* [5]. For the general case of a power system with an arbitrary number of machines, there are various methods which are basically generalizations of the equal area criterion. These methods are based on the stability theory of energy functions developed by Lyapunov in 1892 [41]. They are usually called *direct methods* because they allow to calculate the CCT without the need of a complete time-domain simulation.

Before discussing any direct method it is convenient to rewrite the system DAEs in terms of the time, as the disturbances change the equations. In general, it is possible to recognize three conditions:

- **Pre-fault**: It is the system condition before the disturbances begin.
- **Fault**: It is the system condition during the fault (a short-circuit normally). It may include reclosing [4].
- **Post-fault**: It is the system condition after the fault has been cleared. The post-fault condition is normally different than the pre-fault condition (fault clearing normally requires the disconnection of the faulted line or element).

These three conditions can be expressed in equations as:

$$\dot{\vec{y}}(t) = \vec{f}_P(\vec{x}, \vec{y}(t), \vec{z}(t)), \qquad t < t_F \tag{3-127}$$
$$\vec{0} = \vec{g}_P(\vec{y}(t), \vec{z}(t), t), \qquad t < t_F \tag{3-128}$$
$$\dot{\vec{y}}(t) = \vec{f}_F(\vec{x}, \vec{y}(t), \vec{z}(t)), \qquad t_F \leq t < t_F + t_{cl} \tag{3-129}$$
$$\vec{0} = \vec{g}_F(\vec{y}(t), \vec{z}(t), t), \qquad t_F \leq t < t_F + t_{cl} \tag{3-130}$$
$$\dot{\vec{y}}(t) = \vec{f}(\vec{x}, \vec{y}(t), \vec{z}(t)), \qquad t_F + t_{cl} < t \tag{3-131}$$
$$\vec{0} = \vec{g}(\vec{y}(t), \vec{z}(t), t), \qquad t_F + t_{cl} < t \tag{3-132}$$

Where f_P and g_P represent the pre-fault DAEs, f_F and g_F represent the fault DAEs and f and g represent the post-fault DAEs. The pre-fault condition is of minimal interest as it corresponds to the steady state of the power system. The fault condition determines the initial state of the post-fault condition. The post-fault condition determines the stability of the system under the given fault. In conclusion, the stability of the system is reduced to the stability of the set of DAEs described by Equation 3-131 and 3-132, given the initial conditions determined by Equations 3-129 and 3-130. The CCT then corresponds to the maximum value of t_{cl} for which the post-fault condition is stable.

3.3.1. Lyapunov's Method

Define the following system of autonomous (time independent) differential equations with equilibrium point (steady state) at the origin:

$$\dot{\vec{y}} = \vec{f}(\vec{y}) \tag{3-133}$$

$$\vec{0} = \vec{f}\left(\vec{0}\right) \tag{3-134}$$

In systems where the equilibrium point (EP) is not at the origin a simple substitution of variables can shift the state-space in order to have the EP at the origin, so there is no loss of generality. Lyapunov established in his work that the stability of an EP of a set of differential equations can be asserted without numerical integration. The only requirement is the definition of what is called *Lyapunov function* or *energy function* $W(\vec{y})$. It is possible to define various energy functions for the same set of differential equations. The EP is *asymptotically stable* [42] if and only if there exists at least one energy function satisfying the following conditions over the neighbourhood (also called *region of attraction* or *stability region*) of the EP [4]:

- $W(\vec{y}) > 0, \qquad \vec{y} \neq \vec{0}$
- $W\left(\vec{0}\right) = 0$
- $\frac{dW(\vec{y})}{dt} = \sum_i \frac{\partial W(\vec{y})}{\partial y_i} f_i(\vec{y}) = \vec{\nabla} W(\vec{y})^T \vec{f}(\vec{y}) < 0, \qquad \vec{y} \neq \vec{0}$

Another way of asserting the stability of the EP is by using the *Local Invariant Set Theorem* [42]. This theorem establishes that if the energy function satisfies the inequality $\frac{dW(\vec{y})}{dt} \leq 0$ in a region of the form $W < W_l$ that only contains the EP of interest, then that EP is asymptotically stable. Furthermore, the system state will converge to that EP if the initial point is inside that region.

In the context of power systems, one main conclusion can be drawn: if the fault condition drives the initial state of the post-fault condition outside the region of attraction of the stable EP (SEP), the system will become unstable. Otherwise, the system is stable. The stability problem has been reduced to two subproblems: the construction of a suitable energy function for the power system DAEs and the determination of the largest stability region.

For general power system no suitable energy functions have been found yet [4, 43]. On top of that, Lyapunov's method cannot be applied to non-autonomous equations (a power system perturbed by stochastic load, for example). If these conditions are ignored, direct methods can still be applied. The results will not be exact but they will be accurate enough (although having no theoretical validity). The subproblems now are the construction of an energy function and the determination of a stability region that minimizes the introduced error.

3.3.2. Center of Inertia (COI) Transformation

Before deriving the energy function used in this work, it is convenient to introduced a transformation of the variables that simplify the expressions of the energy function. First, let us define the *Center of Inertia* (COI) of the rotor speeds and angles as:

$$\theta_o = \frac{1}{H_T}\sum_{i=1}^{m} H_i\theta_i \tag{3-135}$$

$$\omega_o = \frac{1}{H_T}\sum_{i=1}^{m} H_i\omega_i \tag{3-136}$$

Where:

$$H_T = \sum_{i=1}^{m} H_i \tag{3-137}$$

The COI transformation for rotor angles and speeds is defined as:

$$\overline{\theta}_i = \theta_i - \theta_o \tag{3-138}$$

$$\overline{\omega}_i = \omega_i - \omega_o \tag{3-139}$$

Where $1 \leq i \leq m$. The COI transformation can be applied to electrical angles too:

$$\overline{\delta}_i = \delta_i - \theta_o \tag{3-140}$$

Where $1 \leq i \leq n$. Notice that θ_o and ω_o vary with respect to time, so the transformation must be applied at each time instant considered.

3.3.3. Transient Energy Function (TEF)

The energy function in Lyapunov's method is a generalization of the energy in mechanical systems. One common example is a spring-mass system. The energy function of that system is simply the sum of the kinetic energy of the mass and the potential energy of the spring. The energy is calculated as *the first integral of the motion*. By analogy, the first candidate energy function for power systems is the first integral of motion. In fact, this candidate has been used previously with satisfactory results [4]. In this work the energy function used is a simplified version of the first integral of motion which is discussed in [43]. The function also includes a term that takes into account the transfer conductances of the power system [4]. The function was derived following the suppositions of section 3.2, specially the no-saliency assumption, and is showed next:

$$W\left(\vec{y}\left(t\right),\vec{z}\left(t\right),t\right) = W_{KE}\left(\vec{y}\left(t\right),\vec{z}\left(t\right),t\right) + W_{PE}\left(\vec{y}\left(t\right),\vec{z}\left(t\right),t\right) \tag{3-141}$$

$$W_{KE}\left(\vec{y}\left(t\right),\vec{z}\left(t\right),t\right) = \omega_s\sum_{i=1}^{m} H_i\overline{\omega}_i^2 \tag{3-142}$$

$$W_{PE}\left(\vec{y}\left(t\right),\vec{z}\left(t\right),t\right)=\sum_{i=1}^{8}W_{PEi} \tag{3-143}$$

Where each potential energy term is defined as (dependence on $\vec{y}\left(t\right)$, $\vec{z}\left(t\right)$ and t is omitted):

$$W_{PE1}=-\sum_{i=1}^{m}\int_{t_F}^{t}D_i\left(\frac{d\overline{\theta}_i\left(\tau\right)}{dt}\right)^2 d\tau \tag{3-144}$$

$$W_{PE2}=-\sum_{i=1}^{m}\int_{t_F}^{t}P_{mi}\left(\tau\right)\left(\frac{d\overline{\theta}_i\left(\tau\right)}{dt}\right)d\tau \tag{3-145}$$

$$W_{PE3}=\sum_{i=1}^{n}\int_{t_F}^{t}P_{li}\left(\tau\right)\left(\frac{d\overline{\delta}_i\left(\tau\right)}{dt}\right)d\tau \tag{3-146}$$

$$W_{PE4}=\sum_{i=1}^{n}\int_{t_F}^{t}\frac{Q_{li}\left(\tau\right)}{V_i\left(\tau\right)}\left(\frac{dV_i}{dt}\right)dt \tag{3-147}$$

$$\begin{aligned}W_{PE5}=&\frac{1}{2}\left[\sum_{i=1}^{m}\left(E'_{di}\left(t\right)I_{di}\left(t\right)+E'_{qi}\left(t\right)I_{qi}\left(t\right)\right)-\sum_{j=1}^{n}Q_{li}\left(t\right)\right]\\&-\frac{1}{2}\left[\sum_{i=1}^{m}\left(E'_{di}\left(t_F\right)I_{di}\left(t_F\right)+E'_{qi}\left(t_F\right)I_{qi}\left(t_F\right)\right)-\sum_{j=1}^{n}Q_{li}\left(t_F\right)\right]\end{aligned} \tag{3-148}$$

$$W_{PE6}=\sum_{i=1}^{m}\int_{t_F}^{t}I_{di}\left(\tau\right)\left(\frac{dE'_{qi}\left(\tau\right)}{dt}\right)d\tau \tag{3-149}$$

$$W_{PE7}=-\sum_{i=1}^{m}\int_{t_F}^{t}I_{qi}\left(\tau\right)\left(\frac{dE'_{qi}\left(\tau\right)}{dt}\right)d\tau \tag{3-150}$$

$$W_{PE8}=\frac{1}{2}\sum_{i=1}^{n}\sum_{j=1}^{n}\int_{t_F}^{t}G_{ij}\left(\tau\right)V_i\left(\tau\right)V_j\left(\tau\right)\cos\left(\overline{\delta}_i\left(\tau\right)-\overline{\delta}_j\left(\tau\right)\right)\left(\frac{d\left(\overline{\delta}_i+\overline{\delta}_j\right)\left(\tau\right)}{dt}\right)d\tau \tag{3-151}$$

As the energy function is expressed in terms of COI variables, it is also called *Transient Energy Function* (TEF) [4]. The terms $P_{li}\left(t\right)$ and $Q_{li}\left(t\right)$ are the active and reactive power demanded by the nonlinear load of node i, respectively. The term $G_{ij}\left(t\right)$ is the real part of $Y_{ij}\left(t\right)$, the ij element of the admittance matrix at time t. The time dependence is stated because of the possible presence of time-varying admittance loads (stochastic loads, for example). The integrals with respect to time imply that the TEF not only depends on the initial point of the post-fault condition, but **how** the system state was driven to that point. Therefore, in order to evaluate the TEF it is necessary to perform a time-domain simulation of the fault condition. Even though a simulation is required, the post-fault condition does not need to be simulated. This greatly reduces the computation time required. The integrals in the TEF can be evaluated numerically with one of the methods presented previously. In this work the integrals were always evaluated using the Implicit Trapezoidal method, even if the simulation was performed using another method. The reason is because Implicit Trapezoidal

introduces a smaller approximation error.

It must be noted that the TEF is constructed for the post-fault equations but it was defined to be zero at the **pre-fault** EP instead of the post-fault EP. There is no problem in doing so, as it will be seen in the next subsection.

3.3.4. Potential Energy Boundary Surface (PEBS) Method

Having defined a TEF, now it is necessary to determine an appropriate stability region. In order to do so, let us refer again to the Local Invariant Set Theorem. This theorem allows asserting the stability of the system in terms of regions of the form $W < W_l$. Therefore, the **largest** stability region can be approximated as $W < W_{cr}$, where W_{cr} is called *critical energy*. Regions of the form $W < W_{cr}$ where W is defined to be zero at the SEP are equivalent to regions of the form $W' < W'_{cr}$ where W' is defined to be zero at another point (the pre-fault EP) [43]. Therefore, the TEF defined in the previous subsection can be used to calculate the stability region of a power system.

Recalling that the fault condition drives the initial point away from the SEP, if the fault lasts long enough it will end up driving the initial point outside of the stability region. Hence, the time instant at which the initial point crosses the stability boundary is:

$$t_{cr} = t_F + t_{CCT} \tag{3-152}$$

Where t_{CCT} is the CCT. The boundary of the stability region is clearly of the form $W = W_{cr}$. Then, t_{cr} is the time at which $W = W_{cr}$. In conclusion, the problem of calculating the CCT reduces to calculating W_{cr}.
There are various methods in the literature for calculating W_{cr}. One logical approach would be to calculate W_{cr} as the largest value of W_l that satisfies the conditions of the Local Invariant Set Theorem. Such calculation cannot be performed exactly, but it can be approximated, as proposed in [38]. The problem is this approach yields very conservative results because the true largest stability region is not necessarily of the form $W < W_{cr}$.

The method implemented in this work is the *Potential Energy Boundary Surface* (PEBS) method proposed in [39], which is based on the equal area criterion. Figure **3-2** shows the potential TEF of a SMIB system using the classical model for the generator (constant E'_{di} and E'_{qi}) [4], and without controllers. The stable equilibrium point is marked with a black dot. With the previous simplifications the potential TEF only depends on the rotor angle θ (subscript dropped because the SMIB only have one generator). In the context of the equal area criterion, the power system can be thought as trying to remove the excess kinetic energy injected by the fault to the generators. In order to do so, the system converts that energy

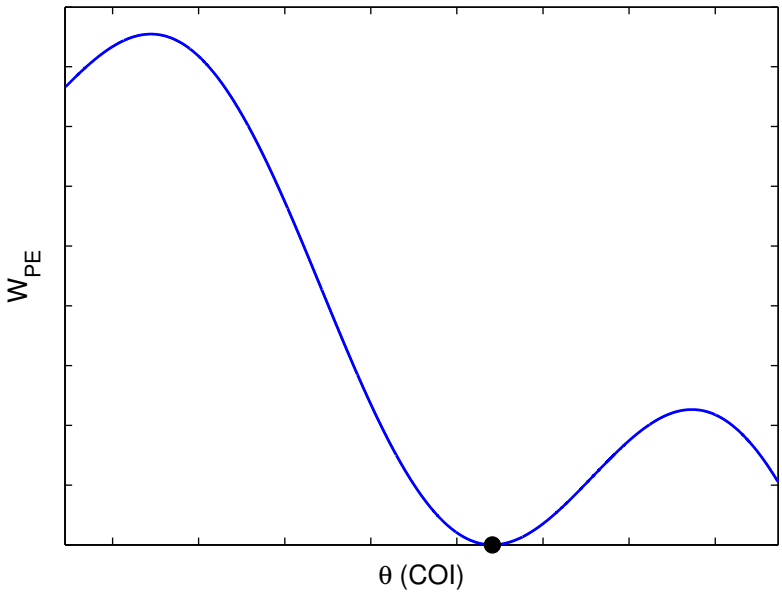

Figure 3-2.: Potential transient energy function of a SMIB system.

into electrical (potential) energy. However, the potential energy is bounded (see Figure **3-2**), so the system cannot remove infinite amounts of kinetic energy. If the total energy surpasses one of the relative maxima of the potential energy, the system will not be able to convert all the excess kinetic energy. This implies the generator speed will never settle to the synchronous value, the rotor angle will increase (or decrease) without bound and the system will be unstable.

Graphically, the system state can be thought as a ball rolling inside a bowl formed by the potential energy graph. When the total energy of the system exceeds one of the relative maxima of the potential energy, the ball will exit the bowl to keep rolling infinitely without ever returning (instability). Otherwise, the ball will keep rolling inside the bowl until it settles down at the bottom (the SEP). The stability region of the SMIB is simply the interval between the two relative maxima shown in Figure **3-2** (the bowl).

The PEBS method is a generalization of the bowl analogy to multimachine power systems. It is based on two suppositions:

- The potential TEF of the multimachine power system conforms a multidimensional "bowl" (for example, see Figure **3-3**).
- The stability region corresponds to the bowl. Therefore, the boundary of the region corresponds to the rim of the bowl.

The execution of the PEBS method is straightforward. The energy function is evaluated multiple times, each one increasing the time value, until the maximum value of the potential

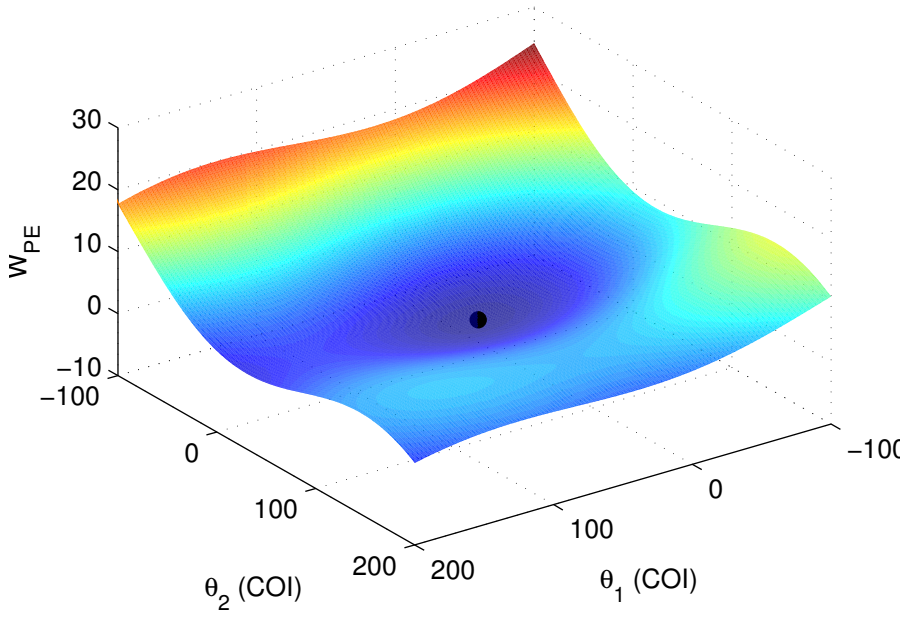

Figure 3-3.: Potential transient energy function of a two-generator system with infinite bus (adapted from [1]).

energy **over the fault trajectory** is found. This value is the critical energy, that is:

$$W_{cr} = \max_{t} W_{PE} \tag{3-153}$$

Then t_{cr} is calculated as the time at which $W = W_{cr}$. Finally, the CCT is calculated from Equation 3-152. Figure **3-4** shows the application of the PEBS method graphically.
There may be cases with various possible values of t_{cr}. In this work it is assumed that the CCT always corresponds to the **lowest** possible value of t_{cr} at which $W = W_{cr}$.

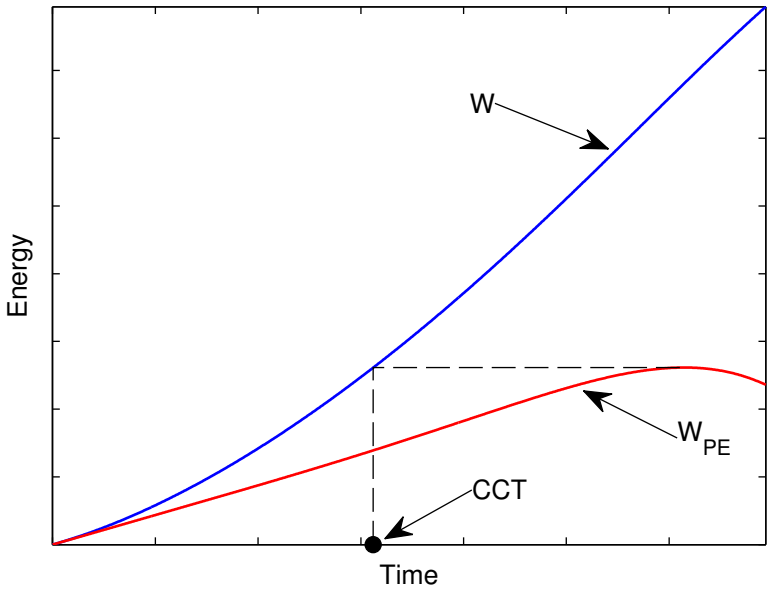

Figure 3-4.: Calculation of the CCT using the PEBS method and assuming $t_F = 0$ (adapted from [2]).

4. Proposed Tuning Methods

The analysis methods described in the previous chapter provide the necessary information to assess the power system and the controllers' response. This chapter presents two proposed methods for controller tuning using the described analysis methods. One method is focused on minimizing the steady state perturbations of the system, whereas the other one is focused on improving the fault response. Both methods take into account the stochastic perturbations produced by the load variations. In order to not having to modify the existent analysis methods to include stochastic effects, a simple approach for treating the stochastic load perturbations as time-dependent deterministic effects is proposed in the next section.

4.1. Stochastic Load Modelling

The main focus of this work is to take into account the stochastic variations in the power consumption of the loads. A load in a transmission system can represent the consumption of a whole city, with all the devices that are being turned on and off continuously. These events produce unpredictable changes on the consumption of the load. As these variations cannot be known with certainty, it is necessary to use appropriate stochastic models to represent them. Stochastic load effects have already been studied in the literature [44, 2, 45, 46]. This work follows the models of [44] and [2] and represents the stochastic load variations as *White Gaussian Noise* (WGN). WGN is defined as the derivative of a standard Wiener process $W_P = \{W_P(t),\ t \geq 0\}$ (do not confuse W_P with an energy function) which satisfies the following conditions [44]:

- $W_P(t)$ is continuous.
- $W_P(0) = 0$ with probability 1.
- For any $t \geq 0$, $W_P(t)$ is a random normal variable with variance t. That is:

$$W_P(t) \sim \mathcal{N}(0, t)$$

- The process is independent of its previous values. The difference between two values belongs to the following distribution:

$$W_P(t+h) - W_P(t) \sim \mathcal{N}(0, h), \qquad t, h > 0$$

Where $\mathcal{N}(\mu, \sigma^2)$ denotes a normally distributed random variable with mean μ and variance σ^2. One important property of the normal distribution is the following one:

$$X \sim \mathcal{N}\left(\mu, \sigma^2\right) \Leftrightarrow kX \sim \mathcal{N}\left(k\mu, k^2\sigma^2\right), \qquad k, \mu, \sigma \in \mathbb{R}, \qquad \sigma \geq 0$$

The standard Wiener process can be discretized using a time step h as follows:

$$W_P[k+1] = W_P[k] + \sqrt{k}\xi[k], \qquad W_P[k] = 0$$

Where $W_P[k]$ is the discretized value of $W_P(kh)$ and $\xi[k] \sim \mathcal{N}(0, 1)$.

In this work only constant power and constant admittance loads are considered. For constant power loads the model adopted is the one proposed in [44]. Let $S_{Li}(t)$ be the power consumption of the load of node i at time t, then such consumption can be expressed as:

$$S_{Li}(t) = S_{L0i}(1 + \lambda_i dW_i(t)) = P_{Li}(t) + jQ_{Li}(t) \tag{4-1}$$

Where S_{L0i} is the steady state load consumption and $dW_i(t)$ is a WGN variable. Similarly, for constant admittance loads the model adopted is the one proposed in [2]. Let $Y_{Li}(t)$ be the admittance of the load of node i at time t, then such admittance can be expressed as:

$$Y_{Li}(t) = Y_{L0i}(1 + \lambda_i dW_i(t)) = G_{Li}(t) + jB_{Li}(t) \tag{4-2}$$

Where Y_{L0i} is the steady state admittance. The load processes are independent: $dW_i(t_1)$ and $dW_j(t_2)$ are independent for any valid values of i, j, t_1 and t_2. Notice that these models assume that the power factor remains constant.

The previous models assume the mean load consumption (or admittance) does not change. The previous assumption is not always acceptable. The mean load consumption experiments very low frequency changes associated with the daily (and weekly) periodicity of the load. As this change is very slow, it can be modelled approximately as a linear change. Again, the nature of this change cannot be exactly determined. Thus, the slope of the linear variation is a stochastic variable. The final model for constant power loads can be written as:

$$S_{Li}(t) = S_{L0i}(1 + \lambda_i dW_i(t))(1 + \rho_i t) = P_{Li}(t) + jQ_{Li}(t) \tag{4-3}$$

And for constant admittance loads as:

$$Y_{Li}(t) = Y_{L0i}(1 + \lambda_i dW_i(t))(1 + \rho_i t) = G_{Li}(t) + jB_{Li}(t) \tag{4-4}$$

Where the slope ρ_i is constant during a single observation but varies between observations.

The load variations are stochastic processes that affect the power system response. In fact, the response of the system affected by a stochastic process is a stochastic process as well.

This means the system response now is described by a set of Stochastic Differential Algebraic Equations (SDAEs) instead of a set of DAEs. There are methods for solving sets of SDAEs [44], but they are far more complex than the numerical integration methods explained before, specially when applied to sets of equations of arbitrary size.

One critical observation is that stochastic processes of Equations 4-3 and 4-4 are **independent** of the system response. This implies the stochastic process of the loads and the stochastic process of the system response are **decoupled**, and thus do not need to be calculated simultaneously.

Based on the previous observation, this work proposes the following two-step procedure for calculating observations of the system response:

1. The load variations are calculated first, and the resulting observations are be treated as time-varying deterministic load profiles.

2. Each load profile is inputted to the deterministic power system model (previous chapter) and the response for each input is calculated. The obtained system responses are the desired observations.

The idea is to seize the fact that the loads are the only stochastic components of the power system. By calculating the observations of the loads first, the rest of the process becomes deterministic. After that it can be solved using standard numerical integration methods. Figure **4-1** shows graphically this procedure.

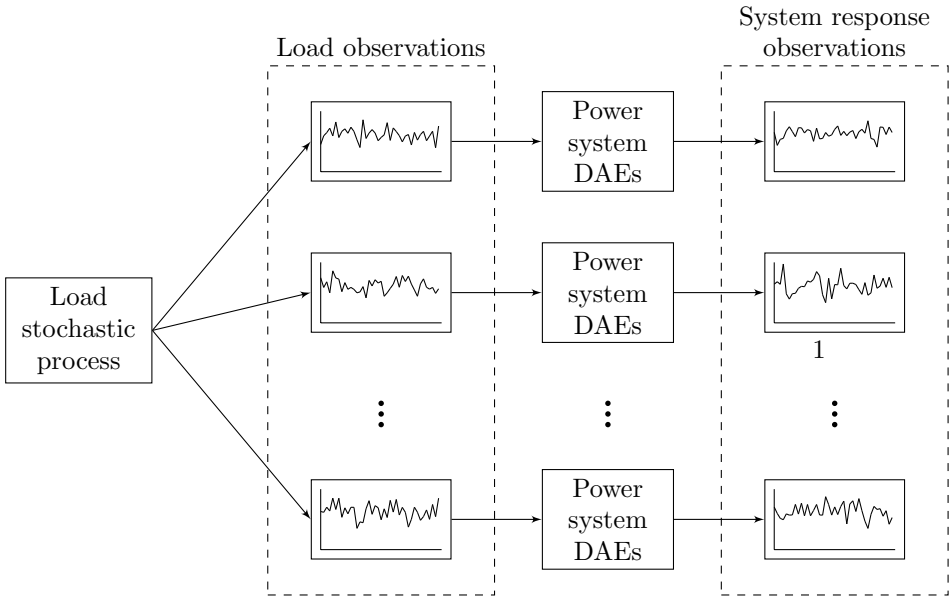

Figure 4-1.: Procedure for calculating the observations of the power system response.

The load variation processes must de discretized in order to be used in Step 2. For constant power loads Equation 4-3 is discretized using a time step h as:

$$S_{Li}[k] = S_{L0i}\left(1 + \lambda_i\sqrt{h}\xi_i[k]\right)(1 + \rho_i hk) = P_{Li}[k] + jQ_{Li}[k] \tag{4-5}$$

Where $S_{Li}[k]$ is the discretized value of $S_{Li}(kh)$ and $\xi_i[k] \sim \mathcal{N}(0,1)$. Similarly, for constant admittance loads Equation 4-4 is discretized using a time step h as:

$$Y_{Li}[k] = Y_{L0i}\left(1 + \lambda_i\sqrt{h}\xi_i[k]\right)(1 + \rho_i hk) = G_{Li}[k] + jB_{Li}[k] \tag{4-6}$$

Where $Y_{Li}[k]$ is the discretized value of $Y_{Li}(kh)$. In this work the slopes ρ_i will be assumed to follow an uniform distribution. The load processes are independent: $\xi_i[k]$ and $\xi_j[l]$ are independent for any valid values of i, j, k and l. Similarly, ρ_i and ρ_j are independent for any valid values of i and j. The variables $\xi_i[k]$ and ρ_i can be calculated using a Random Number Generator (RNG).

4.2. Steady State Tuning

The stochastic load variations affect the power systems continuously, all the time. Even when no disturbances are present, strictly speaking the power system is not at steady state. The system keeps oscillating continuously around the SEP because the loads are continuously perturbing it. This is illustrated in Figure **4-2**. The magnitude of the oscillations is small, but that does not make them less problematic. Small oscillations can produce *resonance* in the power system, eventually leading it to instability[1]. This section discusses the first tuning method proposed, which aims to minimize the steady state oscillations produced by the stochastic load variations.

The purpose of the AVR is to keep the voltage of its respective generator at its specified (steady state) value. Ideally, the control action of the AVR should keep the generator voltage constant regardless of any transient event happening on the system. In reality the generator voltage suffers a transient variation after the event occurs, and the magnitude of such variation is a measure of the quality of the AVR. Therefore, the AVR tuning can be performed by minimizing the magnitude of the transient variations of the voltage. More formally, such variations can be measured using an error integral criterion like the Integral Absolute Error (IAE). Applying the IAE criterion to the AVR of generator i yields (assuming the time period of interest starts at 0):

$$IAEV_i(\vec{x}) = \int_0^\infty |V_i(\vec{x}, t) - V_{0i}|\, dt \tag{4-7}$$

[1]This phenomenon is the main subject of study of the the field of *small-signal stability* [15, 4, 22].

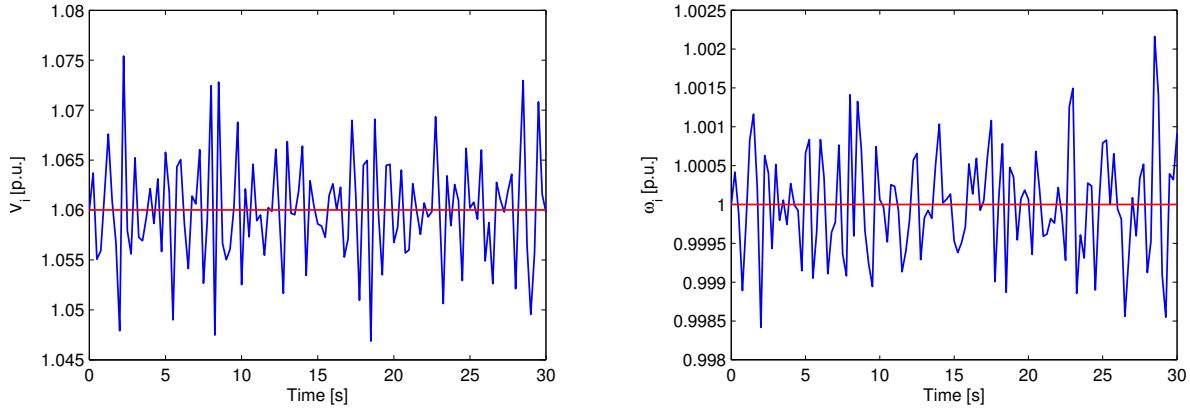

(a) Generator voltage.

(b) Generator speed.

Figure 4-2.: Simulation of a generator in a system with stochastic load perturbation (observed response in blue, ideal response in red).

Where $V_i(\vec{x}, t)$ is the voltage at time t of generator i given the controller parameter values of $\vec{x}$, and $V_{0i} = V_i(\vec{x}, 0)$. The voltage curve can be found, along with the rest of the system variables, through time-domain simulation. The simulation (and thus the generator voltage), depend on $\vec{x}$. It must be noted that the steady state value of the voltage is independent of the controller and thus it is written as the constant V_{0i}. Notice that as $V_i(\vec{x}, t)$ is found through the simulation, the voltage is only known up to the final simulation time t_f and the integral in (26) must be truncated:

$$IAEV_i(\vec{x}) = \int_0^{t_f} |V_i(\vec{x}, t) - V_{0i}|\, dt \tag{4-8}$$

Similarly, applying the IAE criterion to the governor of generator i yields:

$$IAE\omega_i(\vec{x}) = \int_0^{t_f} |\omega_i(\vec{x}, t) - 1|\, dt \tag{4-9}$$

A single metric of quality of the response of the power system generators can constructed as a weighted sum of all the previously defined IAEs:

$$f_s(\vec{x}) = \frac{\sum_{i=1}^{m} [w_{Vi} IAEV_i(\vec{x}) + w_{\omega i} IAE\omega_i(\vec{x})]}{\sum_{i=1}^{m} [w_{Vi} + w_{\omega i}]} \tag{4-10}$$

$$f_s(\vec{x}) = \frac{\sum_{i=1}^{m} \left[w_{Vi} \int_0^{t_f} |V_i(\vec{x}, t) - V_{0i}|\, dt + w_{\omega i} \int_0^{t_f} |\omega_i(\vec{x}, t) - 1|\, dt\right]}{\sum_{i=1}^{m} [w_{Vi} + w_{\omega i}]} \tag{4-11}$$

It is evident that if the value of $f_s(\vec{x})$ is smaller, the response of the system generators is better. The vales of the weights can be adjusted to give more importance to certain generators. In this work the value of w_{Vi} was set to 1 if generator i had AVR. If not w_{Vi} was set

to 0. Similarly, the value of $w_{\omega i}$ was set to 1 if generator i had governor. If not $w_{\omega i}$ was set to 0.

It must be noted that the system response is a stochastic process, and thus $f_s(\vec{x})$ is a random variable. In order to have a reliable deterministic metric, a new function is defined as the expected value of $f_s(\vec{x})$:

$$f_o(\vec{x}) = \mathbb{E}[f_s(\vec{x})] \tag{4-12}$$

The proposed tuning method consists in finding the vector of controller parameters $\vec{x}^\star$ which minimizes the following optimization problem:

$$\vec{x}^\star = \min_{\vec{x}} f_o(\vec{x}) \tag{4-13}$$

It must be noted that $f_o(\vec{x})$ is a parameter of the random variable $f_s(\vec{x})$, and as such it can only be estimated. In this work, $f_o(\vec{x})$ was estimated by taking the average of a set of samples of $f_s(\vec{x})$. The simulations required to calculate $f_o(\vec{x})$ are performed with the stochastic load variations as the only disturbances of the power systems (no other disturbances or faults are considered). It must be noted that the estimation of $f_o(\vec{x})$ is also a random variable.

4.3. Fault Response Tuning

The stochastic variation of the load introduces variability to the CCT, such that a single fault can present different values of CCT. This is illustrated in Figure **4-3**. The observations of the stochastic CCT are calculated by applying the PEBS method in an analogous as the stochastic system response. This section discusses the second tuning method proposed, which aims to maximize the CCT and minimize its variability.

In order to achieve a robust fault response, not only the CCT must be maximized, but its variability must be reduced as well. This is equivalent to maximizing the mean CCT and minimizing its variance. To achieve both objectives simultaneously, the following objective function can be used:

$$f_a(\vec{x}) = \sigma_C^2(\vec{x}) - \mu_C^2(\vec{x}) \tag{4-14}$$

Where $\vec{x}$ is the vector of tunable parameters, μ_C is the mean of the CCT of the considered fault, and σ_C^2 is the population variance of the CCT of the considered fault. The objective of the tuning process is to improve the fault response of a power system for any given fault. Therefore, the objective function should have information of all possible faults. However, in large scale systems the number of elements that can suffer a fault is too high, making computationally impossible to consider them all. For that reason the objective function is defined as a weighted sum of estimated minimum CCTs for a selected subset of the possible faults in the power system. The subset of faults and their weights can be selected

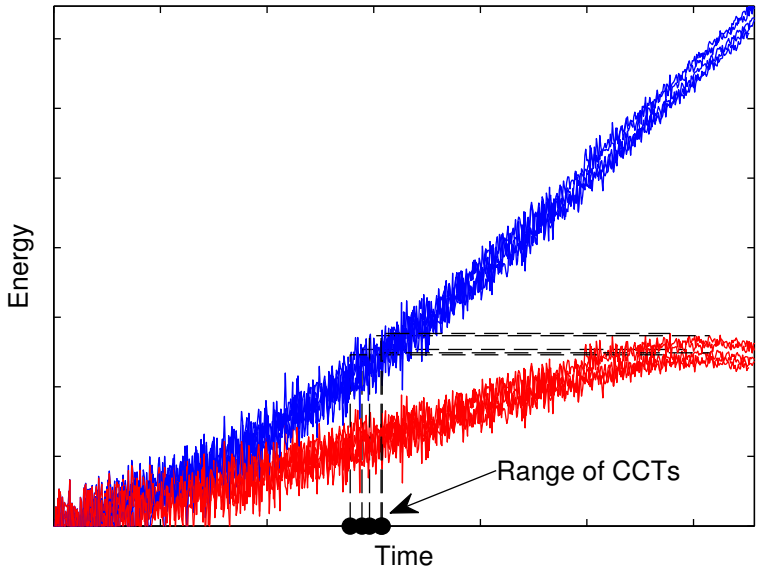

Figure 4-3.: Implementation of the PEBS method with stochastic load perturbation.

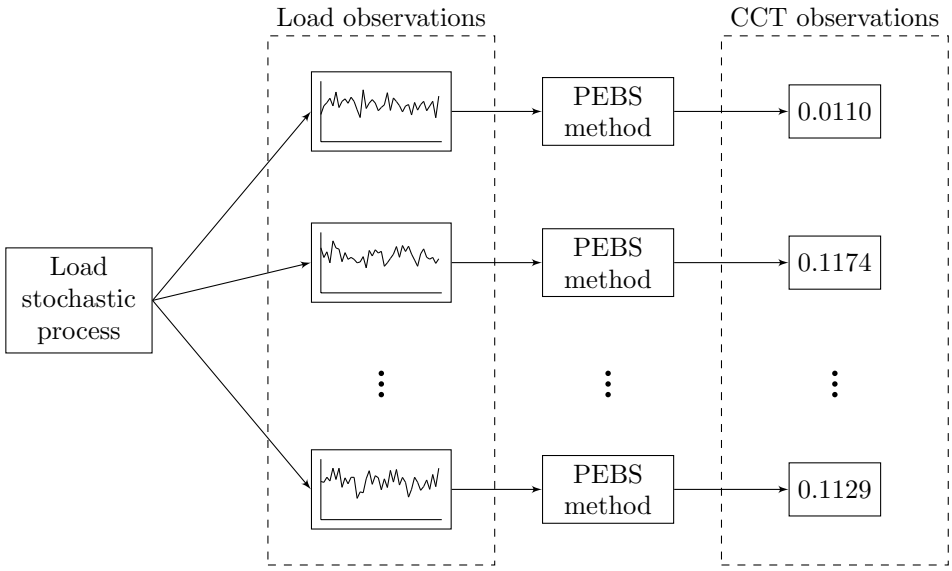

Figure 4-4.: Procedure for calculating the observations of the CCT.

to be give greater importance to the most critical faults, while considering at the same time representative faults of all the areas of the power system. The proposed objective function can be expressed as follows:

$$f_b(\vec{x}) = \frac{\sum_{i=1}^{|F_s|} w_i \left[\sigma_{Ci}^2(\vec{x}) - \mu_{Ci}^2(\vec{x})\right]}{\sum_{i=1}^{|F_s|} w_i} \tag{4-15}$$

Where F_s is the subset of faults considered, $|F_s|$ is the number of faults in the set F_s, w_i is the weight of fault i of the set, μ_{Ci} is the mean of the CCT of fault i and σ_{Ci}^2 is the population variance of the CCT of fault i. As the mean and population variance cannot be exactly known, they must be estimated with the average and the sample variance. The proposed objective function is now written as follows:

$$f_o(\vec{x}) = \frac{\sum_{i=1}^{|F_s|} w_i \left[\frac{1}{n_s-1}\sum_{k=1}^{n_s}\left[\tau_{Cik}(\vec{x}) - \frac{1}{n_s}\sum_{l=1}^{n_s}\tau_{Cil}(\vec{x})\right]^2 - \left(\frac{1}{n_s}\sum_{k=1}^{n_s}\tau_{Cik}(\vec{x})\right)^2\right]}{\sum_{i=1}^{|F_s|} w_i} \tag{4-16}$$

$$f_o(\vec{x}) = \frac{\sum_{i=1}^{|F_s|} w_i \left[\frac{1}{n_s-1}\left[\left(\sum_{k=1}^{n_s}\tau_{Cik}^2(\vec{x})\right) - \frac{1}{n_s}\left(\sum_{k=1}^{n_s}\tau_{Cik}(\vec{x})\right)^2\right] - \left(\frac{1}{n_s}\sum_{k=1}^{n_s}\tau_{Cik}(\vec{x})\right)^2\right]}{\sum_{i=1}^{|F_s|} w_i} \tag{4-17}$$

$$f_o(\vec{x}) = \frac{\sum_{i=1}^{|F_s|} w_i \left[\frac{1}{n_s-1}\sum_{k=1}^{n_s}\tau_{Cik}^2(\vec{x}) - \frac{2n_s-1}{n_s^2(n_s-1)}\left(\sum_{k=1}^{n_s}\tau_{Cik}(\vec{x})\right)^2\right]}{\sum_{i=1}^{|F_s|} w_i} \tag{4-18}$$

Where $\tau_{Cik}(\vec{x})$ is the k-th sample of the CCT of fault i and n_s is the number of CCT samples taken (it is assumed to be the same for all faults). Notice that $\tau_{Cik}(\vec{x})$ is **not** a random variable, it is a sample.

The proposed tuning method consists in finding the vector of controller parameters $\vec{x}^\star$ which minimizes the following optimization problem:

$$\vec{x}^\star = \min_{\vec{x}} f_o(\vec{x}) \tag{4-19}$$

The samples of the CCT required to evaluate $f_o(\vec{x})$ are calculated using the PEBS method. It must be noted that $f_o(\vec{x})$ is a random variable corresponding to the estimation of $f_b(\vec{x})$.

4.4. Optimization Using Cuckoo Search

The two tuning methods presented before were expressed as optimization problems of stochastic continuous functions. This work proposes using the metaheuristic Cuckoo Search for solving these optimization problems.

The original Cuckoo Search (CS) method [10] is a metaheuristic for global optimization of continuous functions which is based on the brood parasitism of the cuckoos. The cuckoos put their eggs in the nests of other species of birds for the host bird to hatch the eggs. Cuckoos usually remove some eggs of the host bird to increase the probability of their own eggs hatching. The host bird can also detect the alien eggs, in which case she can remove them from the nest or migrate to another place and build a new nest there. The CS method makes an analogy where the eggs represent candidate solutions, the nests represent sets of candidate solutions and the cuckoos represents agents in charge of creating new solutions. In this case it is assumed that each nest contains only one egg and there is only one cuckoo per nest, therefore eggs, nests and cuckoos can be considered as the same. This method is based on three idealized rules:

- Each cuckoo lays one egg at a time, in a randomly chosen nest.
- Nests with eggs of high quality are carried over to the next generation.
- The number of nests is fixed and each egg laid by a cuckoo has a probability p_a of being discovered by her host bird. If an egg is discovered, the host bird can dump it or build a new nest. As it was assumed that each nest has one egg, if an alien egg is discovered the host bird will replace it with a randomly generated egg.

A pseudo-code of the method based on the previous rules is shown in Algorithm 1. A fully implemented MATLAB® version of the algorithm is provided by the authors in [47]. The only metaparameters of the algorithm are p_s and p_a. The default values of p_s and p_a, according to the authors [10], are $p_s = 25$ and $p_a = 0.25$. The authors also state that the performance of the algorithm has very low sensitivity to the metaparameters [10], so most of the time the default values were used. To generate new solutions the method uses Lévy flights, which means a new solution $\vec{x}^{(l+1)}$ is generated using $\vec{x}^{(l)}$ as:

$$\vec{x}^{(l+1)} = \vec{x}^{(l)} + \vec{\alpha} \circ \overrightarrow{\text{Lévy}}(\beta) \tag{4-20}$$

Where $\vec{\alpha}$ represents the step length in each dimension (normally taken as 1 for all dimensions, as in this work), $\circ$ represents the Hadamard (elementwise) product and $\overrightarrow{\text{Lévy}}(\beta)$ is a vector of random independent variables following a Lévy distribution:

$$\left\{\overrightarrow{\text{Lévy}}(\beta)\right\}_i \sim u = t^{-\beta}, \qquad 1 < \beta \leq 3 \tag{4-21}$$

Algorithm 1 Cuckoo Search

begin
  define objective function $f_o(\vec{x})$
  generate initial population of p_s nests $\vec{x}_i$ and evaluate their fitness
  while $(t < MaxGeneration)$ or $(StopCriterion)$ **do**
    generate a random cuckoo using a Lévy flight and evaluate its fitness F_i
    choose a random nest j whose fitness is F_j;
    if $(F_i < F_j)$ **then**
      replace nest j with cuckoo i
    end if
    a fraction p_a of the worst nests are abandoned and replaced with randomly generated new nests
    keep the nests with the best quality
    rank nests and find the current best one
  end while
  output best solution
end

The Lévy distribution has and infinite mean and an infinite variance, and the scale of the distribution is controlled with the parameter β, which was chosen to be 1.5. To computationally generate numerical samples of the Lévy distribution the Mantegna algorithm was used [48]. It must noted that, although not explicitly stated in the algorithm, the nest population must be confined to a finite search space defined by the user. For the controller tuning the search space can be defined as the range of admissible or typical parameter values.

5. Test and Results

This chapter discusses the different tests performed for validating the proposed tuning methods. The development of the tests is explained in detail and the obtained results are discussed.

5.1. IEEE14: Steady State Tuning

This section discusses the test performed to validate the proposed steady state tuning method. The test consisted on the tuning of the generator controllers of the IEEE (Institute of Electrical and Electronics Engineers) 14 bus system, widely known in the literature as IEEE14. The oneline diagram of the system is shown in Figure **5-1**.

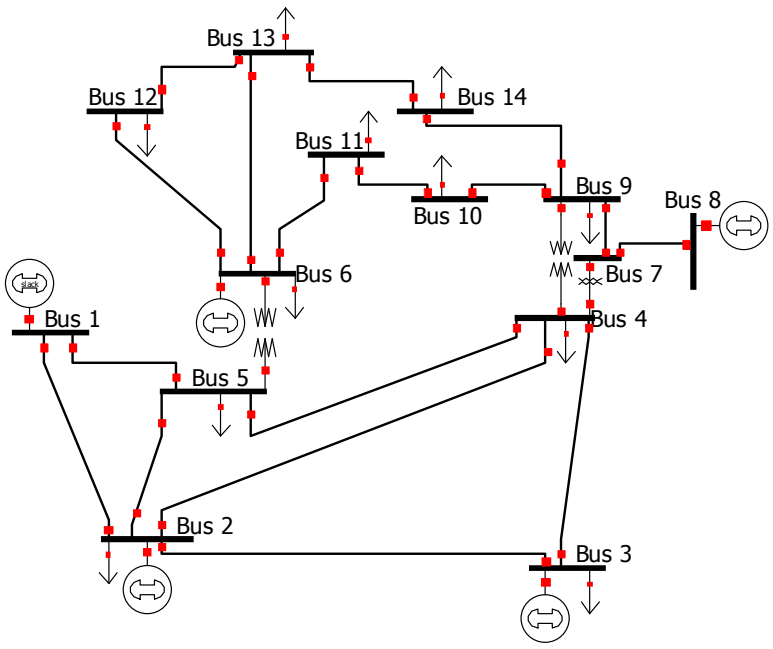

Figure 5-1.: Oneline diagram of the IEEE14 system.

The complete data of the system is available in [49]. The original IEEE14 system does not have generator or controller data, but in 2015 Demetriou et. al. estimated the generator

and controller data of the IEEE14 and other reference systems [50]. The controller and generator data used for the IEEE14 system can be found in [3]. The generators of nodes 3, 6 and 8 act as synchronous condensers. For convenience, the armature resistance (R_{ai}) of the synchronous condensers was neglected. The complete data with this modification can be found in Appendix A. The tunable parameters estimated in [50] are presented on Table **5-1**.

Table 5-1.: Tunable parameters of the IEEE14 system [3].

Parameter	**Value [p.u.]**
Amplifier Gain, Generator 5 (node 8), K_{A5}	50
Amplifier Gain, Generator 4 (node 6), K_{A4}	25
Amplifier Gain, Generator 3 (node 3), K_{A3}	400
Amplifier Gain, Generator 2 (node 2), K_{A2}	400
Amplifier Gain, Generator 1 (node 1), K_{A1}	400
Speed Droop, Generator 2 (node 2), R_2	0.05
Speed Droop, Generator 1 (node 1), R_1	0.05

Generators 3 to 5 act as synchronous condensers and thus do not have governor.

In this test the error function was calculated using simulations of 30 seconds, using the implicit trapezoidal method and a time step of 0.2 seconds. The parameters λ_i were set at a value of 0.5 % for all the loads, and the parameters ρ_i were set to vary uniformly between ± 0.2 %. The loads were modelled with the constant power model (independent of voltage).

The controller tuning was performed using two methods: the *Response Surface method* (classical approach in the field of design of experiments [51]) and the steady state tuning method. The obtained results were used to compare both methods.

In order to perform the optimization through the Response Surface method, a statistical model must be constructed. The possible factors influencing the value of the objective function are the controller parameters. Before constructing the model, an experiment must be carried out to detect which of the factor have a significant influence over the response variable (the objective function).

5.1.1. Screening Experiment

The screening experiments are applied to detect the significant factors of a process. The non-significant factors are free to be set on any convenient value, as they do not have much

impact on the response of the process. The possible factors influencing the process can be too much to be tested thoroughly; therefore the screening process must require an amount of runs as low as possible.

A common screening experiment is the 2^k factorial design, in which the process is executed 2^k times, varying the value of the possible factors from their minimum value to their maximum value, performing all the possible combinations of factor values [51].

In this test, a 2^7 factorial design with no repetitions (1 sample per point of the design) was selected. In order to execute the experiment, the experimental region was defined by setting the levels of operation of the factors, based on the typical values they can take [27]. The values of the factor levels are in Table **5-2**.

In the experiment, the error function is evaluated with each possible combination of the factor levels, for a total of $2^7 = 128$ runs.

Table 5-2.: Design factor levels.

Design Factor	**Low Level**	**High Level**
Amplifier Gain, Generator 5 (node 8), K_{A5}	25	500
Amplifier Gain, Generator 4 (node 6), K_{A4}	25	500
Amplifier Gain, Generator 3 (node 3), K_{A3}	25	500
Amplifier Gain, Generator 2 (node 2), K_{A2}	25	500
Amplifier Gain, Generator 1 (node 1), K_{A1}	25	500
Speed Droop, Generator 2 (node 2), R_2	0.02	0.1
Speed Droop, Generator 1 (node 1), R_1	0.02	0.1

The process is not only affected by the variation of the factors, but by the interaction between factors as well. The significance of the factors and its interactions is tested through an *Analysis of Variance* (ANOVA). The total amount of effects plus their interactions y $2^7 - 1 = 127$, and they cannot be tested all at once, so some factors or interactions must be discarded as non-significant beforehand. To do this, a normal probability plot of the factors and interactions is drawn. The factors and interactions close to the normal line can be represented as a whole set of normal residuals. This means the effect of these factors and interactions do not have a significant influence over the response variable, and they can represent the normal residuals on the fixed effects model of the ANOVA.

For simplicity, the effect of each factor (tunable parameter) will be coded with a letter, and

interactions will be coded as the concatenation of those letters. The coding of the effects is shown in Table **5-3**.

Table 5-3.: Design factor coding.

Parameter	Value [p.u.]
Amplifier Gain, Generator 5 (node 8), K_{A5}	A
Amplifier Gain, Generator 4 (node 6), K_{A4}	B
Amplifier Gain, Generator 3 (node 3), K_{A3}	C
Amplifier Gain, Generator 2 (node 2), K_{A2}	D
Amplifier Gain, Generator 1 (node 1), K_{A1}	E
Speed Droop, Generator 2 (node 2), R_2	F
Speed Droop, Generator 1 (node 1), R_1	G

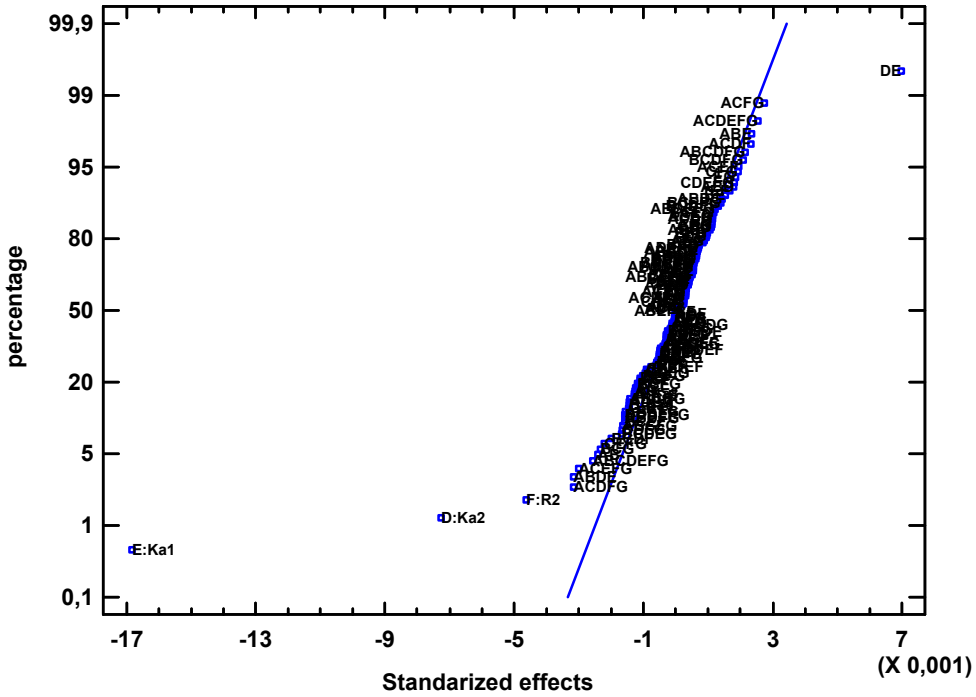

Figure 5-2.: Normal plot of the effects (2^7 factorial experiment).

The factor and interaction effects were drawn in the normal probability plot of Figure **5-2**. From the normal plot it can be concluded that the significant effects are effects D, E, F and DE. A multifactor ANOVA was performed for these effects. In order for the ANOVA to be statistically valid, the following three assumptions must hold:

- The variances of the levels of each factor must be equal (homoscedasticity).
- The residuals of the samples must be normally distributed.
- The residuals of the samples must be independent.

The equality of variance assumption was tested using the Levene's test with a significance $\alpha = 0.05$. The factor E showed significant differences in its variances, as its P-Value was lower than the significance. The exact value is shown in Table **5-4**:

Table 5-4.: Levene's test for factor E.

Levene's test		
Factor	*Test*	*P-Value*
E	43.144	$1.20598 \cdot 10^{-9}$

In order to correct the violation of the homoscedasticity assumption, the data was transformed using the power transform $y^* = y^\lambda$. The value of λ was calculated using the Box-Cox method [51], and it was found to be -0.722. However, this value of λ was not adequate to correct the variances. By trial and error an adequate value $\lambda = -1.3$ was found. The Levene's test was applied to the significant factors using the transformed data, and the results are shown in Table **5-5**:

Table 5-5.: Levene's test for for the significant factors with transformed data.

Levene's test for transformed data		
Factor	*Test*	*P-Value*
D	3.5685	0.0611839
E	3.4545	0.065413
F	1.1893	0.277553

As all the P-Values are greater than the significance, then it can be concluded that the homoscedasticity assumption holds. A multifactor ANOVA was then applied to the transformed data, using the same significance of the Levene's test. The results are shown in Table **5-6**:

Table 5-6.: ANOVA table for the 2^7 factorial experiment.

SoV	*SS*	*DoF*	*MS*	*Fo*	*P-Value*
D	16847.5	1	16847.5	21.88	0.0000
E	277651	1	277651	360.54	0.0000
F	20878.6	1	20878.6	27.11	0.0000
DE	5749.52	1	5749.52	7.47	0.0072
Residuals	94720.9	123	770.089		
Total	415847	127			

The meaning of the headers is the following [51]:

- *SoV:* Source of Variation.
- *SS:* Square Sum of Errors.
- *DoF:* Degrees of Freedom.
- *MS:* Mean Square Sum.
- *Fo:* Fisher Statistic.

It can be concluded that the effects D, E, F and DE have a significant influence over the response variable. To validate the results of the ANOVA, the other two assumptions must be verified. The residuals were calculated using the fixed effects model of the ANOVA. The Shapiro-Wilks test was performed on the residuals to verify that they follow a normal distribution. The result of the normality test is shown in Table **5-7**.

Table 5-7.: Shapiro-Wilks test for the residuals.

Test	*P-Value*
Shapiro-Wilks	0.3839

As the P-Value of the Shapiro-Wilks test is greater than the significance, it can be concluded that the residuals are normal. The normal plot of the residuals in Figure **5-3** serves to graphically verify the results of the Shapiro-Wilks test.

To verify the independence of the residuals, they were arranged by the time each associated datum was obtained, and the lag 1 of the autocorrelation was calculated. The value obtained

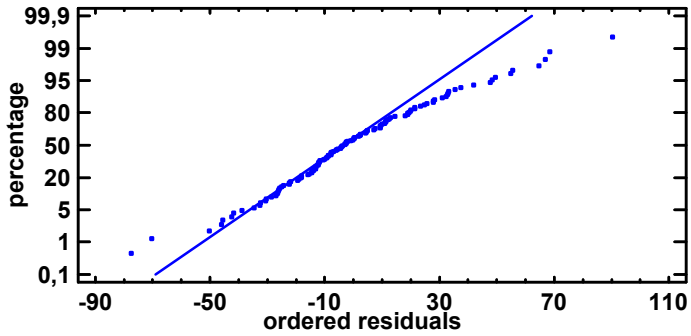

Figure 5-3.: Normal plot of the residuals.

was -0.0303988, which is lower than zero. Therefore, it can be concluded that the residuals are independent.

As the three assumptions of the ANOVA were validated, it can be concluded that the results of the ANOVA are statistically valid.

5.1.2. Regression Model Experiment

From the results of the screening experiment, the significant factors are D, E, and F (K_{A2}, K_{A1} and R_2, respectively). Factors A, B, C and G (K_{A5}, K_{A4}, K_A3 and R_1, respectively) are not significant and therefore there is no need to change them. For this reason, the non-significant factors are set to their normal operating values.

The next step to perform the Surface Response method consists in finding an adequate regression model of the response variable (the objective function in this case). This model must be able to represent the nonlinearity and any other type of trend of the response variable over the experimental region.

The 2^k factorial design does not provide enough data to capture the nonlinearity of the process. A more detailed experiment, like the 3^k factorial design, is required in order to construct appropriate nonlinear regression models. The 3^k factorial design is an experiment similar to the 2^k factorial design, with the difference that an intermediate level is introduced. The values of the factors at the intermediate level are the means of the values at the low and high levels.

As in this test there are 3 significant factors, a 3^3 factorial experiment with no repetitions (1 sample per point of the design) was performed to collect the required data for the regression model. The values of the factors at the different levels are shown in Table **5-8**.

Table 5-8.: Factor levels of the 3^3 factorial design.

Factor	Low Level	High Level	Medium Level
K_{A2}	25	262.5	500
K_{A1}	25	262.5	500
R_2	0.02	0.06	0.1

5.1.3. Response Surface Method

The data collected with the 3^k factorial design can be used to construct a regression model fitting the response variable inside the experimental region. The model can be optimized with classical optimization techniques, and if the optimum point is inside the experimental region, then is also an optimum point of the response variable. If not (the optimum point is found at the boundary of the experimental region), the whole process (including the screening experiment and regression model experiment) must be repeated over a new experimental region containing the expected optimum point. This must be done because the regression model is only valid over the experimental region. If another region is suspected of containing the optimum point, then it must be properly sampled first. The regression model of the response variable is often called the Response Surface of the process, and because of that reason this technique is called Response Surface method.

After obtaining the data from the 3^3 factorial design, a regression model was applied to fit the obtained data. Through trial and error, the following model structure was obtained:

$$f'_o = c_1 + c_2 K_{A2} + c_3 K_{A1} + c_4 K_{A1}^2 + c_5 K_{A2}^2 K_{A1} \tag{5-1}$$

By applying nonlinear regression coefficients c_1 to c_5 were calculated, obtaining the final regression model:

$$f'_o = 0.0518 - 4.5868 \cdot 10^{-5} K_{A2} - 1.4479 \cdot 10^{-4} K_{A1} + 1.6678 \cdot 10^{-7} K_{A1}^2 + 1.8613 \cdot 10^{-10} K_{A2}^2 K_{A1} \tag{5-2}$$

The statistical significance of the model was verified by applying an ANOVA (significance level $\alpha = 0.05$). The results are shown in Table **5-9**:

Table 5-9.: ANOVA table for the regression model.

SoV	*SS*	*DoF*	*MS*	*Fo*	*P-Value*
Model	0.002801	4	0.000700	7.5615	0.000544
Error	0.002038	22	$9.26 \cdot 10^{-5}$		
Total	0.004839	26			

If the variation produced by the model were not statistically significant, the model would not be appropriate to explain the behaviour of the response variable. The statistical significance of each term of the model was verified too. The verification was made using hypotheses tests with significance level $\alpha = 0.05$. The results are shown in Table **5-10**:

Table 5-10.: Hypothesis tests for the significance of the model terms.

Term	*Coefficient*	*LB 95 %*	*UB 95 %*	*to*	*P-Value*
Constant	0.051822	0.040385	0.063258	9.3974	$3.69 \cdot 10^{-9}$
K_{A2}	$-4.58 \cdot 10^{-5}$	$-7.74 \cdot 10^{-5}$	$-1.43 \cdot 10^{-5}$	-3.0158	0.006357
K_{A1}	-0.000144	-0.000225	$-6.41 \cdot 10^{-5}$	-3.7233	0.001181
K_{A1}^2	$1.66 \cdot 10^{-7}$	$2.23 \cdot 10^{-8}$	$3.11 \cdot 10^{-7}$	2.3943	0.025602
$K_{A2}^2 K_{A1}$	$1.86 \cdot 10^{-10}$	$8.02 \cdot 10^{-12}$	$3.64 \cdot 10^{-10}$	2.1672	0.041315

Where the following headers mean:

- *LB 95 %:* Lower bound of the confidence interval (confidence level 95 %).
- *LB 95 %:* Upper bound of the confidence interval (confidence level 95 %).
- *to:* T-Student statistic.

The residuals of the model are plotted against each factor in Figures **5-4**, **5-5** and **5-6**. There is no obvious pattern in the plotted residuals, so they represent typical random variables, and it can de concluded that the regression model is statistically valid.

The model does not include any term involving R_2, which may seem contradictory because the screening experiment labelled it as significant. However, the regression model has been proved to be statistically valid, and therefore there is no contradiction. Remember that the screening experiment takes less samples of each factor than the 3^k experiment. Because of this, the data used to calculate the regression model is more representative of the experimental region than the data used on the screening experiment, and the statistical conclusions

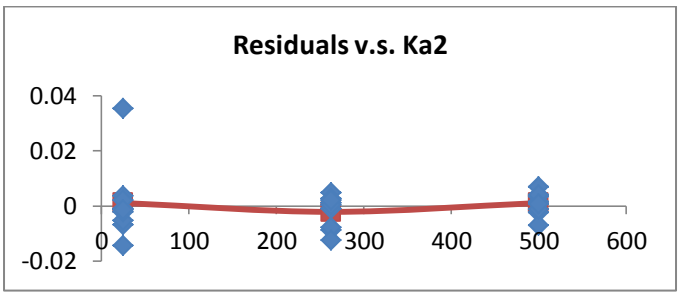

Figure 5-4.: Residuals v.s K_{A2}.

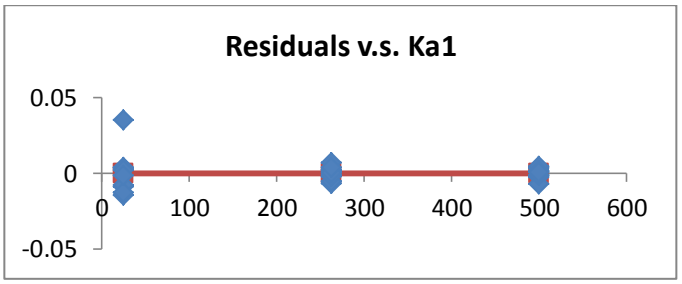

Figure 5-5.: Residuals v.s K_{A1}.

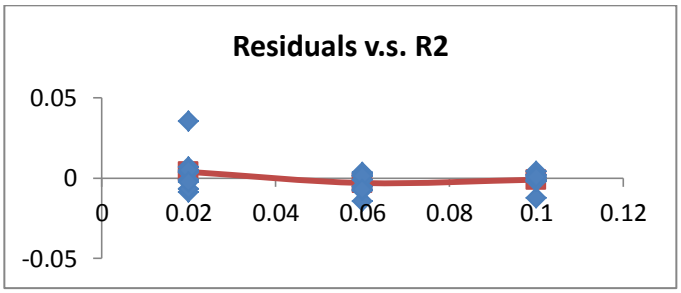

Figure 5-6.: Residuals v.s R_2.

derived from the regression model are more robust than the ones from the screening experiment. As R_2 does not affect the value of the regression model, there is no need to change it, and it was set at its normal operating value.

Finally, as the model is only valid inside the experimental region, the optimization can be formulated as:

$$\min_{[K_{A1}\ K_{A2}]} f'_o \tag{5-3}$$

Subject to:

$$25 \leq K_{A1} \leq 500 \tag{5-4}$$

$$25 \leq K_{A2} \leq 500 \tag{5-5}$$

The optimization was performed in Microsoft® Excel, and the optimal parameters obtained were:

$$K_{A1} = 373.26 \tag{5-6}$$

$$K_{A2} = 330.10 \tag{5-7}$$

Taking into account that the others factors were kept at their normal values, the optimal set of parameters found are shown in Table **5-11**.

Table 5-11.: Controller parameters found with the Response Surface method.

Parameter	**Optimal Value [p.u.]**
K_{A5}	400
K_{A4}	400
K_{A3}	400
K_{A2}	330.10
K_{A1}	373.26
R_2	0.05
R_1	0.05

5.1.4. Proposed Tuning Method

The Response Surface method proved that the only significant variables for the response of the IEEE14 system under stochastic loads are K_{A1} and K_{A2}. Therefore, the vector of tunable parameters for this test is the following:

$$\vec{x} = [K_{A1}\ K_{A2}]^T \tag{5-8}$$

The rest of AVR gains and the governor droops are set as constants equal to their normal operating values. The steady state tuning method was performed the optimal values of K_{A1} and K_{A2}. In order to do so, the objective function f_o was calculated as a 10 sample average of the metric f_s. The Cuckoo Search method was implemented with parameters $p_s = 25$ and $p_a = 0.25$. Cuckoo Search was programmed to stop after 20 generations (iterations). No other stopping criterion was implemented. The search space was restricted to the experimental region of the Response Surface method. Therefore $\vec{x} \in [25, 500]^2$. The optimal vector of controller parameters found with the steady state tuning method was the following:

$$\vec{x}^\star = [221.39\ 27.78]^T \tag{5-9}$$

Taking into account that the others factors were kept at their normal values, the optimal set of parameters found are shown in Table **5-12**.

Table 5-12.: Controller parameters found with the steady state tuning method.

Parameter	**Optimal Value [p.u.]**
K_{A5}	400
K_{A4}	400
K_{A3}	400
K_{A2}	27.78
K_{A1}	221.39
R_2	0.05
R_1	0.05

5.1.5. Comparison of Methods

Both of the previous methods yielded a set of controller parameters that is expected to improve the performance of the IEEE14 system under stochastic loads with respect to the

original set of parameters. In order to check whether this is true or not, and to compare both methods and determine which one shows better performance, a single factor ANOVA was performed. The factor was the set of parameters and the levels were the set found with both methods and the original set. This is shown in Table **5-13**.

Table 5-13.: ANOVA factor and its levels.

Factor	**Levels**		
Parameter set	Original (1)	Response Surface (2)	Steady state tuning (3)

Set 1 corresponds to the original set of parameters, Set 2 corresponds to the set of parameters found with the Response Surface Method, and Set 3 corresponds to the set of parameters found with the steady state tuning method. 20 samples of the objective function for each set of parameters were taken to perform the ANOVA. The data is shown in Table **5-14**.

Table 5-14.: Samples of the objective function.

Experiment data					
Set 1	**Set 1**	**Set 2**	**Set 2**	**Set 3**	**Set 3**
0.0291	0.02742	0.02451	0.02502	0.02152	0.02198
0.02491	0.0263	0.01869	0.02338	0.01977	0.02467
0.02453	0.02997	0.01928	0.02392	0.02128	0.02181
0.02573	0.0284	0.01847	0.02561	0.01992	0.01868
0.02315	0.0263	0.02375	0.02235	0.01922	0.02178
0.02558	0.02234	0.02089	0.02008	0.02077	0.01996
0.02783	0.0267	0.02042	0.01912	0.02169	0.0204
0.02902	0.02528	0.02081	0.02034	0.02264	0.02189
0.02521	0.03024	0.02297	0.01889	0.02019	0.01807
0.02754	0.02689	0.02415	0.02116	0.0258	0.02084

The results of the ANOVA are shown in Table **5-15**.

Table 5-15.: ANOVA table for the parameter sets.

SoV	*SS*	*DoF*	*MS*	*Fo*	*P-Value*
Parameter set	0.000364	2	0.000182	41.1027	$8.88 \cdot 10^{-12}$
Error	0.000253	57	$4.43 \cdot 10^{-6}$		
Total	0.000617	59			

In order for the ANOVA to be statistically valid, its assumptions must be validated. The equality of variance assumption was tested using the Levene's test with a significance $\alpha = 0.05$. The results are shown in Table **5-16**. As the P-Value is greater than α, it can be concluded that the homoscedasticity assumption holds.

Table 5-16.: Levene's test for the parameter sets.

Levene's test		
Factor	*Test*	*P-Value*
Parameter set	1.77711	0.178368

To validate the assumption of normally distributed residuals, the Shapiro-Wilks test was performed to verify that they follow a normal distribution. The result of the normality test is shown in Table **5-17**.

Table 5-17.: Shapiro-Wilks test for the residuals.

Test	*P-Value*
Shapiro-Wilks	0.4952

As the P-Value of the Shapiro-Wilks test is greater than the significance, it can be concluded that the residuals are normal. The normal plot of the residuals in Figure **5-7** serves to graphically verify the results of the Shapiro-Wilks test.

To verify the independence of the residuals, they were arranged by the time each associated datum was obtained, and the lag 1 of the autocorrelation was calculated. The value obtained was -0.193298. The 95 % confidence interval of the lag 1 of the atocorrelation is $[-0.059733, 0.446329]$. As the confidence interval contains the value 0, it can be concluded that the residuals are independent.

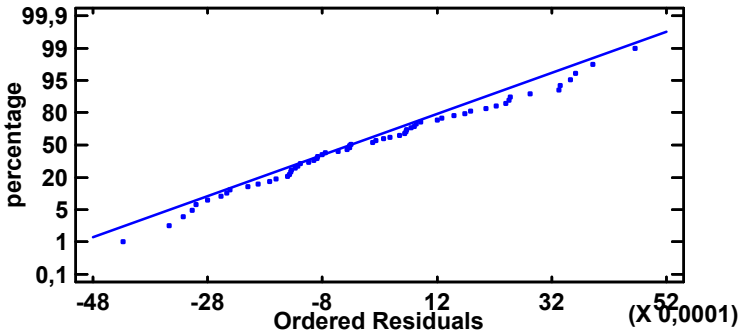

Figure 5-7.: Normal plot of the residuals.

As the three assumptions of the ANOVA were validated, it can be concluded that the results of the ANOVA are statistically valid.

From the results of the ANOVA it is clear that parameter sets have significant effect over the response of the IEEE14 system affected by stochastic loads. The *multiple range test* was implemented to detect significant differences in the values of the objective function for each parameter set. The test was performed using the HSD (Honset Significant Difference) Tukey method with significance $\alpha = 0.05$ [51]. The Tukey method was preferred over more popular methods (Duncan, Least Significant Difference (LSD) for example) because it allows to control the significance. The *homogeneous regions* derived from the multiple range test are shown in Table **5-18**.

Table 5-18.: Homogeneous regions of the performance of the parameter sets.

Parameter set	**Objective function average**	**Homogeneous regions**[1]	
1	0.02662		
2	0.02169		
3	0.02114		

[1] Calculated using Tukey HSD method (HSD=0.001605).

From the homogeneous regions it is clear the performance of the set of parameters obtained with both methods is significantly better than the performance of the original set of parameters. Another conclusion that there is no significant difference in the performance of the set of parameters obtained with both methods. This is remarkable, the steady state tuning with just 20 iterations of Cuckoo Search was able to achieve the same statistical performance of the Response Surface method. On top of that, the Response Surface method has very disadvantages compared to the proposed steady state tuning method:

- The effects considered for the ANOVA of the screening experiment have to be selected based on the normal plot of the effects. This process is not algorithmic, so an appropriate selection of effects depends on the knowledge and experience of the designer.
- The ANOVA of the screening experiment must satisfy the assumptions of the fixed effects models. If not the sample data must be transformed in a way that an ANOVA applied to the transformed data would satisfy those assumptions. The process of selecting an appropriate transformation is not algorithmic and depends on the knowledge and experience of the designer (the are algorithmic procedures like the Box-Cox method but they might fail, as in the case of this test). In the worst of cases, if no appropriate transformation is found, the experiment must be discarded. In that case it would be necessary to design a more appropriate screening experiment, or to resort to an entirely distinct method.
- The process of selecting an appropriate structure for the regression model is not algorithmic and depends on the knowledge and experience of the designer. If not appropriate structure if found, the Response Surface method cannot be applied.
- The number of samples required for the experiments scale exponentially with the number of tunable parameters. Therefore, it is not possible to perform this method on large scale power systems without making coarse approximations and assumptions (fractioned factorial experiments [51]).

The proposed steady state tuning method does not have any of this disadvantages and yet it manages to achieve a statistically equal level of performance.

5.2. IEEE9: Fault Response Tuning

This section discusses the test performed to validate the proposed fault response tuning method. The test consisted on the tuning of the generator controllers of the IEEE 9 bus system, widely known in the literature as IEEE9. This system is the same 9 bus system of the Western System Coordinating Council (WECC). The complete data of the system is available in [4]. The IEEE9 system does not have governor data, so it is assumed the generators only have AVRs. The AVR amplifier gains of the IEEE9 system generators are shown in Table **5-19**.

Table 5-19.: AVR amplifier gains of the IEEE9 system generators [4].

Parameter	Value [p.u.]
Amplifier Gain, Generator 1 (node 1), K_{A1}	20
Amplifier Gain, Generator 2 (node 2), K_{A2}	20
Amplifier Gain, Generator 3 (node 3), K_{A3}	20

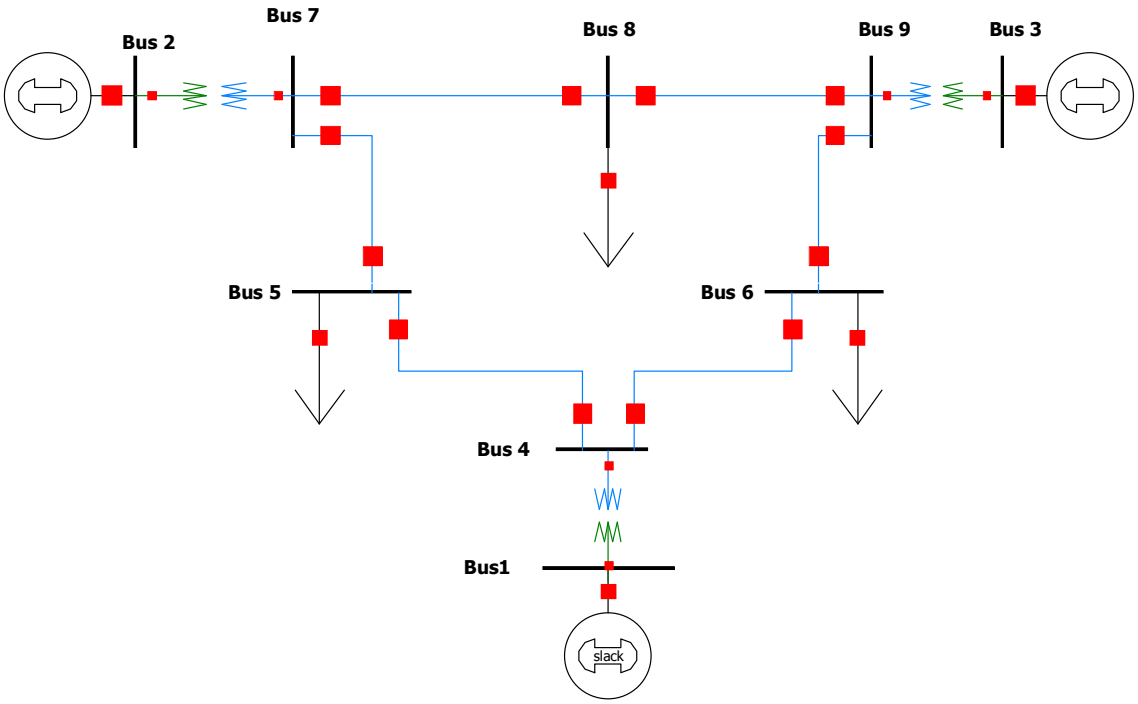

Figure 5-8.: Oneline diagram of the IEEE9 system.

Figure **5-8** shows the oneline diagram of the IEEE9 system. For this tests the following changes were made to the IEEE9 system:

- The generators' damping coefficients D_i were assumed to be zero.
- The generator of node 1 (generator 1) is assumed to be ideal. Therefore, the voltage of node 1 remains constant.

The data of the modified IEEE9 system can be found in Appendix B. As generator is assumed to behave as a perfect voltage source, there is no need to solve any of its algebraic or differential equations. Also, there is no need to tune the AVR of generator 1. This way, the vector of tunable parameters for this tests is the following:

$$\vec{x} = [K_{A2}\ K_{A3}]^T \tag{5-10}$$

The fault response tuning requires calculating the CCT using the PEBS method, which in turn requires a small time domain simulation to calculate the energy function. The time domain simulation was performed using the Explicit Euler method with a time step of $5 \cdot 10^{-4}$ seconds. The parameters λ_i were set at a value of 0.5 % for all the loads, and the parameters ρ_i were all set to 0. The loads were modelled with the constant admittance model. The set of considered faults consisted of the two following faults:

- **Fault 1:** A direct (no fault impedance) balanced three-phase short circuit at the line between nodes 4 and 5. The short circuit was placed at 50 % of the line length.
- **Fault 2:** A direct (no fault impedance) balanced three-phase short circuit at the line between nodes 6 and 9. The short circuit was placed at 50 % of the line length.

The weight of each fault was set to 1.

5.2.1. Initial Exploration

Before proceeding to perform the fault response tuning, it is necessary to define the search space of the tuning method. A feasible region of the AVR tunable parameters was estimated for that purpose. Such region was defined based on the typical values the AVR gains can have, according to [27]. The feasible region was defined as the rectangle $[20, 520] \times [20, 520]$. An initial exploration of the objective function over the search space was then performed. The search space was divided in a 21×21 grid, and the value of the objective function at each point of the grid was calculated The objective function was calculated using 20 samples of each CCT. The values at the grid points were used to plot a estimated surface of the objective function, which is shown in Figure **5-9**.

It is clear from Figure **5-9** that the objective function tends to decrease with increasing values of the AVR gains. To determine the search space of the tuning method a more detailed inspection of the surface was performed over the subregion $[320, 520] \times [320, 520]$. The result is shown in Figure **5-10**.

It can be appreciated from Figure **5-10** that the decreasing trend of the objective function over the subregion $[320, 520] \times [320, 520]$ is not as strong as over the whole feasible region. The minimum value of the objective function over the grid points is found at $[495, 520]$.

5.2.2. Parameter Tuning

The selected search space for the tuning was the rectangle $[420, 520] \times [420, 520]$, therefore $\vec{x} \in [420, 520]^2$. For the tuning method the objective function was calculated using 2 samples

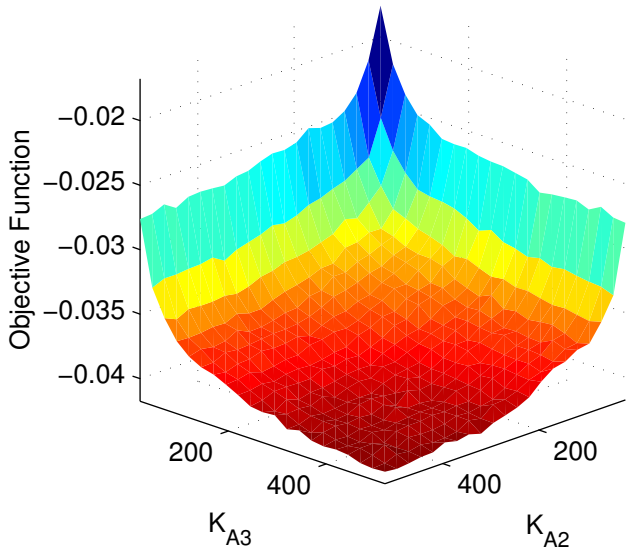

Figure 5-9.: Estimated surface plot of the objective function.

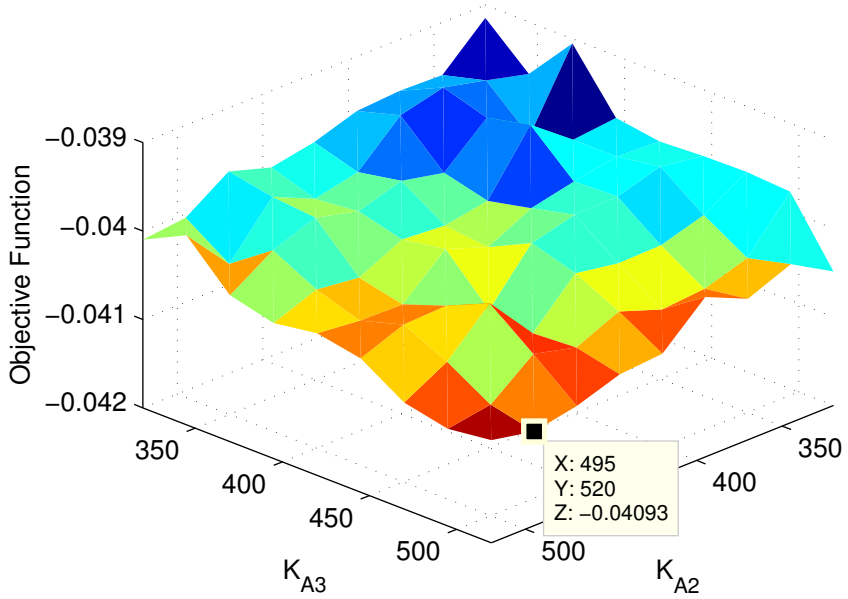

Figure 5-10.: Estimated surface plot of the objective function (zoomed in).

of each CCT. The Cuckoo Search method was implemented with parameters $p_s = 25$ and $p_a = 0.25$. Cuckoo Search was programmed to stop after 500 generations (iterations). No other stopping criterion was implemented. The optimal vector of controller parameters found with the fault response tuning method was the following:

$$\vec{x}^{\star} = [518.81\ 518.88]^T \tag{5-11}$$

5.2.3. Tuning Quality

The objective function can only be estimated, and those estimations are stochastic variables. Therefore, it is not possible to check the optimality of the solution using analytic criteria (first and second order conditions [30], for example). However, it is still possible to statistically check that the CCTs with the tuned parameters are higher than the CCTs with the original parameters. Figures **5-11** and **5-12** show estimates of the probability distribution function (PDF) of the CCTs of the considered faults with the original and tuned parameters. A total of 4000 samples were taken to generate all the estimated PDFs, 1000 samples per PDF.

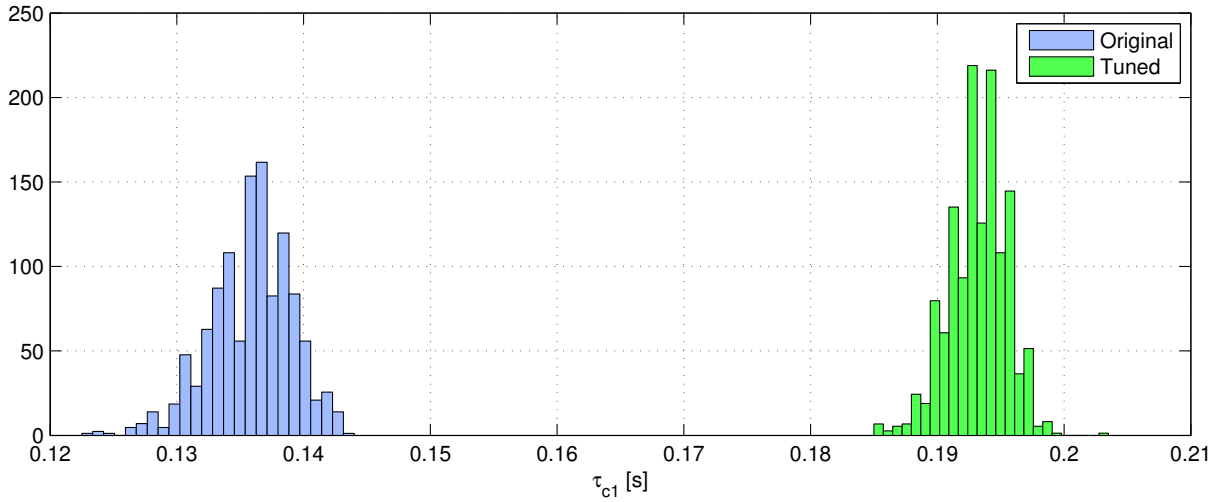

Figure 5-11.: Estimated PDFs of the CCTs of fault 1 with the original and tuned parameters.

Table **5-20** shows different statistics of the CCT of each parameter set and fault, calculated using the 4000 samples of the histograms.

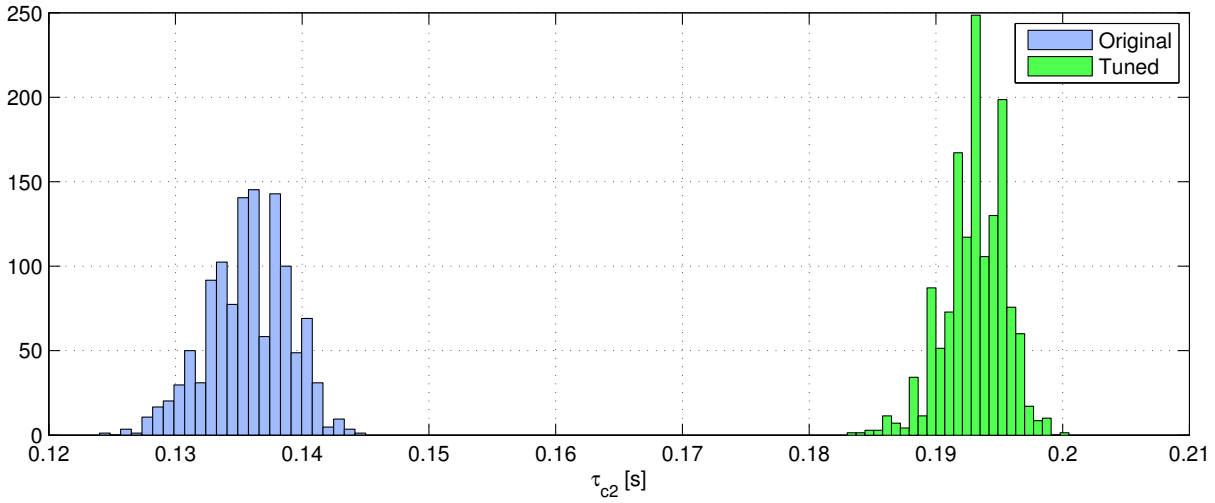

Figure 5-12.: Estimated PDFs of the CCTs of fault 2 with the original and tuned parameters.

Table 5-20.: CCT statistics for different parameter sets and faults.

Parameter set	Fault number	Average [ms]	Standard deviation [ms]	Minimum value [ms]	Maximum value [ms]
Original	1	135.854	3.236	122.5	144
	2	135.747	3.189	124	145
Tuned	1	193.192	2.326	185	203.5
	2	193.15	2.392	183	200.5

From the figures and the table it is clear that the tuned parameter set produces a significant increase of the mean CCT of the considered faults. The tuned parameter set also produces a significant reduction of the standard deviations of the CCT for the considered faults. These conclusions can be statistically proved with hypotheses tests for the variances and difference of means (significance level $\alpha = 0.05$) [51]. The results are shown in Tables **5-21** and **5-22**.

Table 5-21.: Hypotheses tests of the variances of the CCTs.

Fault number	Fo	P-Value	Conclusion
1	1.9352	$2.36327 \cdot 10^{-25}$	Variance decreased
2	1.7785	$8.20367 \cdot 10^{-20}$	Variance decreased

Table 5-22.: Hypotheses tests of the means of the CCTs.

Fault number	to	P-Value	Conclusion
1	454.95	0	Mean increased
2	455.35	0	Mean increased

5.2.4. Error Quantification

The PEBS method gives only an approximate value of the CCT. The CCT value can be obtained with arbitrarily small precision using time domain simulation (this was discussed previously in Chapter 3). In order to quantify the approximation error of the PEBS method, The CCTs of a large set of faults were calculated with both PEBS method and time domain simulation. The CCTs calculated with time domain simulation have an accuracy of +0.5 ms (the true CCTs are at most 0.5 ms greater than the calculated ones). The set of faults considered consists on direct balanced three-phase short circuits at each of the lines of the IEEE9 system. Each short circuit was placed at 50 % of the length of the respective line.

The aim of this procedure is to quantify the approximation error of the PEBS method, so no stochastic load variations was considered. The reason is that the natural variability of the CCT due to the stochastic load might be confused with the approximation error of the PEBS method. As no stochastic load is considered, the CCTs become deterministic so it is only needed to calculate them once. The deterministic CCTs were calculated for both the original and tuned set of parameters. The obtained CCTs and their errors are shown Table **5-23**.

Table 5-23.: Deterministic CCTs of various faults for both parameter sets.

Parameter set	**Faulted element**	**CCT (PEBS) [ms]**	**CCT (simulation) [ms]**	**Error [ms]**	**Error [%]**
Original	Line 4-6	169.5	202.5	-33	16.3 %
	Line 4-5	140	159.5	-19.5	12.2 %
	Line 5-7	89.5	64	25.5	39.8 %
	Line 6-9	135	147	-12	8.2 %
	Line 7-8	129	120.5	8.5	7.1 %
	Line 8-9	156	177	-21	11.9 %
Tuned	Line 4-6	230	528.5	-298.5	56.5 %
	Line 4-5	196	648.5	-452.5	69.8 %
	Line 5-7	148	119.5	28.5	23.8 %
	Line 6-9	213.5	190.5	23	12.1 %
	Line 7-8	171.5	146.5	25	17.1 %
	Line 8-9	209	211.5	-2.5	1.2 %

From Table **5-23** it is clear that the approximation error of the PEBS method can vary greatly between distinct faults. In this case, the relative error can vary from 1.2 % to 69.8 %. The tuned parameter set not only improved the CCTs of the two faults initially considered, but it also improved the CCTs of all other line faults. Although no stochastic load was considered, the increase in the CCTs is significant enough to overcome the variability of the stochastic CCTs. On interesting fault is the one occurring at line 4-5 (which was initially considered as well), the true increase of its CCT is multiple times greater than the calculated with the results of the PEBS method.

6. Conclusions and Future Work

6.1. Conclusions

This work describes the mathematical description and the implementation of two new tuning methods for controller tuning in a power system. One tuning method is focused on the steady state response and the other is focused on the fault response. A major novelty of these tuning methods is that they take into account the stochastic variations of the power system loads by modelling their observations as time-dependent processes.

The tuning methods were described as optimization problems. For the steady state tuning, the objective function was defined as the weighted average of the integral absolute errors of the controlled variables' responses. These errors are calculated using time domain simulations, which are calculated using numerical methods for solving systems of differential and algebraic equations.

For the fault response tuning, the objective function was defined as the weighted average of the difference of variances and squared means of the critical clearing times (CCTs) of a defined set of faults. The critical clearing times are calculated using the Potential Energy Boundary Surface (PEBS) method, which is base on the stability theory of Lyapunov.

The optimization problems of the tuning methods are solved using the metaheuristic Cuckoo Search. Cuckoo Search has been designed primarily to solve continuous optimization problems like the ones of the tuning methods. It also has the advantage that only one metaparameter apart from the population size must be specified.

The proposed steady state tuning method was tested against the Surface Response method in the IEEE14 system. The set of parameters obtained with the steady state tuning after only 20 iterations of Cuckoo Search achieved the same statistical performance of the set of parameters obtained with the Response Surface method. The steady state tuning proved to be a better alternative than the Response Surface method in the sense that it is a completely algorithmic procedure that does not depend on the compliance of a set of assumptions nor the experience of the user.

From the previous test it is also concluded that neither the AVRs of the synchronous con-

densers nor the governors have a significant effect on the response of the IEEE14 system affected by stochastic loads. This is not unexpected because the apparent powers generated by the synchronous condensers are much lower than that of the rest of generators. Also, the governors have relatively high time constants due to the inertia of the mechanical elements considered in their models. For this reason, it is normal for the governors to have no significant impact on the system response affected by the high frequency stochastic variations of the loads.

The proposed fault response tuning was tested by using it to tune the controllers of the IEEE9 system, considering a set of two specific faults. A sample set of the CCTs of both faults with the original and tuned set of parameters was taken to estimate their probability distribution functions and some other statistics like the mean and standard deviation. From the results it is concluded that the tuned set of parameters increases the CCTs of the considered faults and reduces their variances, thus achieving a better and more robust fault response. These conclusions were validated using hypotheses tests of the variances and means.

The deterministic (without considering stochastic loads) CCTs of a larger set of faults of the IEEE9 system were calculated with time domain simulation to quantify the approximation error of the PEBS method. The relative error varied greatly for each fault of the set. Also the CCT estimations obtained with the PEBS method can either be optimistic or pessimistic with no particular trend. However, when considering the tuned set of parameters the deterministic CCTs were higher for all the faults. This shows that although the approximation error of the PEBS method can vary greatly, it can still be used to successfully improve the CCT, hence improving the fault response of the system.

6.2. Future Work

The proposed tuning methods have been developed and tested in detail, considering the stochastic variation of loads. However, the proposed methodologies can be extended in various ways. Future work can consider implementing stochastic variations on the generators to model renewable energy sources. Another possible research would be testing other methods for fast calculation of the CCT with low approximation error, apart from the PEBS method. Also, a research of interest would be extending the proposed tuning methods to other types of controllers present on power systems (power system stabilizers, FACTS, for example).

The proposed tuning methods have been tested thus far using computer simulations. Implementations of these tuning methods on real power systems would provide additional validation to the already obtained results.

From the conclusions of this work one logical question arises: do the AVR of synchronous condenser and governors have a significant impact on the response of a power system affected by stochastic loads? Future research can focus on solving this question on general large-scale power systems.

A. Appendix: Modified IEEE14 System and Controller Data

Table A-1.: Modified IEEE14 line and transformer data (base power 100 MVA).

From node	To node	R [p.u.]	X [p.u.]	B [p.u.]	Tap	Phase shift [°]
1	2	0.01938	0.05917	0.0528	-	-
1	5	0.05403	0.22304	0.0492	-	-
2	3	0.04699	0.19797	0.0438	-	-
2	4	0.05811	0.17632	0.034	-	-
2	5	0.05695	0.17388	0.0346	-	-
3	4	0.06701	0.17103	0.0128	-	-
4	5	0.01335	0.04211	0	-	-
4	7	0	0.20912	0	0.978	0
4	9	0	0.55618	0	0.969	0
5	6	0	0.25202	0	0.932	0
6	11	0.09498	0.1989	0	-	-
6	12	0.12291	0.25581	0	-	-
6	13	0.06615	0.13027	0	-	-
7	8	0	0.17615	0	-	-
7	9	0	0.11001	0	-	-
9	10	0.03181	0.0845	0	-	-
9	14	0.12711	0.27038	0	-	-
10	11	0.08205	0.19207	0	-	-
12	13	0.22092	0.19988	0	-	-
13	14	0.17093	0.34802	0	-	-

The values of **Tap** and **Phase shift** correspond to the magnitudes and angles of the trans-

formers' voltage ratio, respetively. Therefore, elements with valid **Tap** are transformers, and the rest are lines.

Table A-2.: Modified IEEE14 power flow data.

Node	**Type**	V **[p.u.]**	P_L **[MW]**	Q_L **[MVAR]**	P_G **[MW]**	B_{sh} **[MVAR]**
1	Slack	1.06	-	-	232.4	-
2	PV	1.045	21.7	12.7	40	-
3	PV	1.01	94.2	19	-	-
4	PQ	-	47.8	-3.9	-	-
5	PQ	-	7.6	1.6	-	-
6	PV	1.07	11.2	7.5	-	-
7	PQ	-	-	-	-	-
8	PV	1.09	-	-	-	-
9	PQ	-	29.5	16.6	-	19
10	PQ	-	9	5.8	-	-
11	PQ	-	3.5	1.8	-	-
12	PQ	-	6.1	1.6	-	-
13	PQ	-	13.5	5.8	-	-
14	PQ	-	14.9	5	-	-

Values of B_{sh} correspond to the nominal power of shut capacitor and reactors. A positive value indicates a capacitor, and a negative value indicates a reactor. The slack node voltage angle is assumed to be 0°.

Table A-3.: Modified IEEE14 generator data.

Node	S_{rated} **[MVA]**	H **[s]**	D **[p.u.]**	R_a **[p.u.]**	X_d **[p.u.]**	X_q **[p.u.]**	X'_d **[p.u.]**	X'_q **[p.u.]**	T'_{d0} **[s]**	T'_{q0} **[s]**
1	448	2.656	2	0.0043	1.67	1.6	0.265	0.46	0.5871	0.1351
2	100	4.985	2	0.0035	1.18	1.05	0.22	0.38	1.1	0.1086
3	40	1.52	0	0	2.373	1.172	0.343	1.172	11.6	0.159
6	25	1.2	0	0	1.769	0.855	0.304	0.5795	8	0.008
8	25	1.2	0	0	1.769	0.855	0.304	0.5795	8	0.008

The values of S_{rated} are the rated apparent power of the generators. The generator p.u. data uses the generator p.u. base, and must be base-changed to 100 MVA before using it.

Table A-4.: Modified IEEE14 AVR data.

Node	T_R **[s]**	K_A **[p.u.]**	T_A **[s]**	V_{RMAX} **[p.u.]**	V_{RMIN} **[p.u.]**	K_E **[p.u.]**	T_E **[s]**	K_F **[p.u.]**	T_F **[s]**
1	0	50	0.06	1	-1	-0.0465	0.52	0.0832	1
2	0.06	25	0.2	1	-1	-0.0582	0.6544	0.105	0.35
3	0	400	0.05	6.63	-6.63	-0.17	0.95	0.04	1
6	0	400	0.05	4.407	-4.407	-0.17	0.95	0.04	1
8	0	400	0.05	4.407	-4.407	-0.17	0.95	0.04	1

The AVR p.u. data uses their respective generators' p.u. base, but there is no need to base-change them before using them.

Table A-5.: Modified IEEE14 governor data.

Node	P_{MAX} **[p.u.]**	R **[p.u.]**	T_D **[s]**	T_ω **[s]**	T_S **[s]**	T_B **[s]**	T_P **[s]**	F **[p.u.]**
1	0.87	0.05	0.1	0	0.3	0.05	10	0.25
2	1.05	0.05	0.09	0	0.2	0.3	0	1

The governor p.u. data uses their respective generators' p.u. base. The values of P_{MAX} and R must be base-changed to 100 MVA before using them.

B. Appendix: Modified IEEE9 System and Controller Data

Table B-1.: Modified IEEE9 line and transformer data (base power 100 MVA).

From node	To node	R [p.u.]	X [p.u.]	B [p.u.]	Tap	Phase shift [°]
4	6	0.017	0.092	0.158	-	-
4	5	0.01	0.085	0.176	-	-
5	7	0.032	0.161	0.306	-	-
6	9	0.039	0.17	0.358	-	-
7	8	0.0085	0.072	0.149	-	-
8	9	0.0119	0.1008	0.209	-	-
1	4	0	0.0576	0	1	0
2	7	0	0.0625	0	1	0
3	9	0	0.0586	0	1	0

The values of **Tap** and **Phase shift** correspond to the magnitudes and angles of the transformers' voltage ratio, respetively. Therefore, elements with valid **Tap** are transformers, and the rest are lines.

Table B-2.: Modified IEEE9 power flow data.

Node	**Type**	V **[p.u.]**	P_L **[MW]**	Q_L **[MVAR]**	P_G **[MW]**	B_{sh} **[MVAR]**
1	Slack	1.04	-	-	-	-
2	PV	1.025	-	-	163	-
3	PV	1.025	-	-	85	-
4	PQ	-	-	-	-	-
5	PQ	-	125	50	-	-
6	PQ	-	90	30	-	-
7	PQ	-	-	-	-	-
8	PQ	-	100	35	-	-
9	PQ	-	-	-	-	-

Values of B_{sh} correspond to the nominal power of shut capacitor and reactors. A positive value indicates a capacitor, and a negative value indicates a reactor. The slack node voltage angle is assumed to be 0°.

Table B-3.: Modified IEEE9 generator data.

Node	S_{rated} **[MVA]**	H **[s]**	D **[p.u.]**	R_a **[p.u.]**	X_d **[p.u.]**	X_q **[p.u.]**	X'_d **[p.u.]**	X'_q **[p.u.]**	T'_{d0} **[s]**	T'_{q0} **[s]**
1	100	∞	0	0	0	0	0	0	∞	∞
2	100	6.4	0	0	0.8958	0.8645	0.1198	0.1969	6	0.535
3	100	3.01	0	0	1.3125	1.2578	0.1813	0.25	5.89	0.6

The values of S_{rated} are the rated apparent power of the generators. The generator p.u. data uses the generator p.u. base, and must be base-changed to 100 MVA before using it. Notice that the slack generator (node 1) is assumed to be ideal and behave like a perfect voltage source.

Table B-4.: Modified IEEE9 AVR data.

Node	T_R [**s**]	K_A [**p.u.**]	T_A [**s**]	V_{RMAX} [**p.u.**]	V_{RMIN} [**p.u.**]	K_E [**p.u.**]	T_E [**s**]	K_F [**p.u.**]	T_F [**s**]
1	0	20	0.2	∞	$-\infty$	1	0.314	0.063	0.35
2	0	20	0.2	∞	$-\infty$	1	0.314	0.063	0.35
3	0	20	0.2	∞	$-\infty$	1	0.314	0.063	0.35

The AVR p.u. data uses their respective generators' p.u. base, but there is no need to base-change them before using them.

Bibliography

[1] T. Athay, R. Podmore, and S. Virmani, "A practical method for the direct analysis of transient stability," *IEEE Transactions on Power Apparatus and Systems*, vol. PAS-98, no. 2, pp. 573–584, 1979.

[2] T. Odun-Ayo and M. L. Crow, "An analysis of power system transient stability using stochastic energy functions," *International Transactions on Electrical Energy Systems*, vol. 23, no. 2, pp. 151–165, 2013.

[3] P. Demetriou, M. Asprou, J. Quiros-Tortos, and E. Kyriakides, "IEEE 14-bus modified test system data," accessed: 2017-11-20. [Online]. Available: http://www.kios.ucy.ac.cy/testsystems/images/Documents/Data/IEEE%2014.pdf

[4] P. W. Sauer and M. A. Pai, *Power System Dynamics and Stability*. Prentice Hall, 1997.

[5] W. D. Stevenson and J. J. Grainger, *Power System Analysis*. New York: McGraw-Hill, 1994.

[6] G. Ziegler and N. B. Nichols, "Optimum setting for automatic controllers," *Trans. ASME*, vol. 64, pp. 759–768, 1942.

[7] C. K. Sanathanan, "A frequency domain method for tuning hydro governors," *IEEE Transactions on Energy Conversion*, vol. 3, no. 1, pp. 14–17, 1988.

[8] G. Shabib, M. A. Gayed, and A. M. Rashwan, "Optimal tuning of PID controller for AVR system using modified particle swarm optimization," in *14th International Middle East Power Systems Conference (MEPCON'10)*, 2010.

[9] J. E. Lansberry, L. Wozniak, and D. E. Goldberg, "Optimal hydrogenerator governor tuning with a genetic algorithm," *IEEE Transactions on Energy Conversion*, vol. 7, no. 4, pp. 623–630, 1992.

[10] X. S. Yang and S. Deb, "Cuckoo search via Lévy flights," in *2009 World Congress on Nature Biologically Inspired Computing (NaBIC)*, 2009, pp. 210–214.

[11] G. Zhang, "Marine diesel-generator excitation controller based on adaptive on-line ga tuning pid," in *Proceedings of the 30th Chinese Control Conference*, 2011, pp. 3868–3871.

[12] G. Shahgholian, M. Maghsoodi, M. Mahdavian, S. Farazpey, M. Janghorbani, and M. Azadeh, "Design of fuzzy+PI controller in application of TCSC and PSS for power system stability improvement," in *2016 13th International Conference on Electrical Engineering/Electronics, Computer, Telecommunications and Information Technology (ECTI-CON)*, 2016, pp. 1–6.

[13] H. Lomei, M. Assili, D. Sutanto, and K. M. Muttaqi, "A new approach to reduce the nonlinear characteristics of a stressed power system by using the normal form technique in the control design of the excitation system," *IEEE Transactions on Industry Applications*, vol. 53, no. 1, pp. 492–500, 2017.

[14] R. K. Pandey and D. K. Gupta, "Intelligent multi-area power control: Dynamic knowledge domain inference concept," *IEEE Transactions on Power Systems*, vol. 32, no. 6, pp. 4310–4318, 2017.

[15] P. Kundur, *Power System Stability and Control*. New York: McGraw-Hill, 1994.

[16] ABB, "Power capacitors and harmonic filters, buyer's guide," Catalog, 2013. [Online]. Available:
https://search-ext.abb.com/library/Download.aspx?DocumentID=1HSM954332-00en&LanguageCode=en&DocumentPartId=&Action=Launch

[17] S. J. Chapman, *Electric Machinery Fundamentals*, 4th ed. New York: McGraw-Hill, 2005.

[18] A. E. Fitzgerald, C. Kingsley, and S. D. Umans, *Electric Machinery*, 6th ed. New York: McGraw-Hill, 2005.

[19] W. H. Hayt and J. E. Kemmerly, *Engineering Circuit Analysis*, 2nd ed. New York: McGraw-Hill, 1971.

[20] H. Saadat, *Power System Analysis*. New York: McGraw-Hill, 1999.

[21] W. H. Hayt, *Engineering Electromagnetics*, 5th ed. New York: McGraw-Hill, 1989.

[22] P. M. Anderson, B. L. Agrawal, and J. E. V. Ness, *Subsynchronous Resonance in Power Systems*. New York: IEEE Press, 1990.

[23] J. Machowski, J. W. Bialek, and J. R. Bumby, *Power System Dynamics: Stability and Control*. Chichester, United Kingdom: John Wiley & Sons, Ltd., 2008.

[24] R. H. Park, "Two reaction theory of synchronous machines – generalized method of analysis – part I," *AIEE Trans.*, vol. 48, pp. 716–727, 1929.

[25] E. Hairer and G. Wanner, *Solving ordinary differential equations II: Stiff and differential-algebraic problems*. Berlin: Springer-Verlag, 1996.

[26] "IEEE recommended practice for excitation system models for power system stability studies," *IEEE Std. 421.5*, 2005.

[27] P. M. Anderson and A. A. Fouad, *Power System Control and Stability*. Hoboken, NJ: John Wiley & Sons, Inc., 2003.

[28] D. R. Kincaid and E. W. Cheney, *Numerical analysis: mathematics of scientific computing*. American Mathematical Soc., 2002, vol. 2.

[29] M. L. Crow, *Computational Methods for Electric Power Systems*. Boca Raton, FL: CRC, 2009.

[30] J. Nocedal and S. J. Wright, *Numerical Optimization*. Springer, 2006.

[31] B. Stott and O. Alsac, "Fast decoupled load flow," *IEEE Transactions on Power Apparatus and Systems*, vol. PAS-93, no. 3, pp. 859–869, 1974.

[32] W. F. Tinney and C. E. Hart, "Power flow solution by newton's method," *IEEE Transactions on Power Apparatus and Systems*, vol. PAS-86, no. 11, pp. 1449–1460, 1967.

[33] J. R. Magnus and H. Neudecker, "Matrix differential calculus with applications to simple, hadamard, and kronecker products," *Journal of Mathematical Psychology*, vol. 29, pp. 474–492, 1985.

[34] A. Hjorungnes and D. Gesbert, "Complex-valued matrix differentiation: Techniques and key results," *IEEE Transactions on Signal Processing*, vol. 55, no. 6, pp. 2740–2746, 2007.

[35] R. Hunger, "An introduction to complex differentials and complex differentiability," Technische Universität München, Tech. Rep. TUM-LNS-TR-07-06, 2007.

[36] E. Hairer, S. P. Norsett, and G. Wanner, *Solving ordinary differential equations I: Nonstiff problems*. Berlin: Springer-Verlag, 1987.

[37] H.-D. Chiang, F. Wu, and P. Varaiya, "Foundations of direct methods for power system transient stability analysis," *IEEE Transactions on Circuits and Systems*, vol. 34, no. 2, pp. 160–173, 1987.

[38] A. H. El-abiad and K. Nagappan, "Transient stability regions of multimachine power systems," *IEEE Transactions on Power Apparatus and Systems*, vol. PAS-85, no. 2, pp. 169–179, 1966.

[39] N. Kakimoto, Y. Ohsawa, and M. Hayashi, "Transient stability analysis of electric power systems via lure type lyapunov functions, parts I and II," *Trans. IEE of Japan*, vol. 98, 1978.

[40] F. A. Rahimi, M. G. Lauby, J. N. Wrubel, and K. L. Lee, "Evaluation of the transient energy function method for on-line dynamic security analysis," *IEEE Transactions on Power Systems*, vol. 8, no. 2, pp. 497–507, 1993.

[41] A. M. Lyapunov, *The General Problem of the Stability of Motion*. London: Taylor and Francis Ltd., 1992.

[42] J. E. Slotine and W. Li, *Applied Nonlinear Control*. Englewood Cliffs, NJ: Prentice hall, 1991.

[43] K. R. Padiyar, *Power System Dynamics – Stability and Control- Second Edition*. Hyderabad, India: B.S. Publications, 2000.

[44] K. Wang and M. L. Crow, "Numerical simulation of stochastic differential algebraic equations for power system transient stability with random loads," in *2011 IEEE Power and Energy Society General Meeting*, 2011, pp. 1–8.

[45] T. Odun-Ayo and M. L. Crow, "Structure-preserved power system transient stability using stochastic energy functions," *IEEE Transactions on Power Systems*, vol. 27, no. 3, pp. 1450–1458, 2012.

[46] K. Wang and M. L. Crow, "The fokker-planck equation for power system stability probability density function evolution," *IEEE Transactions on Power Systems*, vol. 28, no. 3, pp. 2994–3001, 2013.

[47] X. S. Yang and S. Deb, "Cuckoo Search (CS) Algorithm," accessed: 2017-11-20. [Online]. Available: https://www.mathworks.com/matlabcentral/fileexchange/29809-cuckoo-search–cs–algorithm

[48] R. N. Mantegna, "Fast, accurate algorithm for numerical simulation of Lévy stable stochastic processes," *Phys. Rev. E*, vol. 49, pp. 4677–4683, 1994.

[49] R. D. Zimmerman, C. E. Murillo-Sánchez, and D. Gan, "MATPOWER," accessed: 2017-11-20. [Online]. Available: http://www.pserc.cornell.edu/matpower/

[50] P. Demetriou, M. Asprou, J. Quiros-Tortos, and E. Kyriakides, "Dynamic IEEE test systems for transient analysis," *IEEE Systems Journal*, vol. PP, no. 99, pp. 1–10, 2017.

[51] D. C. Montgomery, *Design and analysis of experiments*, 2nd ed. New York: John Wiley & Sons, Inc., 1984.